#261

FINAL REPORT

RECOVERY OF SANTA MONICA BAY FROM SLUDGE DISCHARGE

Submitted To

Environmental Monitoring Division
Hyperion Treatment Plant
12000 Vista del Mar
Playa del Rey, California 90291

by

Dr. Bruce Thompson, Project Manager
Southern California Coastal Water Research Project
646 W. Pacific Coast Highway
Long Beach, California 90806

March 1992

TABLE OF CONTENTS

LIST OF FIGURES & TABLES

TABLES

FIGURES

I. EXECUTIVE SUMMARY

Sludge was discharged from the Hyperion Treatment Plant's 7-mile outfall into the Santa Monica Submarine Canyon since 1957. This discharge created an area of approximately 20 sq. mi. that had elevated contaminants in the sediment and altered biological assemblages (Figure 1). The discharge of sludge was terminated in November 1987. This event provided a unique opportunity to study the recovery of the Bay ecosystem from sludge disposal. The objectives of this study were to provide an assessment of the recovery of the Bay, and to study the rates and processes of recovery from sludge discharge which may be useful in evaluating ocean disposal options in the future.

This study included a wide range of oceanographic, sediment, and biological measurements. Sampling was started a year and a half prior to discharge termination to document conditions in the Bay under full discharge. Recovery of the Bay was followed at the same sites for three years after discharge termination, through August 1990.

During full sludge discharge, the sediments in the canyon were characterized by extremely high organic content, sulfides, and contaminant concentrations. Only a few unusual benthic species could exist in the sludge field. This gradient of sediment contamination and altered benthic communities are typical of point source discharges.

Since the termination of sludge discharge into the Bay, complete recovery has not yet occurred in the Santa Monica Canyon, but nearly all parameters measured show trends towards recovery. Recovery will be considered complete when the marine life in the old sludge field is similar to that at the reference sites off Malibu.

The sediment in the Santa Monica Canyon are subjected to very high currents, both up and down the canyon. These currents can resuspend sediments to such a degree that sedimentation in the canyon was not noticeably affected by sludge discharge. Currents may also aid recovery by scouring and/or burying the sludge field.

As of August 1990, most of the contaminants in the sludge field have decreased in concentration. Most notably, the sulfide levels in the old sludge field have decreased to nearly background levels, and PCBs and PAHs have decreased by about 49% and trace metals have decreased by 53-59%.

Nearly ten times more benthic species now inhabit the old sludge field than did under full sludge discharge. The entire benthic community is changing and is becoming more like those in the reference areas off Malibu. However, some of the most common and abundant species that usually live in those reference areas are not yet established in the canyon.

Recovery of fish in the canyon is extremely slow, however some trends towards recovery have been observed. Abundances of both white croaker and Dover sole have decreased in the canyon since sludge discharge termination, while Pacific sanddabs, typical of reference areas, are beginning to move back into the canyon. Fish diseases, such as fin erosion and epidermal tumors, have nearly disappeared from Dover sole caught near the old sludge field, and the levels of PCBs has decreased in their tissues.

The toxicity of the sediments in the old sludge field to the amphipod *Grandidierella* has also decreased considerably. Based on the most recent tests (August 1990) the sediment in the old sludge field is no more toxic than sediment in the reference areas.

Although recovery is proceeding in the Bay, the process is very slow. Forecasts for full recovery suggest that the old sludge field may not recover for more than ten years. This important study should be continued through full recovery to verify these forecasts and to fully understand recovery from sludge discharge.

II. ACKNOWLEDGMENTS

This study was funded by the City of Los Angeles, Department of Public Works, Bureau of Sanitation. We are grateful for their support of this unique and important study. We thank Dr. Sam Cheng, Dr. John Dorsey (co-principal investigator), and Mr. Ken Ludwig for their support and cooperation.

We would like to acknowledge numerous people at SCCWRP and at the Hyperion Treatment Facility that helped during this project. Nearly all of the SCCWRP staff has participated in one form or another; their contributions are listed below.

Foremost recognition goes to the field sampling crew: the crew of the MARINE SURVEYOR, Captain Steve Kmeth, Pete Christy, and Bill Schafer, and to Marine Coordinator Harold Stubbs and Dario Diehl of SCCWRP.

During the course of the study, staff of the Environmental Monitoring Division, Dr. John Dorsey, Jim Roney, Ann Martin, Tony Phillips, John Shisko, and Karen Smith assisted with sample collection. SCCWRP staff Ken Schiff, Henry Schafer, Rich Gossett, Larry Cooper, Jim Laughlin, Pat Hershelman, David Tsukada, Diane O'Donohue, and others also helped with sample collection.

Grab sample sorting was done by Tara Beaton, Diane O'Donohue, David Tsukada, Darrin Greenstein, Larry Cooper, and Andrew Jirik of SCCWRP.

Trace metals and CHN analyses were conducted by Pat Hershelman at SCCWRP. Trace metals were also measured at West Coast Analytical Co., Monrovia, CA. Trace organics were measured by Rich Gossett, Skip Westcott, Azra Kahn, Marilyn Castillo, Valerie Raco, Rika Jain, and Chuck Ward at SCCWRP. Sediment grain-size analysis was done by David Tsukada at SCCWRP. Dr. Robert Eganhouse provided supervision and wrote the analytical methods section in Appendix 3.

Dr. Tareah Hendricks of SCCWRP analyzed the CTD, sediment trap, and current meter data, and wrote the Oceanographic Conditions section of this report.

Steve Bay and Darrin Greenstein of SCCWRP conducted the sediment toxicity tests. Steve Bay also wrote the Sediment Toxicity section of this report.

Mr. Larry Cooper and Dr. Jeff Cross of SCCWRP wrote the Dover sole population section.

Analysis and writing of the remainder of the report was done by Dr. Bruce Thompson of SCCWRP, co-principal investigator.

We are particularly grateful for the assistance of Dr. Bob Smith and his staff at EcoAnalysis, Inc., in Ojai, California, for their consultation and production of the multivariate data analysis included in this report.

Production and word processing was done by Elena K. Preston.

III. INTRODUCTION

The City of Los Angeles' Hyperion Treatment Plant began discharging sewage sludge from its 7-mile outfall in 1957. During that time, approximately four million gallons of sludge per day was discharged into the head of the Santa Monica Submarine Canyon at a depth of 100 m (Figure 1). During full sludge discharge, numerous monitoring and research samples were collected from the area near the outfall, thus the effects of sludge discharge were well documented (Hume *et al.* 1962; Bascom *et al.* 1978; Hyperion Treatment Plant Monitoring Reports).

Sludge discharge into the Bay was terminated in November 1987. This event presented an opportunity to study the recovery of the Bay from sludge discharge. In anticipation of this event, this study was designed to include sampling both before and after discharge termination.

The objectives of this study were to measure the sequence of events and rates of recovery from sludge discharge in order to infer and understand the process of Santa Monica Bay recovery. To accomplish this, we used a multidisciplinary approach that included sampling physical oceanographic, sediment chemistry, and biological parameters.

This is a final report of our findings through August 1990. As will be shown, complete recovery of the Santa Monica Canyon has not occurred, and it will be important to continue sampling there before conclusions about recovery rates and processes can be made. Additionally, the tremendous amount of data collected on this unique project will require much more time to analyze completely. This report is mostly descriptive in nature showing trends in raw data. Detailed analyses of interrelationships among the recovering sediment and biological parameters will continue for several years.

There have been several other studies of recovery from sewage and sludge discharge. All of these have been conducted at shallower depths (<30 m). The most well known study of recovery was from organic pulp mill discharge in Sweden (Rosenberg 1976). He showed initial recovery from elevated sediment organic material, sulfide levels to be rapid, requiring less than one year, but complete recovery required more than five years. He noted that the recovery process occurred generally in reverse of the degradation of the area by the discharge.

Another well known study of recovery is that of Sanders *et al.* (1980), on the west Falmouth oil spill. In contrast to Rosenberg's study, they found recovery to be very slow. After five years, traces of #2 fuel oil still existed in the sediment at the most contaminated sites, species composition, diversity, and abundances were just beginning to be normal.

Figure 1 Chart of Santa Monica Bay showing sampling locations for this study. Inset is an enlarged view of the station arrangement in Santa Monica Canyon. Contours of benthic assemblages are based on a survey by Bascom (1978) and was the basis for our site location selections.

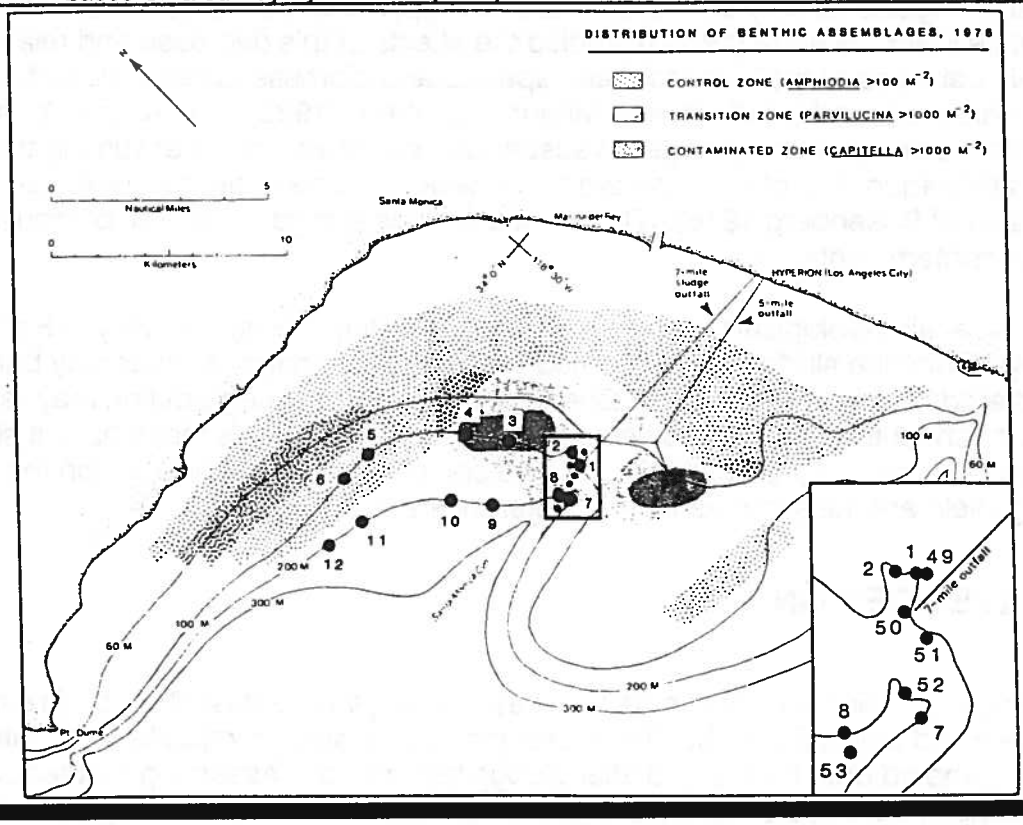

The differences in recovery time between Rosenberg's and Sanders' studies may be related to the presence of contaminants (oil) in Sanders' study which made recovery proceed much slower. More recent experiments of recovery have supported this idea. Containers of sludge and non-sludge sediments were used in a Scottish loch by Eleftheriou *et al.* (1982). They showed that the sediments had returned to background levels after eight months, but that the infauna remained "depressed" and suggested that this was due to the persistence of toxic effects. Mesocosm experiments (MERL) showed benthic infaunal changes of polluted sediments from the Providence River in five months, however contaminants (trace metals and chlorinated hydrocarbons) were still detectable in the sediments (Oviatt *et al.* 1984). Their experiments suggested that contaminants will remain in the sediments for a long time following source removal, but their finding of rapid infaunal recovery is in contract with Sanders' and Eleftheriou's studies.

In southern California, there have been several studies of improvement following abatement of discharge. Reish (1959) studied improvement following oil refinery discharge in Los Angeles Harbor and related infaunal improvement to changes in dissolved oxygen content of the water presumably caused by the termination of the discharge.

In 1971, the Orange County Sanitation Districts switched their sewage discharge from a 1-mile outfall (20 m) to their existing outfall at 60 m. In a study of recovery from the 1-mile outfall, Smith (1974) found that sediment organic material and sulfide reached background (control) levels in three months. The infaunal number of species remained rather constant, but densities decreased to background levels within a year. In 1974, Greene (1976a) resampled Smith's sites and found further decreases in sediment organic material and sulfide levels and significantly lower infaunal diversity. However, he attributed these decreases to episodic wave scour rather than improvement from sewage discharge. In 1975, the Los Angeles County Sanitation Districts began to decrease their discharge of solids at White Point. Greene (1976b) studied the effects of this decrease and related decreases in densities of "pollution tolerant" species and biomass to reduced particulate emissions which reduced sulfide levels. Mearns and Word (1982) used regressions to predict benthic biomass from changes in suspended solids emissions assuming that the processes and sequences of changes are the reverse of those of degradation. (Similar to the conclusion of Rosenberg 1976). These assumptions should be tested, particularly in the presence of contaminants.

Several physical and biological processes may be operating during recovery in Santa Monica Bay. Since the sludge field is located in a canyon, burial and scour may bury the sludge and erode it down the canyon. Chemical and biological degradation may reduce the contaminant concentrations. As the sediment changes, the animals that inhabit it should also change. Recovery will be considered to be complete when the animals on the seafloor in the sludge field are the same as those in reference areas.

IV. SURVEY DESIGN

Optimal sampling design for environmental effects surveys were described by Green (1979) and Bernstein and Zalinski (1983). These designs require sites in impacted and reference areas to be sampled both before and after sludge termination. Assuming that recovery is the reverse of impact, we adopted these designs for this study.

Our station locations were based on the results of previous surveys of sludge discharge effects in Santa Monica Bay (Bascom 1978) which showed three zones of biological effects: a contaminated zone nearest the outfall, transition zone, and a reference zone. We placed duplicate sites "down-current" in each of these zones at two depths, 100 and 200 m. Additionally, we reestablished five sites in the canyon axis sampled by Bascom (1978), for a total of 17 sites (Figure 1).

Sampling was begun in February 1986 and was conducted three times over the subsequent 18 months (winter and summer) until sludge discharge was terminated in November 1987 (Table 1, Appendix 1 and 2). As discussed above, we thought that recovery would be rapid initially, so sampling was conducted quarterly during the first year following termination. It was hoped that such frequent sampling would define more accurately the dynamics of the recovery process. However, as will be shown, we were incorrect in our assumption of rapid recovery. Semi-annual sampling was resumed in 1989 through the end of our contract in August 1990. A total of 11 sampling cruises were completed and 187 sediment and infaunal samples were collected over the five-year duration of the study.

Recovery of the Santa Monica Bay ecosystem will be evaluated in several ways. Recovery will be considered complete when the values for any given parameter (e.g. sulfides in sediment, numbers of fish caught per trawl, etc.) are statistically no different than at the reference sites. As will be shown, the numerous parameters measured in this study are recovering at different rates, thus an unambiguous single recovery endpoint cannot not be observed.

The biological assemblages (communities) of the Bay's ecosystem are of the greatest concern and were the primary focus of this study. Recovery of the benthic infauna, megafaunal invertebrates, and fish in the Santa Monica Canyon to reference conditions will provide the best demonstration of recovery. Based on the pre-termination sampling, we redefined the zones of impact described by Bascom (1978). Multivariate data analysis was used to show which sites had similar biological assemblages. Changes in species composition and abundances at these site groupings, or assemblages, will be followed through time until they are similar to those in the reference areas.

All of the samples collected were not analyzed. Benthic infauna and sediment contaminant analyses (trace metals and organics) from Cruise 4 (January 1988) were deleted by agreement with the Project Officer (Dr. Sam Cheng). Those analyses were replaced with the deep sediment coring and sediment toxicity samples that were added-on. Additionally, concentrations of trace metals in muscle tissues are still being analyzed. An addendum to this report will be provided upon completion.

Parameters Sampled

A variety of oceanographic, sediment, and biological parameters were sampled during each sampling period. These activities are shown on Table 1.

Detailed descriptions of the methods of sample collection and analysis are included in Appendix 3. Briefly, current meters, sedimentation traps, and water column profiles of conductivity, temperature, depth, and dissolved oxygen were measured at selected sites during each sampling period. The objective of this sampling was not to obtain detailed records, but to obtain some idea of how currents in the Santa Monica Canyon behaved and insure that unusual oceanographic events, such as El Niño or up-welling would not confound the sequences of recovery.

Sediment samples for chemistry analyses and benthic macrofauna were collected using separate 0.1 m^2, chain-rigged Van Veen grab samples at each site. A 7.6 m otter trawl was used to collect megabenthos and fish.

The approximate boundaries and depth of the sludge field was measured using the SCCWRP sediment corer (Bascom *et al.* 1982).

Sediment toxicity testing was conducted several times during the study. Sediments from the field samples were returned to the lab and the amphipod *Grandidierella japonica* was used as a test organism.

Table 1 Listing of sampling times and activities showing numbers of samples collected during each cruise. Station locations are shown on Figure 1 and exact locations and times are listed in the Appendices.

	Pre-Termination			Termination of sludge discharge	Post-Termination							
	1986		1987		1988				1989		1990	
Cruise	Feb. 1	Aug. 2	Sept. 3	Nov.	Jan. 4	Apr. 5	Aug. 6	Nov. 7	Jan. 8	Aug. 9	Jan. 10	Aug. 11
Task												
Sediments												
Grain Size	17	17	17		17	17	17	17	17	17	17	17
TOC & TON	17	17	17		17	17	17	17	17	17	17	17
Sulfides	17	17	17		17	17	17	17	17	17	17	17
CHCs	17	17	17		17	17	17	17	17	17	17	17
PAHs	17	17	17		17	17	17	17	17	17	17	17
Metals	17	17	17		17	17	17	17	17	17	17	17
Cores		3				10		10		10		10
Biology												
Infauna (grabs)	17	17	17		17	17	17	17	17	17	17	17
Megafauna (trawls)	12	12	12		12		12		12	12	12	12
Tissue contaminants		6	6				12			12		12
Sediment bioassays			3			4				14	8	32
Oceanography												
CTD/DO profile	6	6	6		6		6		6	6	6	6
Current meters	1				3		3		3	3	3	3
Sediment traps	3				3		3		3	3	3	3

VII. RESULTS

A. Oceanographic Conditions (Dr. Tareah Hendricks)

1. Background

The discharge of organically enriched particles, and associated trace constituents, from the 7-mile outfall has altered the physical and chemical composition of the sediments in the region around the discharge. The fate of the particles in these deposits are dependent on their susceptibility to resuspension, transport, dispersion, and redeposition. Resuspension may occur as a result of the individual or joint effects of biological and physical processes. In this section of the study, we address the physical oceanographic characteristics of the water column, and their possible effects on the ultimate fates of sediment particles.

2. Objective

The objectives of the physical oceanography measurements were: (a) characterize the physical environment in the vicinity of the 7-mile outfall, the canyon, and the surrounding area, and (b) determine if there were any trends in these measurements that are associated with the cessation of the discharge of sludge from that outfall.

3. Study Plan

The physical oceanographic measurements included observations of the temperature, salinity, dissolved oxygen, and light transmission characteristics of the water column, time-series of current velocities in the upper end of Santa Monica Canyon, and measurements of the flux rates of particles settling into sediment traps positioned near the ocean bottom. The methods used for sampling and analysis are detailed in Appendix 3.

4. Results

a. Water Column

The hydrocasts were made at seven of the stations shown in Figure 2. One of them, HR50, is located within the canyon and in close proximity to the terminus of the 7-mile outfall. Discharge from this outfall ceased on November 14, 1987. The water column was sampled on seven occasions between September 1986 and August 1990. Table 2 summarizes the sampling dates.

Figure 2 Station locations - physical oceanography

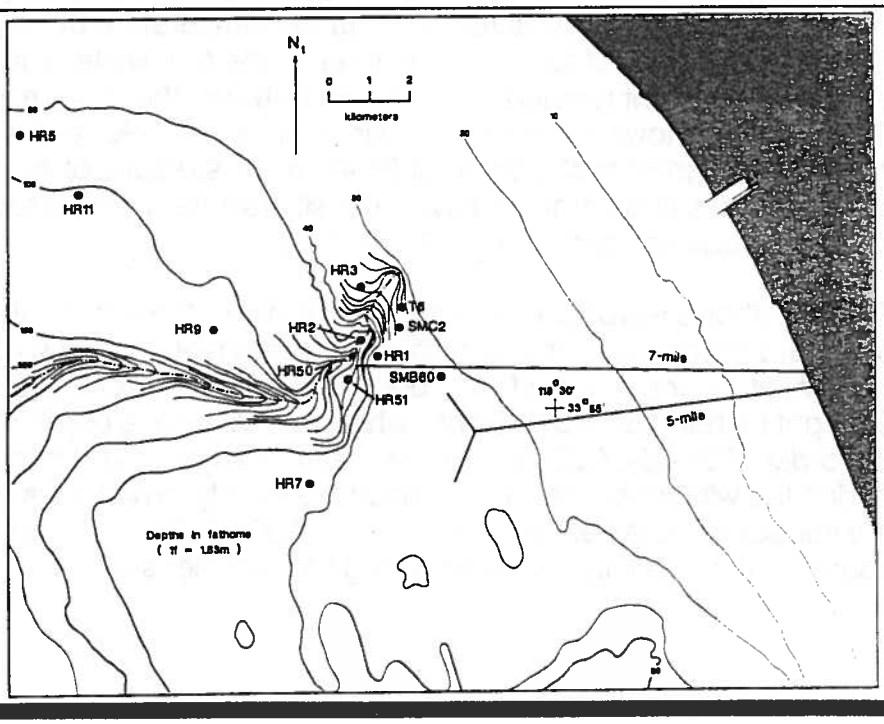

Table 2 Hydrocast Survey Dates			
Date	Cruise #	Cal. Day	Comments
09/03/86	2	CD246	Temperature only, no HR50
02/12/87	4	CD043	None
08/05/88	6	CD218	
01/31/89	8	CD031	
08/24/89	9	CD236	Subsurface Wastefield
02/16/90	10	CD047	None
08/14/90	11	CD226	

Figure 3 shows a typical temperature profile for the water column during the summer season. Surface temperatures were in the range of 17-19°C; temperatures at a depth of 200 m were on the order of 9-10°C. A sharp thermal gradient approximating a thermocline was present during each of the four summer surveys at a depth of 6-20 m. The temperature change across this thermocline was on the order of 5-7°C. At depths in excess of about 40 m, temperature gradients slowly diminished with increasing depth. Although the profiles have similar shapes, the shapes are often shifted in depth, but relative to each other. Part of this offset may be associated with spatial differences within the bay, but vertical excursions associated with internal tides and waves also play a major role.

Figure 4 illustrates a typical thermal stratification of the water column during winter conditions. Temperatures at the 200 m depth similar to those recorded during the summer surveys (ca. 9°), but the temperature of the surface waters had fallen to values of 13-14°C. On three of the four winter surveys, there was an almost constant temperature gradient between the surface waters and the 200 m depth. However, during the winter cruise of 1990, a sharp thermal gradient was present at a depth of 26-42 m. Illustrations of the distribution of temperature, salinity, transmissivity, density (sigma-t), and dissolved oxygen for each cruise are contained in Appendix 3.

Figure 5 shows a typical distribution for salinity in the water column during the summer season. A subsurface salinity minimum of about 33.4-33.5 ppt is present at depths ranging from about 35-55 m. Surface salinities are about 0.15 ppt higher (33.45-33.65 ppt), while the salinity at a depth of 200 m is on the order of 34.05-34.20 ppt. Figure 6 shows a typical distribution of salinity during the winter season. The subsurface salinity minimum is diminished, but the surface salinities are on the order of 33.30-33.50 ppt, or approximately the same as at the salinity minimum during the summer season.

Figure 3 Typical temperature profile - summer

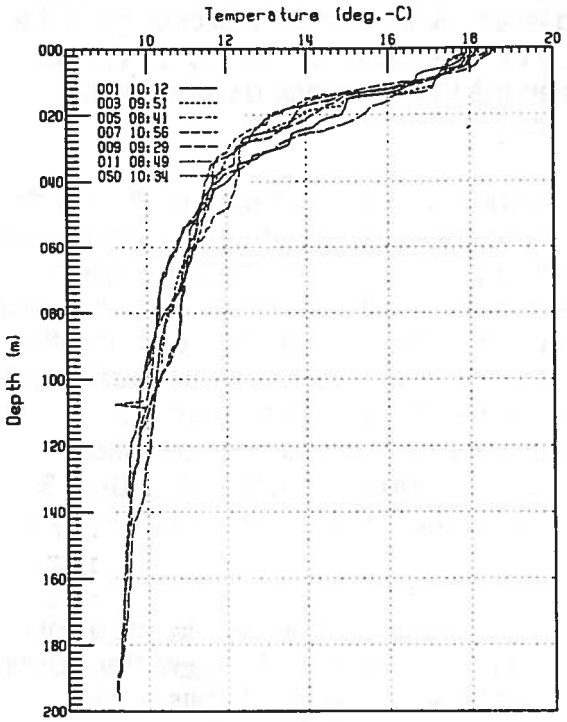

Figure 4 Typical temperature profile - winter

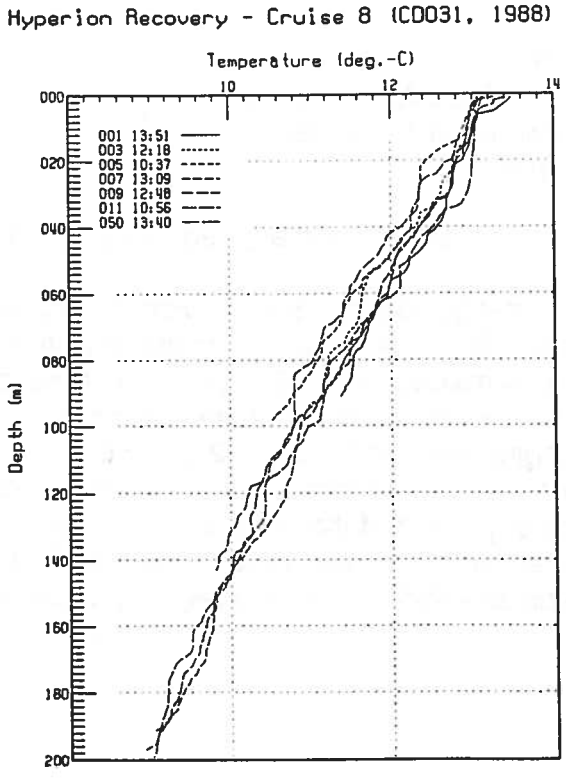

Figure 5 Typical salinity profile - summer

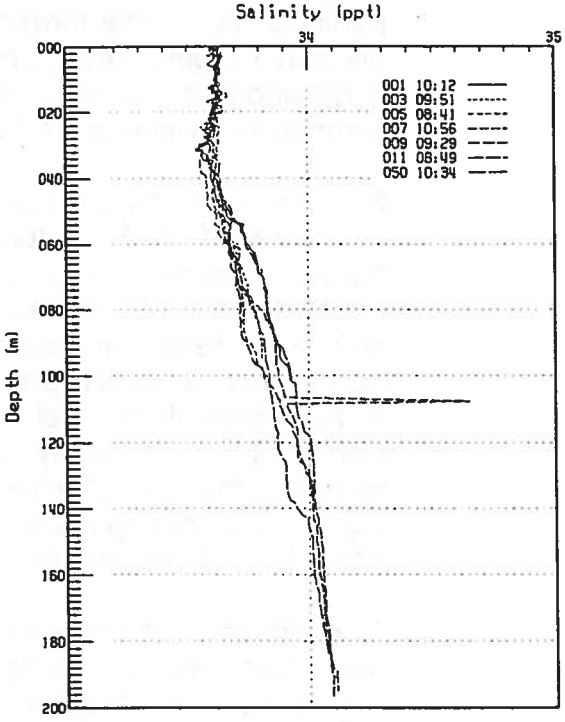

Figure 6 Typical salinity profile - winter

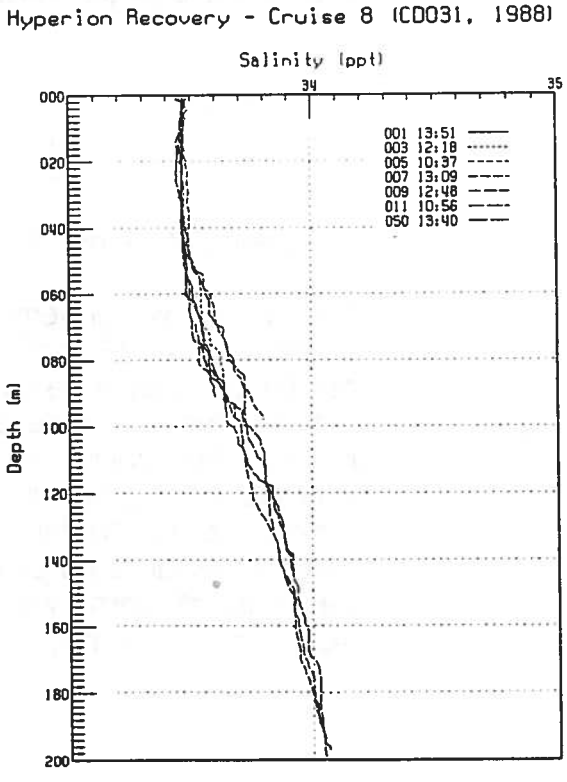

Figure 7 shows one distribution of water transparency during the summer. There is a much greater variation in this parameter between the surveys than for water temperature and salinity. Frequently, there is a local minimum in the transparency within the upper 20 m of the water column that may be associated with phytoplankton production. Secondary minima may or may not be present at greater depths--especially near the bottom, where suspended particles in the water form a nepheloid layer. Since substantial changes take place in the water column transparency between summer seasons, it is not surprising that clear differences between the transparency distributions in summer and winter are difficult to identify.

Figure 8 shows a typical distribution of density in the water column during the summer season. Since temperature gradients dominate the upper portion of the water column, the shape of the density profile is approximately a mirror image of the temperature profile in that region. Similarly, the temperature and salinity gradients are (negatively) correlated in the lower portion of the water column, so the density profile also mirrors the shape of the temperature profile in that region. In general, the water column is stable, with the density increasing monotonically with increasing water depth. Surface densities are related to the surface water temperature, and ranged from about 24.0-24.3 sigma-t units during the summer surveys. At the 200 m depth, the density is about 26.3-26.4 sigma-t units.

As might be expected from the temperature gradients, the density gradient is nearly constant over the upper 200 m of the water column in the winter. During our surveys, the density varied from about 24.9-25.2 sigma-t units at the surface, to about 26.3-26.4 sigma-t units at a depth of 200 m, for an average gradient of about 0.006 sigma-t units per meter. This density gradient is related to the frequency of free oscillations of a perturbation in a density surface (isopycnal surface), and hence to the maximum frequency of oscillation for an internal wave (Brunt-Vaissala frequency).

$$N^2 = -\frac{g}{\rho}\frac{\partial \rho}{\partial z}$$

where:

N	=	Brunt-Vaissala frequency
g	=	gravitational acceleration
rho	=	density

The period of the oscillation is related to the Brunt-Vaissala frequency by: $\tau = \frac{1}{2\pi N}$

The average winter density gradient corresponds to a Brunt-Vaissala frequency of about 7.7×10^{-3} sec^{-1}. Thus the periods of internal waves in these waters can be expected to lie between about 14 minutes and 22 hours (inertial period at this latitude). The density gradient in the lower 100 m of the water column is more variable during the summer, ranging from about 0.6-1.2 times the average winter gradient. The resulting minimum internal wave periods are on the order of 13-18 minutes. In the upper portion of the water column, the density gradients are generally much stronger, resulting a lower bound for the frequency of internal waves that can be as short as two to three minutes in the vicinity of the thermocline.

Figure 7 Example of light transmissivity profile - summer

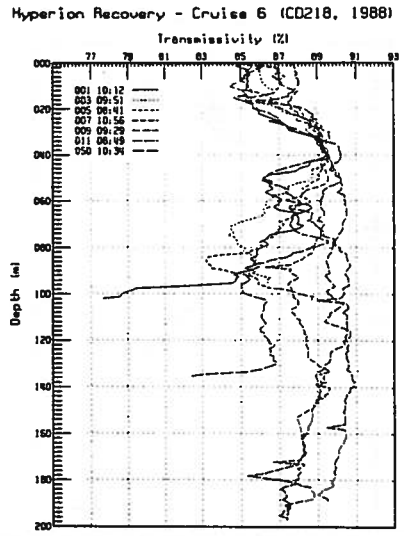

Figure 8 Typical density profile - summer

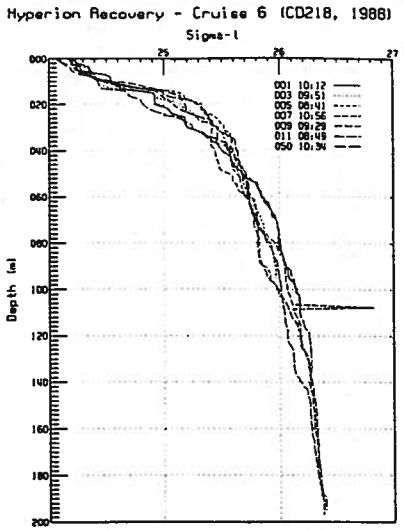

Figure 9 illustrates at typical summer profile of dissolved oxygen (DO). During the summer, the surface DO concentration was on the order of 8.5-9.0 mg/l. A subsurface maximum is often present at a depth of 10-35 m, below which the concentration decreases to a value of about 2.5-3.5 mg/l at a depth of 200 m. Surface DO concentrations in the winter varied from about 5.5-8.7 mg/l. Generally the subsurface maximum was absent. At a depth of 200 m, the DO concentration was about 2.5-3.3 mg/l, or essentially the same as during the summer.

On two of the surveys (Cruise 9, Cruise 11), we detected the presence of wastewater at several of the hydrocast stations. Figure 10 shows the distribution of salinity in the upper 100 m for four of the seven stations during Cruise 9 (the profiles for all the stations are contained in Appendix 1). Anomalous reductions in salinity are evident in the depth range from 16-45 m in the profiles collected at Stations HR50 and HR1--and to a lesser degree, at Station HR7. Anomalous reductions in temperature, light transmissivity, and dissolved oxygen also accompanied the reductions in salinity, and indicate the presence of wastewater from the 5-mile outfall (the 7-mile outfall was no longer in operation).

In order to get a rough idea of the dilution of this wastewater by the entrainment of ambient ocean water during the initial dilution process, we assumed that diffuser acted like a line source and that subsequent dilution due to oceanic mixing was negligible. We further assumed that the ambient water was entrained into the plume in the depth interval of from 56-40 m. The average salinity of the entrained water would be about 33.53 ppt. We assumed that the salinity of the effluent was 0.5 ppt. The salinity at the salinity minimum within the wastefield is about 33.25 ppt.

Figure 9 Typical dissolved oxygen profile - summer

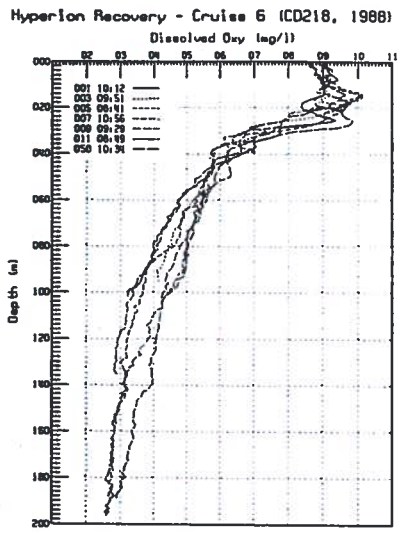

Figure 10 Salinity anomaly within a wastefield

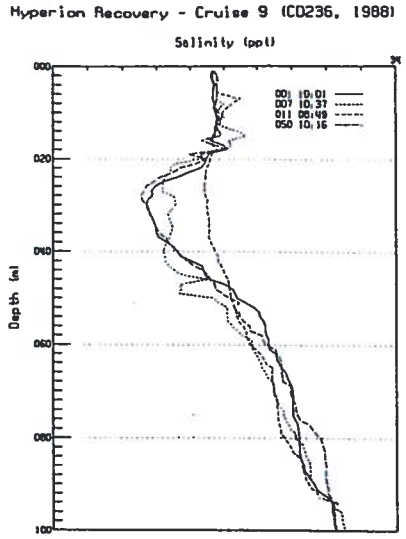

The dilution can be estimated from the salinity mass balance equation: $33.53D + 0.5(1) = 33.25(D+1)$
where: D = volume of entrained ambient water per unit volume of effluent

Solving this equation yields a dilution value of 117:1 (119:1 if the effluent is assumed to have a salinity of 0 ppt). This is the dilution at the depth of maximum wastewater concentration. Theory and laboratory studies indicate that the average dilution of the wastewater in the plume from a line source is equal to twice the minimum dilution within the plume. Thus the average dilution, D_a, would be about 234:1 (Note: the regulatory definition of the dilution is the total volume of wastewater and ambient water for each unit volume of wastewater, so it would be equal to D_a+1, or 235:1).

The reduction in.water temperature in the wastefield (Figure 11) is associated with the entrainment of colder, deeper water during the initial dilution process. The increased density associated with this colder water is required to offset the reduced salinity. The density profiles are shown in Figure 12. No significant anomalies are evident in the presence of the wastefield, indicating that the wastefield is in density equilibrium with the surrounding water.

Particulates in the effluent also decrease the transmissivity of light (Figure 13). The light transmissivity of distilled water for a transmissometer with a 25 cm beam path is about 91.3%. From the profile collected at stations that appear to be free of the presence of wastewater, we find that the reduction associated with the presence of natural particulate material (and absorption) is about 5%. At Stations HR1 and 50, the presence of the wastewater with a suspended solids concentration of about 0.28 mg/l (33 mg/l diluted by 117:1) results in an additional reduction of about 10%.

Figure 11 Temperature anomaly within a wastefield

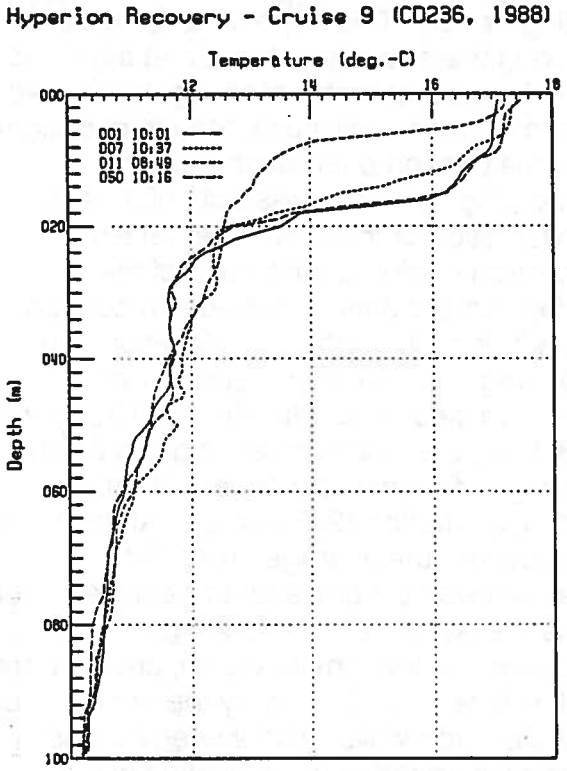

Figure 12 Density profile within a wastefield

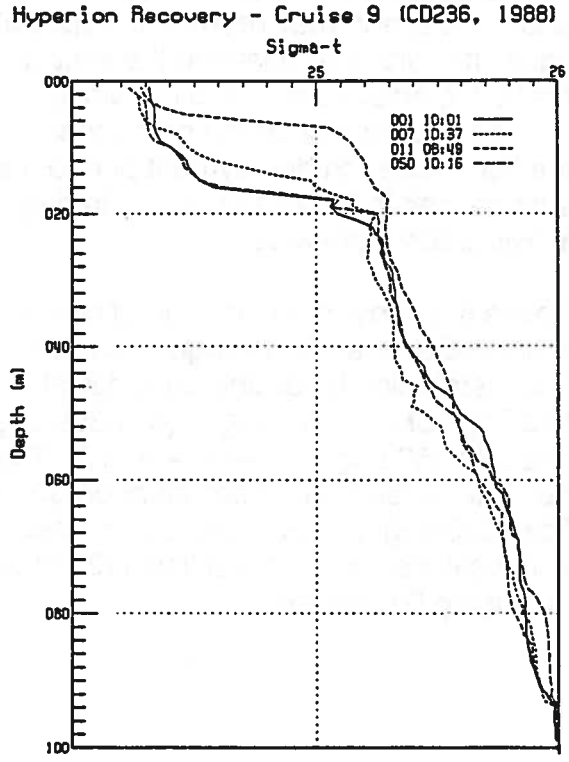

Figure 13 Light transmissivity anomaly within a wastefield

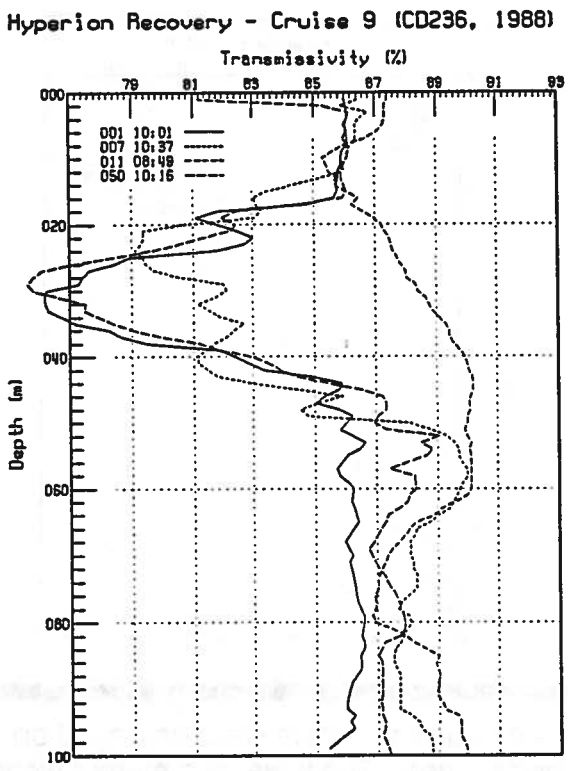

Figure 14 shows the reduction in dissolved oxygen associated with the presence of the wastefield. The maximum reduction is on the order of 1.8 mg/l. Part of this reduction is associated with the entrainment of ambient water during the initial dilution process, since the deeper entrained water has a lower concentration of dissolved oxygen than the ambient water at the wastefield depth.

b. Currents

Basic properties, direction of flow

The current measurements were made at a single mooring (Station HR2) located within the canyon at a depth of 100-108 m (Figure 2), in a region of complex bathymetry.

Figure 14 Dissolved oxygen anomaly within a wastefield

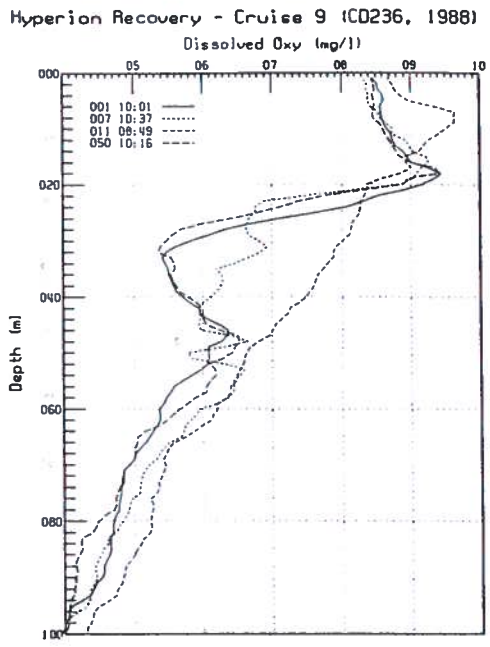

Three current meters were deployed on the mooring. The lower two meters were within the canyon, and were positioned at the elevations of 2 and 10 m above the bottom. The third meter was positioned in the water column above the canyon. Because of the steep slope of the bottom and sides of the canyon there was some variation in the depth of the mooring, and hence the depths of the current meters. The deployment dates and current meter depths for each deployment period are summarized in Table 3.

Table 3
Current Meter Deployments

Deployment Date	Calendar Day	Number Days	CM Elevation (m)		
			Midw.	+10m	+2m
04/21/86	CD111	37	40	90	98
05/28/86	CD148	38	40	90	98
01/14/88	CD014	37	68	98	106
12/21/88	CD354	38	45	na	103
02/28/90	CD060	36	40	90	98
08/13/90	CD256	21	44	94	102

The most common direction of flow at an elevation of 2 m above the bottom within the canyon is parallel to an axis oriented along 015-195 deg.$_m$, or 029-209 deg.$_t$ (Figure 15). This appears to be essentially along the axis of the canyon at the location of the current meter mooring, but a precise comparison is difficult because of changes in the canyon orientation near the mooring, and the possibility of a nearby bifurcation of the axis. The net along-canyon motion during each of the deployment periods was down-canyon (193 deg.$_m$). At the 2 m elevation, the average down-canyon speed was 4.9 cm/sec; at an elevation of 10 $_m$, it was 3.4 cm/sec. Accompanying this down-canyon flow was a weaker net cross-canyon motion (283 deg.$_m$). At the 10 m elevation, the average cross-canyon speed was 3.1 cm/sec, or nearly as strong as the down-canyon flow. Near the bottom, at the 2 m elevation, cross-shore flow is restricted more by the proximity of the canyon walls. The average cross-canyon speed at this elevation was reduced to 1.5 cm/sec. All these averages do not include the deployment beginning on CD354 in 1988. The flow during this period appears to be anomalous, and may represent a special case. It is discussed later in the section entitled "Correlations". The net along-canyon and cross-canyon components of the flows for each deployment period are summarized in Table 4 (X-axis is in deg.$_m$, Y-axis is 90° clockwise).

Above the canyon, the motion of currents is spread over a wider range of angles. The distribution is roughly bimodal, along headings of 300-345 deg.$_m$ (314-359 deg.$_t$) and 030-150 deg.$_m$ (044-164 deg.$_t$). The net flow consists of a consistent on-shore flow (039 deg.$_m$) averaging 2.2 cm/sec and weak net down-coast flow (129 deg.$_m$) averaging 0.8 cm/sec.

Figure 15 Directional probability of ocean and canyon currents

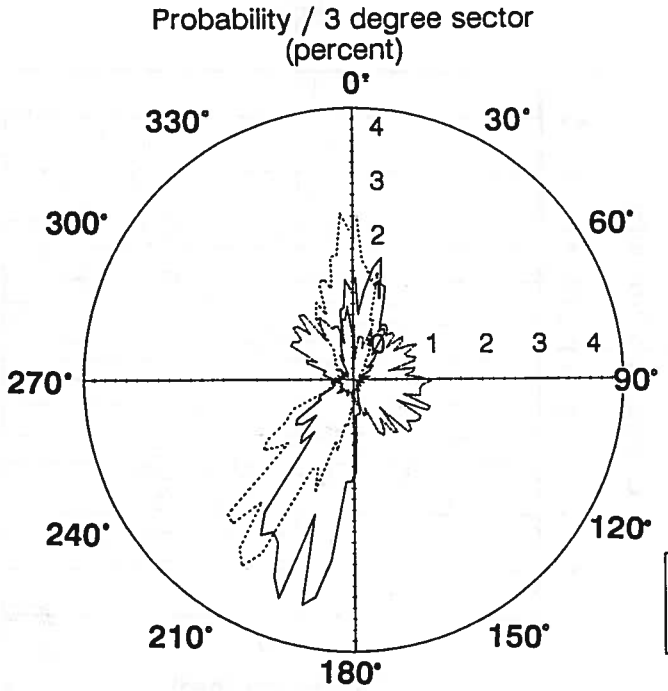

Table 4
Net Velocities (cm/sec) and Variances (cm^2/sec^2)

Date	Elev.	X-Axis	# Days	Vx	Vy	Var-Vx	Var-Vy
CD111, 1986	Midw.	220	37	-3.1	-0.1	32.1	57.0
	10m	201	37	5.4	3.5	171.0	15.2
	2m	193	36	7.4	2.2	211.0	14.2
CD148, 1986	Midw.	209	38	-2.5	-0.6	21.5	37.2
	10m	204	38	3.0	3.4	117.3	12.6
	2m	193	38	4.9	2.3	155.8	10.4
CD014, 1988	Midw.	210	27	-1.6	-0.2	55.1	79.7
	10m	195	36	2.2	2.4	148.1	18.0
	2m	223	37	3.7	2.1	199.9	16.9
CD354, 1988	Midw.	219	38	-2.3	0.1	21.9	58.1
	10m	na	0	na	na	na	na
	2m	194	38	12.6	0.1	486.6	27.6
CD060, 1990	Midw.	225	36	-3.0	-0.3	24.0	63.6
	10m	214	25	2.9	3.5	211.4	29.2
	2m	193	36	5.2	0.2	138.7	11.6
CD256, 1990	Midw.	232	21	-0.4	-3.9	12.6	117.8
	10m	196	18	3.7	2.9	160.9	16.8
	2m	198	21	3.2	0.7	99.4	6.8

Note that the net on-shore flow at a depth of 40-68 m (039 $deg._m$) is essentially opposite to the net down-canyon flow within the canyon (195 $deg._m$) and the net down-coast flow at the 40-68 m depth is opposite to the cross-canyon flow near the bottom of the canyon.

Current Speeds

The median current speeds at the two elevations within the canyon are comparable (ca. 8.1 cm/sec). The median speed above the canyon is about 50% greater (12.0 cm/sec). However, there was a significantly greater incidence of high current speeds recorded by the meters within the canyon. Figure 16 shows the cumulative probability distribution of current speeds for all the data at each of the elevations on the mooring. If the set of current speeds follows a "normal" (Gaussian) distribution, it would plot as a straight line in this figure. However, all the distributions tend to bend to the right, indicating that the currents have a greater fraction of high current speeds than would be expected for a normal distribution. This is particularly true for the currents measured within the canyon.

Figure 17 is analogous to Figure 16, but the logarithm of the current speed has been used in place of the speed as the abscissa.

Figure 16 Current speed probability distribution

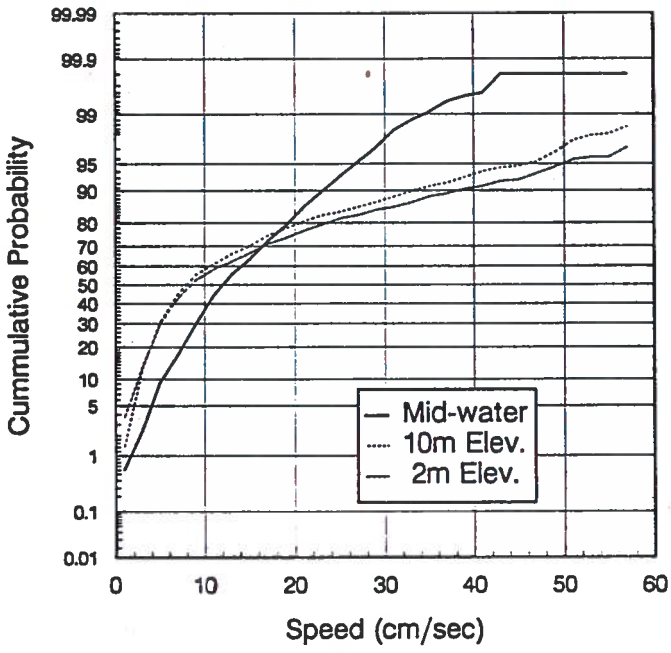

Figure 17 Current speed probability distribution (log-normal)

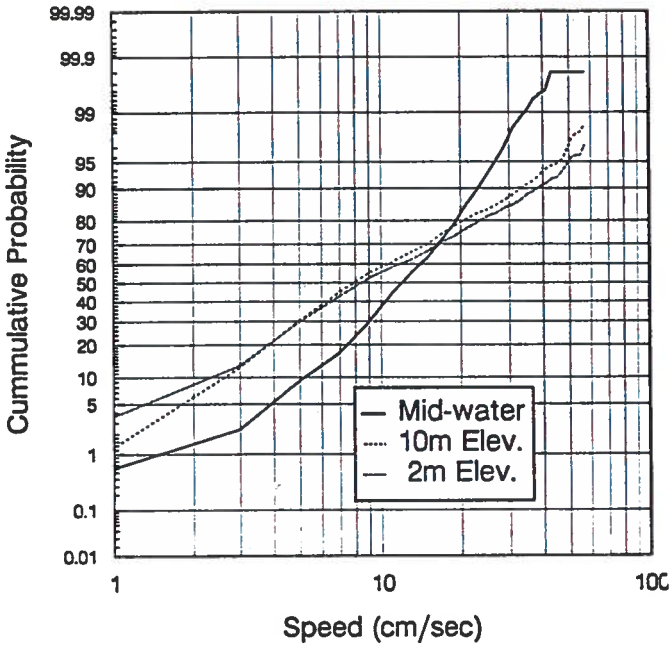

With this modification, the distribution of speeds for both elevations within the canyon (2 and 10 m) can be approximated by straight lines, indicating that they roughly follow a log-normal distribution. The plots have been terminated at a speed of 59 cm/sec since the current meters were not calibrated for speeds in excess of this value. As a result, up to 1.4% of the current measurements within the canyon were not adequately resolved during the deployments. These current speeds are substantially higher than we have measured on the shelf within Santa Monica Bay, or other shelf areas within the Southern California Bight. In contrast to the distribution of current speeds within the canyon, the distribution of the mid-water current speeds is not adequately represented by a log-normal distribution, and falls somewhere between a linear-normal and a log-normal distribution (e.g. a Poisson distribution).

The current speeds at the 10-percentile (low-speed) level are 5.6, 2.5, and 2.6 cm/sec for the mid-water, 2 m elevation, and 10 m elevation flows, respectively. At the 90-percentile (high-speed) level, the corresponding values are 23, 38.3, and 32.6 (mid-water 2 and 10 m). The 99-percentile speeds are approximately 34.4, >59, and >59 cm/sec at the mid-water, 10 m, and 2 m elevations, respectively.

Figure 18 compares the speeds of currents measured at a depth of 40-68 m over the canyon with those measured at a depth of 30-37 m at two stations on the edge of shelf in 57 m of water lying in-shore from the canyon (Stations SMC2 and T6, Figure 2) during other studies from 1988-89. Note that within the canyon, the highest recorded speeds increase with increasing proximity to the bottom. This is in contrast to the situation at the two stations on the shelf, where the highest speeds 2 m above the bottom are less than at mid-water levels (Figure 19). This suggests that while friction with the bottom reduces the near-bottom current speeds, other processes such as the focusing of internal waves (Gordon and Marshall 1976) may enhance the currents at the bottom of this canyon.

Figure 20 shows the distribution of current speeds at the 2 m elevation in the canyon for the winter-spring and late spring-fall periods, averaged over the appropriate deployments. On the average, the currents in the late spring and fall tend to be stronger than in the winter-spring season. However the speeds during the two deployments in the winter-spring were highly variable, and the highest speeds of any deployment were observed during the observations from 12/20/88 (CD354) to 1/25/89 (Figure 20).

Temporal Variability

The currents within the canyon and above the canyon are highly variable in time. An example of the variability in the along- and cross-canyon component of the flows at an elevation of 2 m above the bottom is shown in Figure 21 (the complete set is contained in Appendix 3). Examination of the variations in the along-canyon flow suggests that fluctuations of tidal periodicity make a significant contribution to this variability. In the cross-canyon flows, the fluctuations appear to occur over shorter time-scales. Table 4 lists the variance of the current velocities about the net along- and cross-canyon flows.

We examined the temporal distribution of the time-scales characterizing the fluctuations through the use of a digital fast Fourier transform to convert the original observations from "time space" (i.e. a time-series) to "frequency space" (i.e. amplitude as a function of frequencies representing the observations, instead of the time of the observation). In this analysis, variations along a single axis (e.g. along-shore) are represented as the resultant of combining component flows. Each of these components consists of a sinuosidal variation with a characteristic frequency (or periodicity) and phase (i.e. angle at the beginning of the observations). The computational procedure estimates the amount of the variance ("energy") associated with each of these components. This information can be used to evaluate the distribution of energy as a function of the "persistence" (periodicity) of the variations, and to identify specific frequencies (i.e. tidal frequencies) that may account for a significant fraction of the energy.

Figure 18 Current speeds - above-canyon vs. in-shore shelf

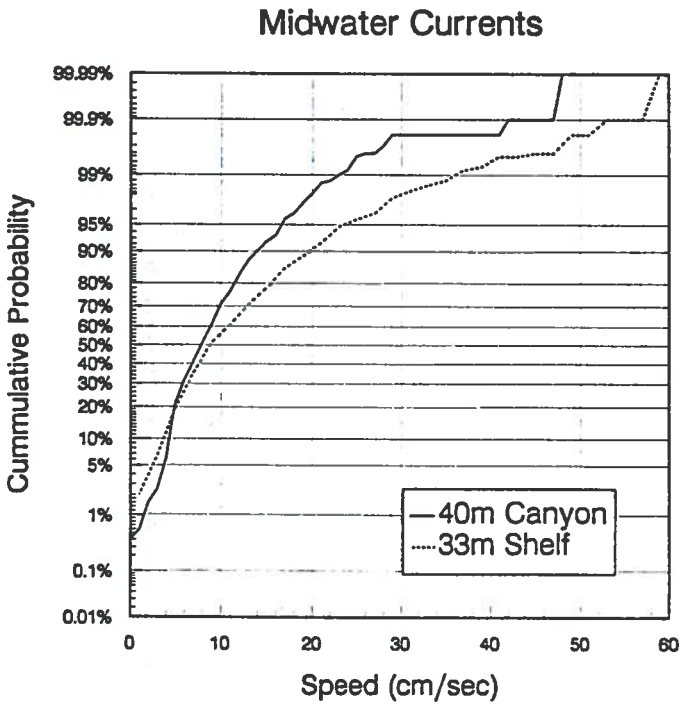

Figure 19 Shelf current speeds - mid-water vs. near-bottom

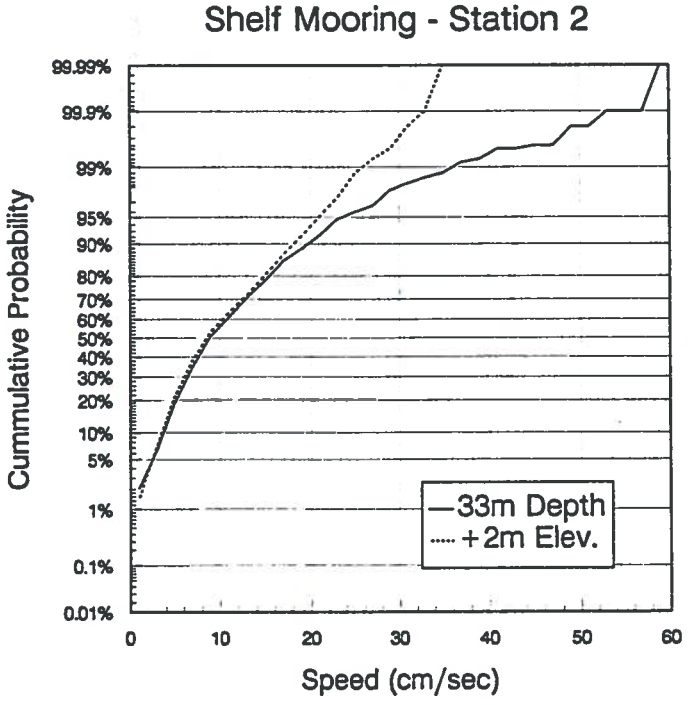

Figure 20 Seasonal dependence of canyon current speeds

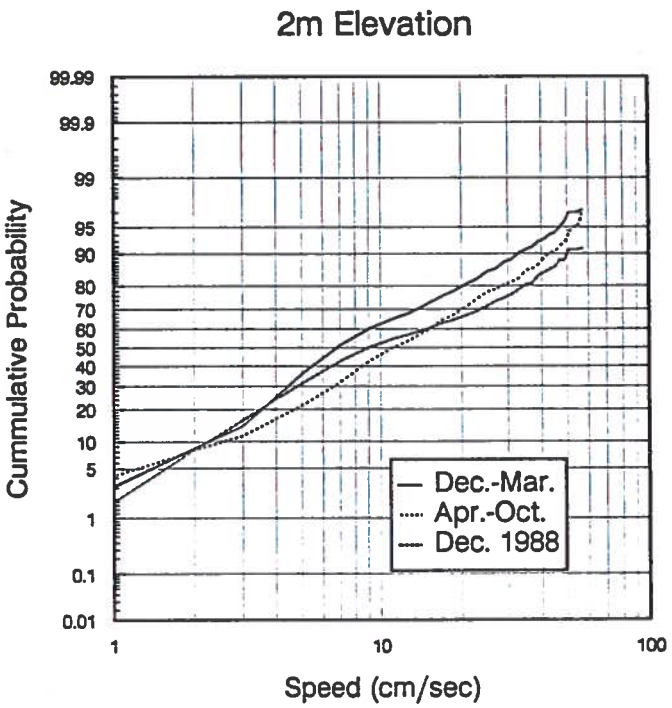

Figure 21 Example of near-bottom canyon current velocities (Vx = along-canyon, + = down-canyon; Vy = cross-canyon, + = up-coast)

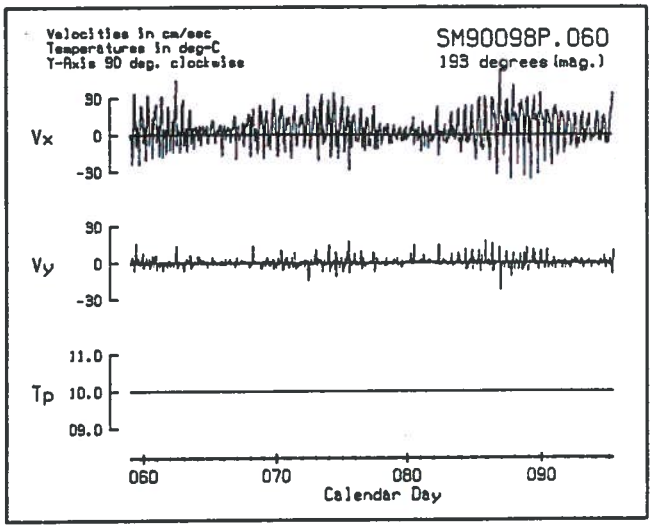

The result of this analysis for the along-canyon component of the currents at an elevation of 2 m is shown in Figure 22. The vertical axis represents the energy associated with each component frequency (termed the "spectral energy density"), while the horizontal axis indicates the frequency of the component. In this case, we have expressed the frequency in terms of the number of cycles per day (cpd). The periodicity associated with each frequency, expressed in days, can be obtained from the inverse of the frequency (i.e. a frequency of two cycles per day would have a periodicity of 1/2 a day, or 12 hours). A number of "spikes" are evident in the figure.

The peaks at frequencies of about two (1.94) and four (3.9) cpd are particularly striking and correspond to the frequency of the principal lunar semi-diurnal tidal component (referred to as the "M2" tidal component) and its first harmonic, respectively. Other possible peaks associated with other tidal components include those at frequencies of 0.6-0.7 cpd (lunar fortnightly, "Mf"), 1 cpd (luni-solar diurnal "K1", principal solar diurnal "P1"), 3 cpd (combination of diurnal and semi-diurnal), and 6 cpd (third harmonic of M2), but the data is too limited to establish this association.

Figure 23 shows that analogous diagram for the cross-canyon flows at the 2 m elevation. There is less evidence of contributions by fluctuations of tidal periodicity in this distribution, and the "tailing off" of the spectral energy density at high frequencies is less evident than in the along-canyon motions. A uniform distribution (spectral energy density independent of frequency) would be indicative of random motions.

In Figure 24, we examine the amount of the variance in the along- and cross-canyon motions associated with the entire range of frequencies. The ordinate represents the cumulative variance as a function of increasing periodicity (= inverse of the frequency). The latter is plotted on abscissa. Note that the total variance associated with the along-canyon fluctuations (ca. 240 cm^2/sec^2) is about 14 times greater than that associated with the cross-canyon fluctuations (ca. 17 cm^2/sec^2). Significant contributions to the variance by spikes in the spectral energy density (e.g. M2, 2*M2 in Figure 21) show up in this diagram as a nearly vertical increase in the variance at the periodicity associated with the spike.

The contributions to the total variance by the M2 tidal component and its first harmonic are clearly evident in the figure and account for about 57% of the total variance (M2: 45%, 2*M2: 12%). About 25% of the variance is associated with periodicities shorter than the first harmonic of the M2 tidal component (i.e. < 6.2 hours), and about 10% is associated with variations that occur more slowly than the M2 tidal component (12.4 hours). Slightly more than 5% is associated with fluctuations that have periodicities in excess of one week.

Figure 25 is the cross-canyon analog to Figure 24. Although the contributions associated with the M2 tidal component and its first harmonic are evident, they represent only a small fraction of the total variance.

Figure 22 Along-canyon spectral energy density 2 m above the bottom (all data)

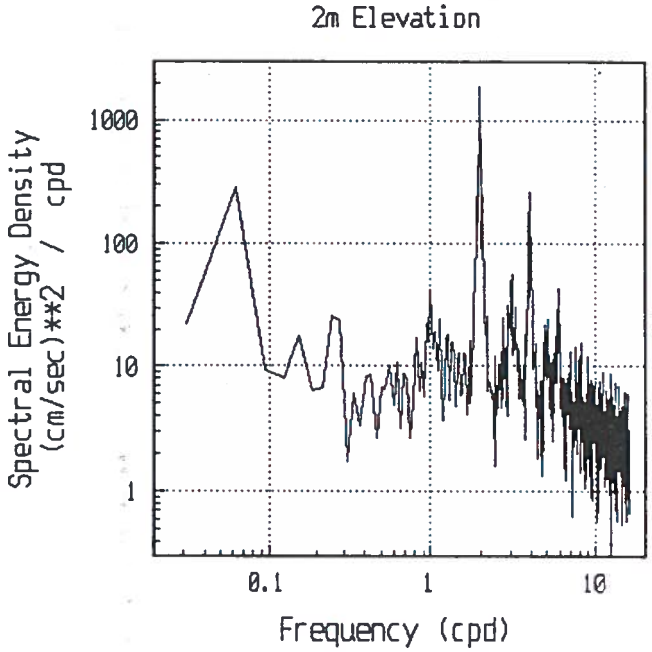

Figure 23 Cross-canyon spectral energy density 2 m above the bottom (all data)

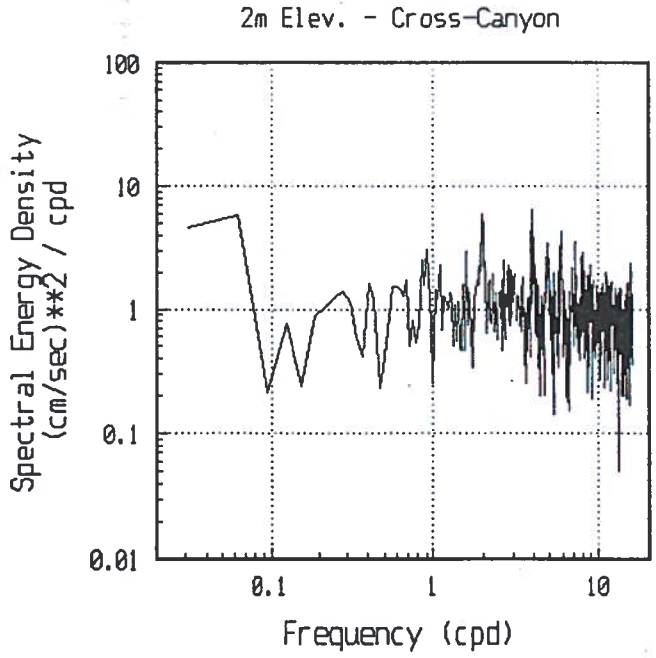

Figure 24 Temporal sources of variance - along-canyon

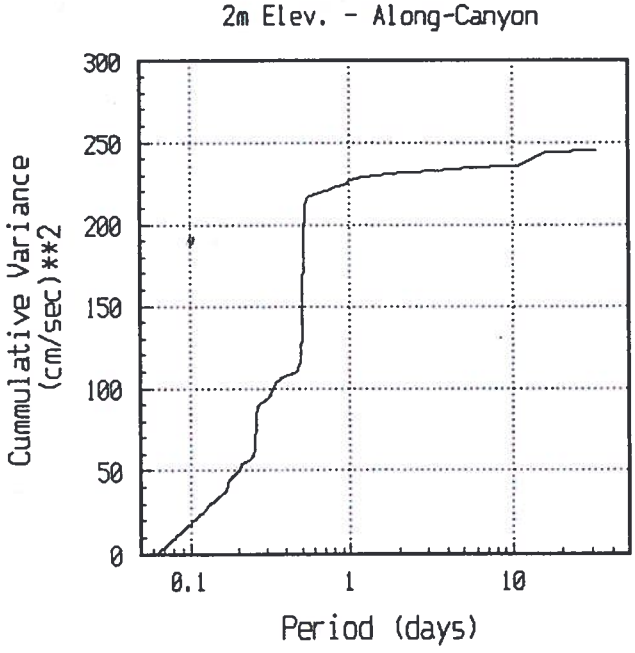

Figure 25 Temporal sources of variance - cross-canyon

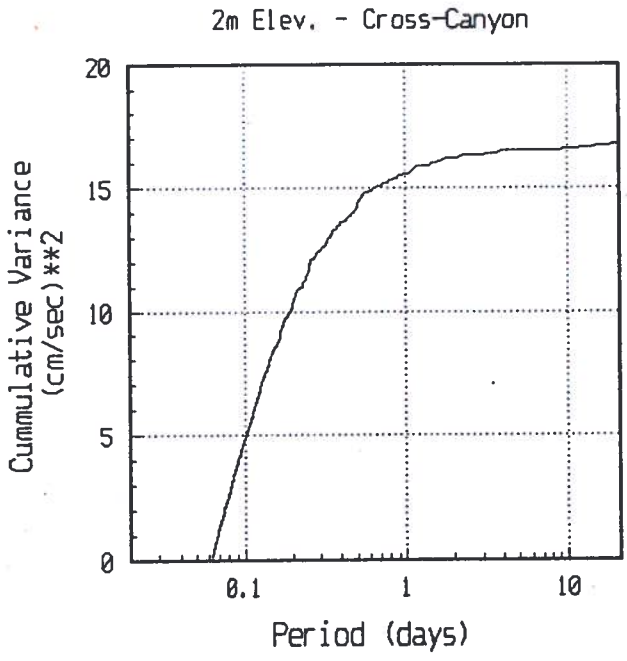

Most of the contribution is associated with periodicities shorter than the first harmonic of the M2 tidal component. There an indication that periodicities shorter, or frequencies higher, than that resolved by the analysis (1.5 hours, 16 cpd, respectively) might make a significant additional contribution to the total variance.

The properties of the mid-water currents (above-canyon) differ substantially from those within the canyon. As noted previously, the principal major axis for variations in these currents is approximately parallel to the general trend of the isobaths on the shelf, or roughly perpendicular to the axis of the canyon. Figure 26 shows the spectral energy distribution for the variations in the currents along this principal major axis of variation. Three features distinguish this spectrum from the spectrum for the along-canyon motions within the canyon: (1) substantial more energy is associated with the subtidal frequencies (e.g. frequencies < 1 cpd), (2) fluctuations of diurnal tidal periodicity (ca. 1 cpd) are clearly present, and (3) the energy associated with the first harmonic of the principal lunar semi-diurnal tidal component (2*M2) is greatly reduced and may be negligible.

Figure 27 illustrates the corresponding energy spectrum for the mid-water motions perpendicular to the principal major axis (i.e. along the principal minor axis). This spectrum differs from the spectrum associated with the principal major axis in that the amount of energy associated with the subtidal frequency fluctuations (< 1 cpd) is reduced (although still enhanced compared with the within canyon currents), and the energy associated with the supertidal frequency fluctuations (> 2 cpd) is enhanced.

Figure 28 shows the cumulative variance as a function of periodicity for fluctuations along the principal major axis. More than one-half of the total variance (56%) is associated with fluctuations that persist longer than the diurnal tides. Variations of diurnal tidal periodicity contribute about 7 cm^2sec^2 to the total variance (ca. 11%); variations of semi-diurnal tidal periodicity contribute about another 7 cm^2/sec^2. Fluctuations occur over times shorter than the semi-diurnal tidal period account for about 16% of the total variance.

Figure 29 is the analog to Figure 28 for the fluctuations along the principal minor axis of the mid-water currents. Variations of diurnal tidal periodicity contribute about 4 cm^2/sec^2 to the total variance (16%); semi-diurnal tidal period fluctuations account for another 4.5 cm^2/sec^2, or 18%.

Thus although the variance associated with tidal fluctuations in the cross-shore direction is less than in the along-shore direction, they contribute a greater percentage to the total variance. Fluctuations that are shorter in duration than the semi-diurnal tidal changes total about 9 cm^2/sec^2, or about the same as the same fluctuations along the principal major axis.

Figure 26 Along-shore (cross-canyon) spectral energy density - mid-water currents

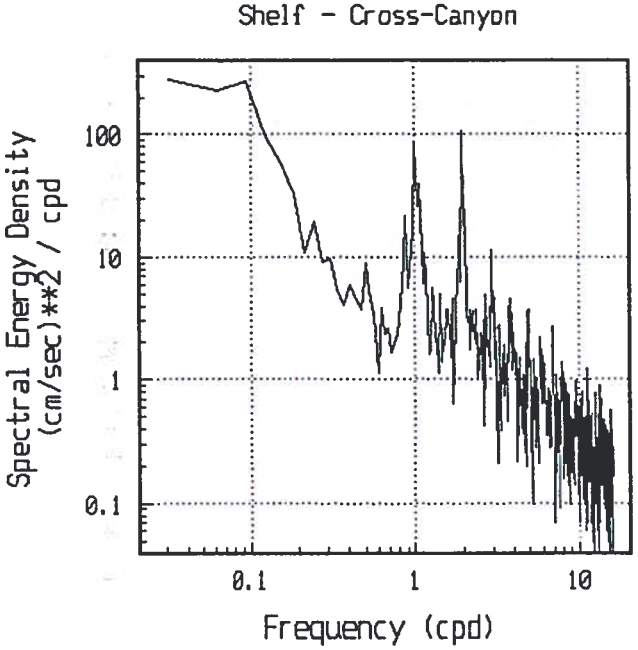

Figure 27 Cross-shore (along-canyon) spectral energy density - mid-water currents

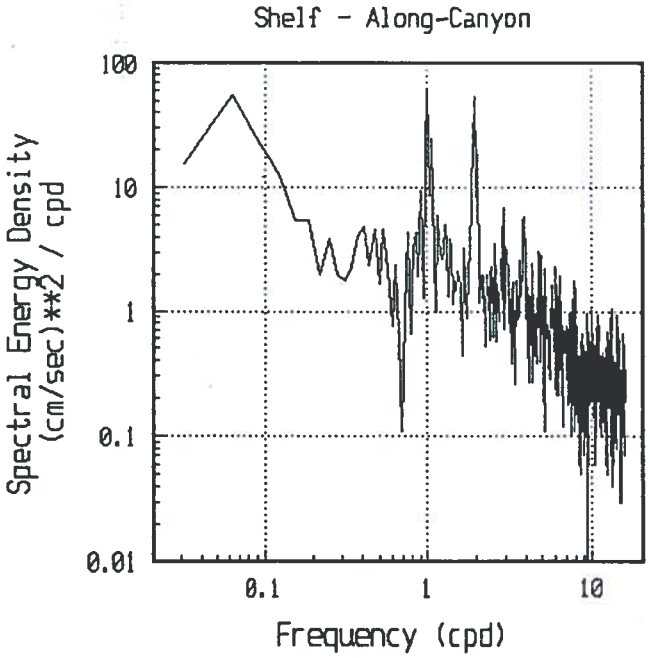

Figure 28 Temporal sources of variance - along-shore (cross-canyon)

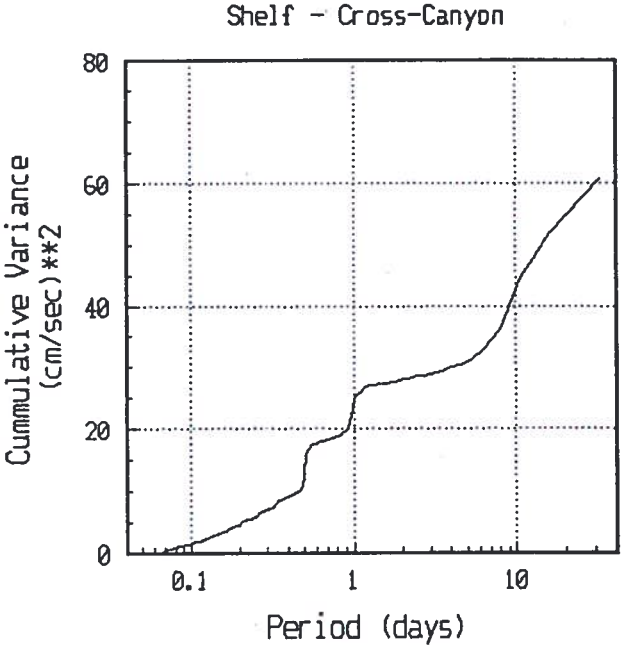

Figure 29 Temporal sources of variance - cross-shore (along-canyon)

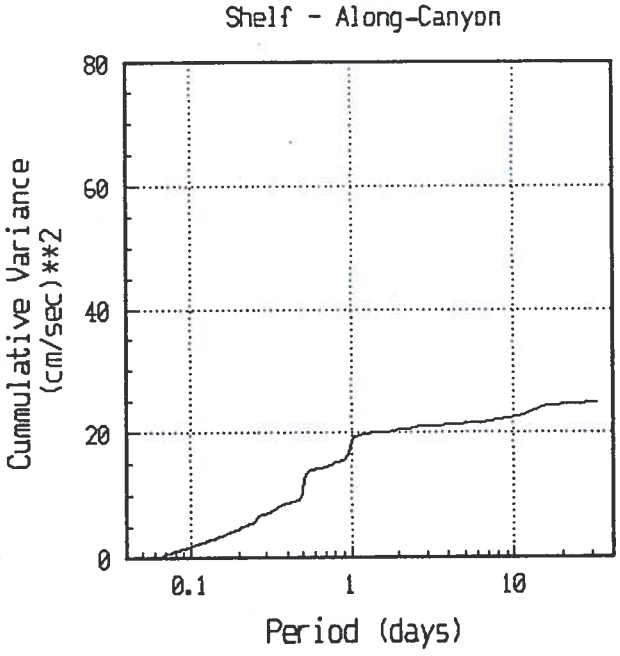

Thus variations characterized by periodicities shorter than the semi-diurnal tidal period (12.4 hours) are nearly isotropic, while fluctuations with periodicities longer than the diurnal tidal periodicity (ca. 24 hours) are strongly anisotropic, i.e. 31 cm^2/sec^2 versus 5 cm^2/sec^2.

Correlations

As noted in the study plan section, running average filters were applied to the original time-series to produce new time-series corresponding to fluctuations of supertidal, tidal, and subtidal frequency. The resultant time-series were used to examine the degree of correlation existing between the flows at the various elevations for each of the frequency bands. Table 5 summarizes the deployment averaged values of the cross-correlation coefficients for the tidal band component of the flows.

Correlations with magnitudes in excess of 0.5 are printed in bold; values are printed in italics when the standard deviation is greater than the magnitude of the average. "A" refers to the along-canyon axis; "X" to the cross-canyon axis.

Table 5
Correlation - Tidal Band

	Midw-A	+10m-A	+2m-A	Midw-X	+10m-X	+2m-X
Midw-A	1.00	*0.04*	*-0.02*	*0.03*	*-0.01*	*0.05*
+10m-A		1.00	**0.78**	*0.14*	0.14	0.18
+2m-A			1.00	*0.19*	0.12	0.12
Midw-X				1.00	*-0.08*	*-0.00*
+10m-X					1.00	0.16
+2m-X						1.00

The correlations are all less than 0.20 (4% of the variance in common) except between the along-canyon flows at elevations of 2 and 10 m. The average correlation for along-canyon tidal fluctuations between this pair of elevations was 0.78. Four out of the five deployments had higher correlation values (0.84 -> 0.97) between these flows, but the average was reduced by a relatively small value for the CD014, 1988 deployment (r=0.34). On two (out of five) occasions, the correlation values between the mid-water cross-canyon flow and the along-canyon flow at the 10 m elevation were between 0.34-0.41. On three (out of six) occasions, the correlation between the mid-water cross-canyon flow and the along-canyon flow at the 2 m elevation was between 0.33-0.37.

The fluctuations of supertidal frequency are the next largest contributors to the total variance for the along-canyon flows (and the largest contributor to the cross-canyon flows) within the seven-canyon. Table 6 summarizes the deployment averaged correlation coefficients for this frequency band.

Table 6
Correlation - Supertidal Frequency

Loc.	Midw-A	+10m-A	+2m-A	Midw-X	+10m-X	+2m-X
Midw-A	1.00	*0.02*	*-0.01*	*-0.07*	*-0.06*	*0.01*
+10m-A		1.00	**0.58**	0.08	-0.12	*0.01*
+2m-A			1.00	0.07	-0.10	-0.08
Midw-X				1.00	*0.02*	*0.04*
+10m-X					1.00	*0.12*
+2m-X						1.00

Again the only correlation coefficient with a magnitude in excess of 0.5 is associated with the along-canyon component of the flows at elevations of 2 and 10 m. As in the case of the fluctuations of tidal periodicity, four of the five deployment periods have correlation values for this pair of flows that are in excess of the average value (0.62 -> 0.79), but the correlation for the CD014, 1988 deployment was only 0.12. No correlation values for the individual deployments for any of the other elements of this matrix have a magnitude in excess of 0.26 (7% of the variance in common), and all but one have a magnitude less than 0.17 (3% of the variance in common).

Table 7 lists the deployment averaged correlation coefficients for the subtidal frequency fluctuations in the currents. As for the other frequency bands, the greatest correlation is associated with the along-canyon flows at elevations of 2 and 10 m. However, there is also a moderately strong correlation between the cross-canyon component of the flow at the 10 m elevation, and its along-canyon component (r=0.62) and the along-canyon component of the flow at an elevation of 2 m (r=0.70). There is also a weaker and negative correlation between the along-canyon flow at the mid-water elevation and that at elevations of 10 m (r=-0.30) and 2 m (r=-0.39). During some of the individual deployments, the magnitudes of the correlation between the along-canyon motions at the mid-water depth and those at the 2 and 10 m elevations within the canyon were in the range of 0.33-0.67.

Table 7
Correlation - Subtidal Frequency

Loc.	Midw-A	+10m-A	+2m-A	Midw-X	+10m-X	+2m-X
Midw-A	1.00	*-0.30*	*-0.39*	*-0.03*	*-0.15*	*0.02*
+10m-A		1.00	**0.71**	*-0.12*	**0.62**	0.38
+2m-A			1.00	*-0.03*	**0.70**	0.32
Midw-X				1.00	*-0.04*	*0.13*
+10m-X					1.00	0.42
+2m-X						1.00

Although the lowest correlation value between the along-canyon motions at the 2 and 10 m elevations was again associated with the CD014, 1988 deployment, the correlation value still remained high (0.61 versus 0.68 -> 0.82 for the other deployments). Correlations between the cross-canyon motions at the 2 and 10 m elevations were in excess of 0.5 (0.51 -> 0.74) during four of the five deployments, but on one occasion (CD256 1990), there was a negative correlation (-0.22) that reduced the average to 0.42.

It is interesting to note that fluctuations of subtidal frequency have the greatest number of correlation values with magnitudes in excess of 0.5-- even though the contribution of this frequency band to the within canyon flows is relatively minor. We noted earlier that the net down-canyon flow was especially fast (ca. 12.5 cm/sec) during the deployment beginning on calendar day 354 (12/28) in 1989 (Table 4). In comparing the subtidal and tidal frequency fluctuations for this period, we were struck by the apparent correlation between the magnitude of the subtidal frequency fluctuations and the amplitude (at the same time) of the fluctuations of tidal periodicity (Figure 30).

To examine the correlation between these motions, we constructed a new time-series from the time-series containing the fluctuations of tidal periodicity. In this new time series, the magnitude of the current replaced its amplitude, so that both up- and down-canyon motions were represented by positive values. We then used our 25-hour running average filter to create a time-series that represents the fluctuations of subtidal frequency in the amplitude of the tidal fluctuations. The correlation between these slow variations in tidal amplitude and the fluctuations of subtidal frequency in the along-canyon motions was then computed. For all the deployments, except that beginning on CD354, the magnitude of the correlation coefficient was less than 0.10 (-0.091 to +0.099). However, for the CD354 deployment, the correlation was 0.87.

We suspect that the combination of a high correlation and a high net down-canyon current speed is an artifact associated with some deficiency in the measurements (or their interpretation). We believe that the most likely source of this artifact is associated with the irregular bathymetry of the canyon and variations in its alignment. Both of these factors can lead to the generation of secondary flows of relatively limited spatial extent. For example, if the current meter mooring was placed near a bend in the canyon during this deployment, the presence of flow direction dependent areas of reduced current strength in the flow (Figure 31) could produce an apparent rectification of the tidal oscillations, leading to large net flow. The possibility of such secondary flows also casts some uncertainty about the validity of our estimates of the average net velocities within the canyon and perhaps even on the direction of flow.

Figure 30 Correlation of subtidal frequency fluctuations in the along-canyon currents with tidal amplitude: a) Tidal component of the flow, b) Subtidal frequency component of the flow, c) Subtidal frequency component of the magnitude of the tidal amplitudes.

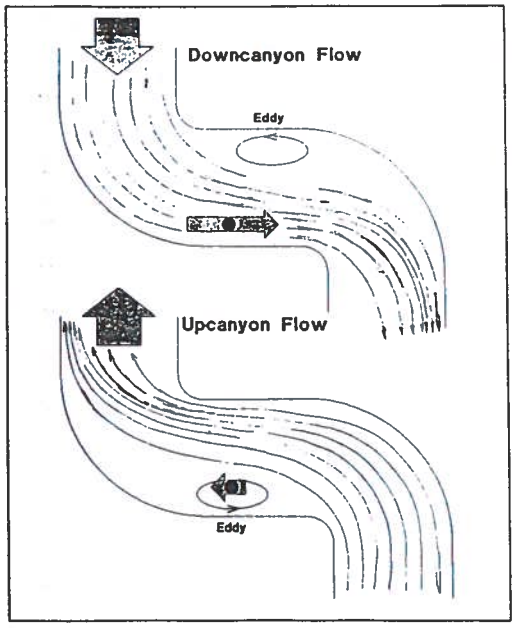

Figure 31 Example of apparent flow rectification by secondary flows

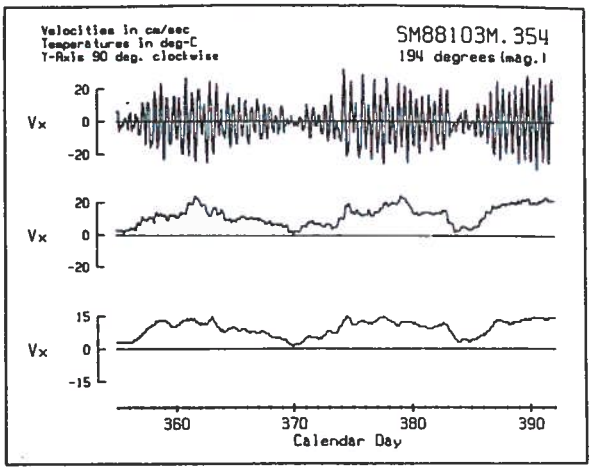

c. Sediment Trap Fluxes

The sediment trap moorings were deployed at three canyon-slope Stations HR1, 2, and 51, and one shelf station (SMB60 Figure 2). The canyon-slope moorings had four traps, positioned at elevations of 1, 4, and 10 m and 60 m above the bottom. The shelf mooring had three traps, at elevations of 0.5, 2, and 5 m above the bottom. The sediment trap moorings were deployed on five occasions for durations ranging from 22-39 days. The deployment periods are summarized in Table 8.

Table 8
Sediment Trap Deployments

Deployment Date	# Days
05/28/86	38
02/29/88	39
09/16/88	36
04/06/90	38
10/04/90	22

Table 9 summarizes the mass fluxes into the sediment traps at each mooring during each of the deployment periods.

With the exception of the last deployment in 1990, the depositional fluxes at the sea-bottom interface are on the order of 2500-5800 mg/cm^2/yr. Comparable flux rates are observed on the shelf (SMB60) and within the canyon (HR1, 2, and 51). These rates appear to be substantially higher than the probable accumulation rate of particulate material on the shelf (ca. 10-100 mg/cm^2/yr), but are comparable with fluxes into sediment traps observed at some other areas on the southern California coastal shelf. It has been speculated that this is the result of a series of resuspension and redeposition of surficial sediment material (Hendricks 1986 and 1987).

Table 9
Sediment Trap Fluxes (mg/cm^2/yr)

Date	HR1	HR2	HR51	SMB60
05/28/86	5446	3889	na	4459
02/29/88	5328	4314	5788	3088
09/16/88	2532	2929	2612	2916
04/06/90	3400	2424	5093	3789
10/04/90	865	441	249	686

Temporal changes in the flux rates are illustrated in Figure 32. The abscissa is expressed as the number of days between the beginning of a deployment and when the discharge through the 7-mile outfall was terminated (November 14, 1987). Two of the deployments precede the termination of the discharge; three deployments follow the termination.

There is a suggestion of both a general decline in the flux rates into the sediment traps and a possible seasonal variation. In order to examine the latter, we compared the fluxes collected during the fall deployments (9/16/88 and 10/4/90) with those made during the winter and spring (2/29/88, 4/6/90, 5/28/86). The results are summarized in Table 10. The fluxes for fall are listed with, and without, the measurements from the 10/4/90 deployment because there appears to be a general, and large, reduction in deposition rate during 1990.

Table 10
Seasonal Trend in Sediment Trap Fluxes (mg/cm^2/yr)

	HR1	HR2	HR51	SMB60
Fall (all data)	1699	1685	1430	1801
Fall (w/o 10/90)	2532	2929	2612	2916
Winter-Spring	4725	3542	5441	3779

Figure 32 Temporal variability in sediment trap fluxes (extrapolated to z=o)

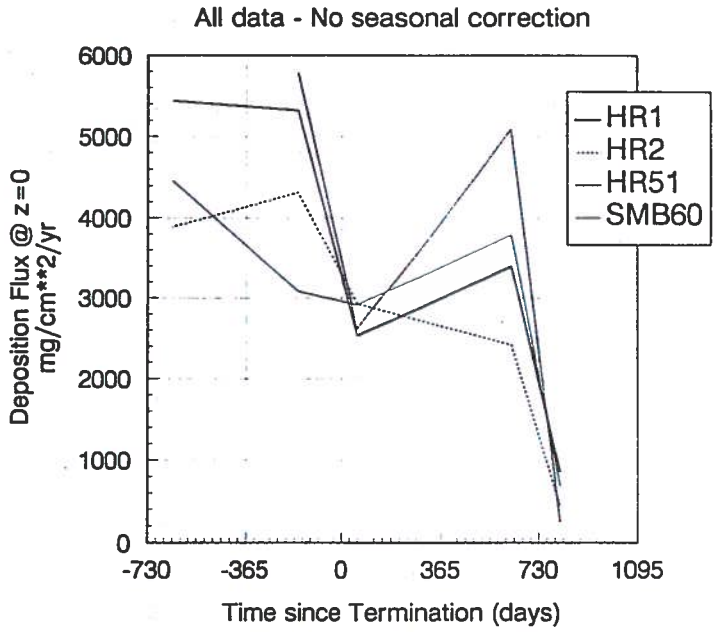

Figure 33 Temporal variability in sediment trap fluxes - corrected for seasonal variability (average of all (traps)

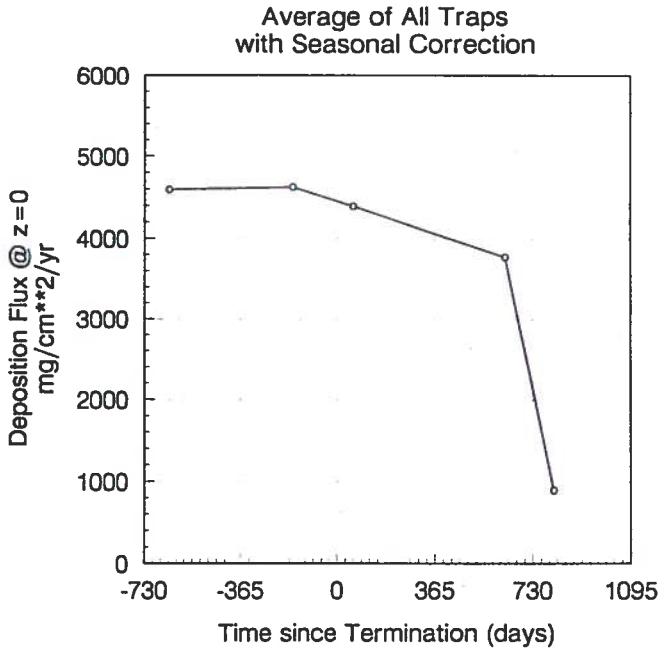

The fluxes for the winter-spring period are on the order of 1.6-2.7 times higher (without the 10/90 measurements and all data, respectively) greater than the fluxes during the fall. We assumed that the winter-spring fluxes were 1.6 times greater than the fluxes during the fall season, modified the fall data to yield a "winter-spring" season equivalent, and averaged all the trap data for a single deployment together. The result is shown in Figure 33 and suggests that the depositional rates into the sediment traps declined only slightly, during the first year and one-half (630 days) following discharge. During the next half year (179 days), there was a substantial decline in the rate.

Figure 34 shows the concentration of total volatile solids (TVS) in the material collected in the traps at an elevation of 0.5 m (SMB60) or 1 m (HR1, 2, and 51) above the bottom. There is a general trend toward declining TVS values during the entire course of the study, including the period prior to the termination of the discharge. The greatest reductions occur at the stations positioned within the canyon (HR1, 2, and 51).

Figure 35 shows the measured trend in the TVS concentrations measured in the trap material collected at an elevation of 60 m above the bottom. Again there is a general trend toward declining TVS values, but the greatest reduction appears to precede the termination of the discharge.

Figure 34 Temporal variability of the organic content (total volatile solids) of the trap material at 0.5-1 m above the bottom

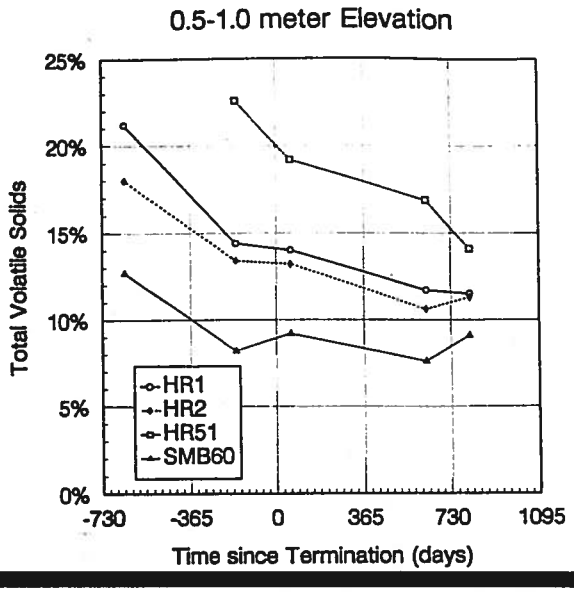

Figure 35 Temporal variability of the organic content (total volatile solids) of the trap material at 60 m above the bottom (canyon and slope moorings)

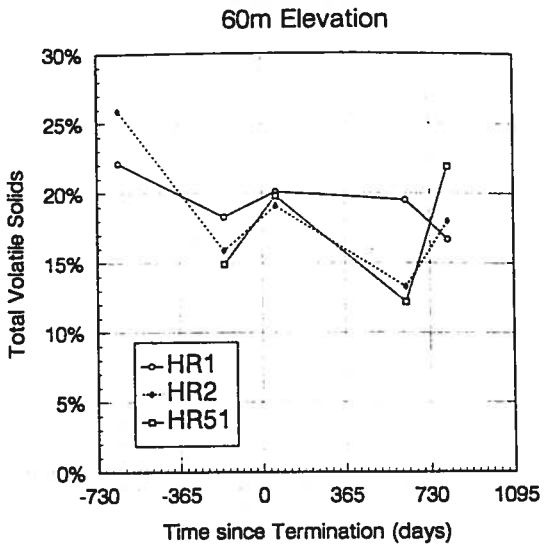

Figure 36 shows the change in the ratio between the TVS concentrations in the sediment trap material collected at an elevation of 60 m above the bottom compared to the TVS values in the material collected at 1 m. Overall there is an upward trend in this ratio, but the trend is not as evident in the samples collected at HR2 as it is at the other two canyon stations.

Table 11 lists the characteristic thickness of the depositional layer and the regression coefficient for a log-linear regression. The average characteristic thickness for the settleable material in the nepheloid layer at the stations within the canyon (HR1, 2, and 51) is 15.2 (+/- 2.9) meters, while the average thickness at the shelf mooring is almost an order of magnitude less at 1.8 (+/- 0.5) m. If it is assumed that the flux rate of particulate material into a trap is proportional to the concentration of settleable matter in the water column at the trap elevation, then the concentration profile of settleable particulate material will have the same shape and characteristic thickness as the deposition flux dependence. The total mass of settleable particulate material in the nepheloid layer is given by the equation:

$$M(h_0) = \int_0^{h_w} F(z, h_0)\, dz$$

where $F(z,h_0)$ is given by Eqn (1) and h_w is the water depth. Since the flux rates into the traps at the sea-bottom interface at the shelf station (SMB60) are comparable with those at the canyon stations (HR1, 2, and 51), this means that the total mass of settleable particulate material contained in the nepheloid layer in the canyon is about 8.5 times greater ($= h_0(\text{canyon})/h_0(\text{shelf})$) than on the shelf.

Figure 36 Ratio of the organic content of the sediment trap material at 60 m above the bottom (compared with 1 m above the bottom)

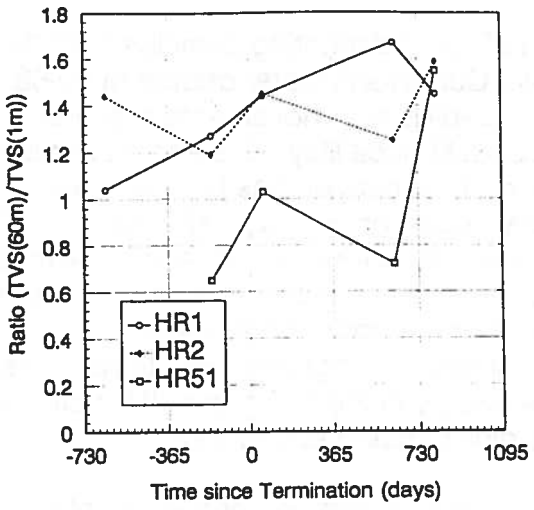

Table 11
Nepheloid Layer Parameters

Date	Sta.	HR1 (N=4)	HR2 (N=4)	HR51 (N=4)	SMB60 (N=4)
05/28/86	h_0	14.5	21.7	na	1.3
	r	-.9999	-.9957	na	na
02/29/88	h_0	10.9	11.5	16.6	1.8
	r	-.9991	-.9990	-.9838	-.9975
09/16/88	h_0	13.3	11.5	17.7	1.9
	r	-.9978	-.9998	-.9933	-.9952
04/06/90	h_0	15.8	15.5	17.3	1.6
	r	-.9981	-.9967	-.9992	-.9998
10/04/90	h_0	14.6	15.3	16.3	2.6
	r	-.9995	-.9991	-.9984	-.9992

5. Discussion and Summary of Oceanographic Results

The waters within Santa Monica Bay were density stratified to some degree during each of the hydrographic surveys. During the winter and spring, the stratification was weak, and the gradient was nearly constant over the upper 200 m of the water column. During the summer, a thermocline was present at depths of 5-35 m, increasing the density stratification of the upper portion of the water column (< 50 m depth). Although we have not modeled the initial dilution process associated with the discharge from the 7-mile outfall, it seems likely that the wastefield associated with this discharge will generally form at some depth above the edges of the canyon and below the thermocline (when it is present).

The discharge of wastewater from both the 5-mile and the 7-mile outfalls have been significant sources of organically enriched particulate material in the inner portion of Santa Monica Bay. In 1987 (the last year of the 7-mile outfall), the mass emissions of total solids from the 7-mile outfall was 59,200 metric tons per year, while the mass emissions of suspended solids from the 5-mile outfall was 30,000 metric tons per year.

The ultimate fate of these particles, and their associated trace constituents, depends on their rate of sedimentation from the water column, the extent of subsequent resuspension, transport, dispersion, and redeposition.

The fates of the organic material and trace constituents are also affected by the uptake and modification by biota, "decay" associated with bacteria and the mobilization of the trace constituents to the water column (or scavenging from the water column). After formation of the wastefield, effluent particles will begin to settle from the wastefield to the ocean bottom. The distribution of these particles, and their rate of sedimentation will depend on the properties of the ocean currents, the particle settling speeds, and the extent of particle changes due to microbial activity or uptake by the biota.

We can get some idea of the likely distribution of the sedimenting particles from the current measurements made during this study. Currents at water depths of 40-68 m in the vicinity of Santa Monica Canyon have properties and movements that are similar to those on the shelf in the interior of Santa Monica Bay. The net movement of the water at this depth in the vicinity of the head of the canyon has both an on-shore component (avg: 2.2 cm/sec) and a down-coast component (avg: 0.8 cm/sec). The variations in these currents are significantly greater than their net speeds. The median current speed is about 12 cm/sec. The temporal properties of the variations depend on the direction of the flow. Variations that are roughly shore parallel are characterized by longer time-scales (i.e. more slowly varying) than variations in the cross-shore direction. More than one-half the energy in the shore parallel fluctuations is associated with time-scales longer than the diurnal tide (i.e. one day).

Within the canyon, at elevations of 2-10 m above the bottom, the properties of the currents are strongly modified by the presence of the canyon. The dominant axis of the fluctuations in the currents is along the axis of the canyon. Variations of semi-diurnal tidal periodicity (and harmonics of this frequency) dominate this flow. Fluctuations with periods longer than the diurnal tidal period account for less than 10% of the energy in this flow. Fluctuations in the cross-canyon direction are predominantly associated with frequencies higher (periodicities shorter) than the semi-diurnal tidal period and its first harmonic (6.2-hour period). In contrast to the along-canyon flows, the latter only make minor contributions to the total energy of this flow. Median speeds for the canyon flows are 8 cm/sec at elevations of 10 and 2 m above the bottom. These median speeds are about two-thirds the mid-water median speed measured above the canyon. However, the canyon currents are much more likely to have extremely high speed currents. For example, the 95-percentile speed for the mid-water (40-68 m depth) currents is about 26 cm/sec, but it is 50 cm/sec for the currents within the canyon at an elevation of 2 m. The currents at an elevation of 10 m are only slightly weaker.

Based on these characteristics, particles initially within the wastefield from the 7-mile outfall can be expected to be carried in-shore and up- and down-coast from the terminus of the outfall (with a net down-coast bias) by the mid-water currents. We will show later that because of the high concentration of solids in the effluent from the 7-mile outfall, some of the particles may have sufficiently high settling speeds so that they were not carried above the canyon during the initial dilution process. These particles would be expected to be dispersed up- and down-canyon from the discharge point, with a net down-canyon bias.

Because the amplitudes of the tidal fluctuations are generally large, some of the particulate material within the canyon may have been carried up over the head of the canyon and dispersed over the adjacent shelf area. Particles from the 5-mile outfall can be expected to be carried both up- and down-coast (again with a net down-coast bias) and on-shore during their initial sedimentation from the wastefield.

The mass emissions of (total) solids from the 7-mile outfall was significantly greater than the mass emissions of (suspended) solids from the 5-mile outfall (e.g. 70,200 metric tons versus 41,700 metric tons for the 7-mile and 5-mile discharges, respectively in 1986). Nevertheless, the sedimentation of particles on the bottom from the 7-mile outfall, compared with that from the 5-mile, is likely to have been even more substantial than indicated by the mass emission rates alone.

Studies of the aggregation of cohesive particles indicate that deposition rate of these particles on the bottom is strongly dependent on the concentration of suspended solids within the wastefield. Farley and Castro (1990) used numerical models to simulate the aggregation of particles under conditions similar to those associated with the discharge of municipal wastewaters from ocean outfalls. The studies were carried out for wastefield thickness of 1 and 10 m. Hendricks (1990) combined the results of the Farley and Castro studies with the assumption of a power-law dependence of the processes on the thickness of the wastefield. With this generalization of the Farley and Castro results, the mass rate of sedimentation of particles out of the wastefield is related to the thickness of the wastefield and the concentration of particles within it by the equation:

$$J_w(H,C) = 0.16H^{1.23}C^{2.3} + 0.174H^{0.33}C^{1.3}$$

where:

	H	=	wastefield thickness (m)
	C	=	concentration of suspended solids (mg/l)
	J_w	=	flux rate of particles leaving the wastefield (gm/m^2/day)
	W_s	=	settling speed of the particles (cm/sec)

Farley and Castro also measured the settling speed of the particles leaving the wastefield. The assumption of a power law dependence for the settling speed on the wastefield thickness results in the equation:

$$W_s(H,C) = 0.0001\ (2.57H^{1.74}C^{1.78} + 0.22H^{0.46}C^{0.36})$$

We can get some idea of the potential significance of aggregation processes on the deposition of particles in the 7-mile effluent by calculating estimates of the flux rate and settling speeds of these particles following discharge.

During the hydrocast surveys, we found evidence of the wastefield from the 5-mile outfall during one of the cruises, and estimated that the average initial dilution was on the order of 235:1. The range of initial dilutions associated with the discharge from the 7-mile outfall were probably no greater than those associated with the 5-mile outfall--and may have been less because of the single port discharge (versus the multiport diffuser on the 5-mile outfall).

In 1987, the concentration of (suspended) solids in the 5-mile effluent was 58 mg/l; in the 7-mile effluent, the concentration of (total) solids was 12,600 mg/l. Assuming an average initial dilution of 235:1, the concentration of solids in the two wastefields were on the order of 0.25 mg/l and 54 mg/l, respectively.

The concentration of solids in the aggregation equations is the combined concentration of effluent and natural particles. For the purposes of calculation, we assume that the concentration of natural particles entrained into the wastefield during the initial dilution process was 0.15 mg/l. We also assume that the thickness of the wastefield is on the order of 20 m, as suggested by the hydrographic data. With these assumptions, the mass flux rate of particles from the wastefield, and their settling speed, for the discharge from the 5-mile outfall are expected to be on the order of:

$$J_w = 1\ gm/m^2/day \qquad W_s = 0.01\ cm/sec$$

With the same assumptions for the wastefield associated with the 7-mile outfall, the flux of aggregated particles from the wastefield, and their settling speed, would be:

$$J_w = 60{,}000\ gm/m^2/day \qquad W_s = 56\ cm/sec$$

Thus aggregation dynamics would indicate that the flux of particles settling from the wastefield associated with the 7-mile outfall was about 60,000 times greater than the sedimentation flux of particles from the wastefield associated with the 5-mile outfall. Similarly, the settling speed of the particles leaving the wastefield from the 7-mile outfall is estimated to be about 6,000 times greater than those settling from the wastefield from the 5-mile outfall. In reality, of course, neither the flux rate nor the settling speed for particles from the 7-mile outfall would be as large as estimated from these equations since turbulent shear would break up the aggregated particles before they reach the size required to produce this rate and speed. Nevertheless, it appears likely that the sedimentation of effluent particles to the ocean bottom from the 7-mile outfall discharge was likely to dominate deposition in the vicinity of the two outfalls to a far greater extent than suggested by the simple 2:1 ratio of their mass emission rates.

Based on these considerations, it would appear that the sedimentation of wastewater particles from the overlying water column should have undergone a substantial reduction following termination of the discharge from the 7-mile outfall. Therefore, it is interesting to note that this termination was not accompanied by an immediate and significant reduction in the fluxes of material into the sediment traps. This lack of an abrupt change in sedimentation rate suggests that either: (a) particulates discharged from the 7-mile outfall did not settle in the vicinity of the sediment trap moorings or, (b) there are significant other sources for material collected by the sediment traps. The first of these hypotheses seems unlikely, given the changes in the biota and sediment composition that are observed at these locations (see sections on Biology).

The most obvious candidate source is the resuspension and redeposition of particle from the bottom. This process is also suggested by the change in the flux into the traps with increasing distance above the bottom.

If resuspension is the source of much of the material in the traps, then termination of the discharge from the 7-mile outfall may only have a delayed effect on the flux rate of material into the sediment traps, and the composition of these particles. Following termination of the discharge, there will still be a reservoir of wastewater material in the sediments around the discharge(s) that can be resuspended and redeposited into the traps. Thus changes in the fluxes into the traps, and the composition of those particles, may only undergo slow changes until: (a) all the wastewater material has been resuspended and transported out of the area (or dispersed and reduced to much lower concentrations), (b) consolidation and bonding of the surface sediments has occurred so that they become resistant to resuspension, or (c) they are buried by the continued sedimentation of natural particulate material.

Moorings containing near-bottom sediment traps were deployed within the canyon and on the adjacent shelf. Depositional fluxes of material into the traps were on the order of 3000-5000 $mg/cm^2/yr$ during most of the four years of observations, but declined precipitously during the last deployment of the study period. Depositional fluxes into the traps declined exponentially with elevation above the bottom. The "characteristic thickness" of the depositional near-bottom layer (i.e. where the flux declined to 1/e of the value at the sea-bottom interface) was about 15 m in the canyon, but only about 2 m on the shelf. This difference is consistent with the properties of the currents within the canyon, compared with those on the shelf.

The sediment trap data indicates that resuspension probably occurs on the shelf and within the canyon. Measurements of the near-bottom currents on the shelf in this area at an elevation of 2 m above the bottom indicates that resuspended particles will be carried off-shore, while undergoing up- and down-coast transport. It can be expected that Santa Monica Canyon will act as an interceptor for some of these particles. Particles settling from the water column into the canyon, or particles resuspended from the shelf and slope and carried into the canyon by the near-bottom flows have a high probability of being resuspended by the strong peak currents that exist on the canyon axis. The net transport of these particles at the location of the current meter mooring will be down-canyon, but with up- and down-canyon dispersion associated with fluctuations in the currents. Since current measurements were only made at a single location within the canyon, we cannot determine how far this down-canyon motion extends along the canyon.

The data we have collected is consistent with the hypothesis of a sediment reservoir of wastewater particles. If that is the case, then the reduction in the deposition rate of particulate material into the traps during the last deployment period of the study might signal the approach of the period of the domination of the resuspension of particles from the 7-mile outfall. However, with only the last sample indicating such a significant reduction, it is not possible to distinguish this possibility from the effects of natural variability in the ocean environment without additional data.

Somewhat more perplexing is the rather steady downward trend in the organic material collected in the traps. Concentrations of particulates collected within the canyon declined steadily during the study both near the bottom (1 m elevation) and in the water column (60 m elevation).

Overall, the rate of reduction was faster near the bottom, so that the ratio of the concentration of organic material near the bottom, relative to that at an elevation of 60 m, tended to increase during the study. Although the concentration of organic material collected by the sediment traps deployed on the shelf also tended to decline during the course of the study, the trend was not as strong as at the canyon locations. We cannot explain these trends. However, it should be noted that there were reductions in the total mass emissions of wastewater particulates from the two outfalls prior to termination of the 7-mile discharge. For example, the emissions of total suspended solids from the 5-mile outfall were almost 40% higher in 1986 (41,700 metric tons) than in 1987 (30,000 metric tons).

B. Sediment Characteristics

1. Conditions under full sludge discharge.

a. Deep sediment cores. Only three exploratory cores were collected in October 1986 prior to sludge discharge termination. These cores showed that the sludge field was 50 cm deep at Station HR50 and over 100 cm deep at Station HR7. Samples collected in 1974 showed a sludge depth of approximately 25 cm. (Mitchell and Schafer 1975).

b. Sediment grain-size and organic content. The most obvious aspect of the sediments in the Santa Monica Canyon under full sludge discharge was the black color and extremely high dissolved sulfide content. Visually, there was little evidence of inorganic sediment (sand and silt), rather it appeared as a thick, black paste.

By weight, the sludge field sediment was composed mostly of sandy-silt, with clay and organic material contributing lesser fractions (Table 12). In comparison, the sediment at the reference sites was mostly silty-sand with much lower clay and organic fractions than in the sludge field.

Imposed on these differences are natural differences in sediment grain-sizes and organic material at different depths (Figures 37-40). Sediments become finer with more organic material in deeper water. There were significant differences in sediment grain-size and organic material parameters between the 100 and 200 m sites (ANOVA, $p < .05$).

The initial location for Station HR6 was in an area with considerable rock and cobble. During the second cruise (August 1986) that station location was moved approximately 100 m to the west where more typical shelf sediments were collected. Additionally, one of the 100 m transition sites (Station HR3) contained more coarse sand and shell debris than the other sites.

The sludge field contained very high concentrations of organic carbon and nitrogen (Figures 41 and 42). Over 11% of the sediment at Stations HR50 and 51 were organic carbon, and over 1% was nitrogen. Organic material was also elevated at contaminated sites adjacent to the sludge field.

The ratio of organic carbon to nitrogen (C:N) in marine sediments is a good indicator of the quality of the organic material. Higher values indicate more refractory, or non-bioactive sediments and lower values indicate more labile sediments. Values in marine sediments are usually near 10 (Emery 1960). Values at the terminus of the old outfall were less than 10 indicating higher than usual nitrogen content (Figure 43), typical of sludge.

Elevated dissolved sulfide concentrations in the sludge field were a direct result of the high organic content of the sludge (Figure 44). Values as high as 489 mg l^{-1} were measured at Station HR51. Sulfides were also elevated in sediment at the contaminated sites near the canyon.

c. Sediment contamination. A total of 35 contaminant compounds were measured in sediments. They are listed in Appendix 4. For this report, we present results for major groups of trace organic compounds: PCBs, DDTs, and PAHs, and four individual trace metals: Ag, Cd, Cu, Zn.

In general, contaminant distributions resulting from sludge discharge were highest in the sludge field at the head of the Santa Monica Canyon nearest the outfall (Stations HR50 and 51) and decreased in concentration farther from the outfall (Figures 44-51). There were order-of-magnitude increases in sulfides, PCBs and PAHs in the sludge field. The 200 m contaminated sites had generally lower concentrations than the 100 m sites, particularly in sulfides which were near reference levels at those sites. These concentric patterns of contaminant distributions are typical of point source discharges.

PCBs were highest at a slightly deeper canyon Station 52 and DDTs were highest at the deepest sites, $\geq$200 m. Hyperion's sludge did not contain high concentrations of DDTs and this anomalous pattern is probably due to transport of DDTs from the Palos Verdes Peninsula.

Contaminant concentrations at the reference sites are all higher than those reported for other, more distant, reference sites (Thompson *et al.* 1987); Ag, PCBs, and PAHs are an order-of-magnitude higher. Although the Santa Monica Bay reference values are higher than normal, the Santa Monica Bay benthic assemblages are very similar to other reference areas. Therefore, it is assumed that recovery of sediments to the Santa Monica Bay levels will also produce reference benthic assemblages.

Figure 37 Distributions of sediment parameters under full sludge discharge. Numbers are means of each parameter, at each station, from three pre-termination cruises (Figures 37-51).

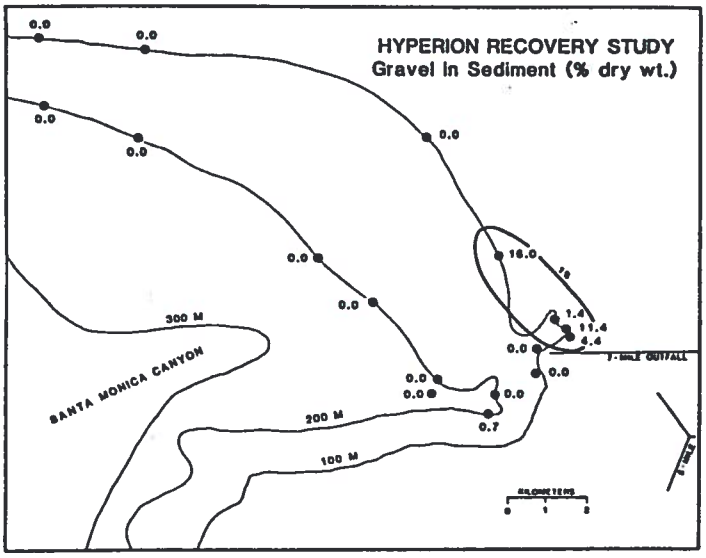

Figure 38

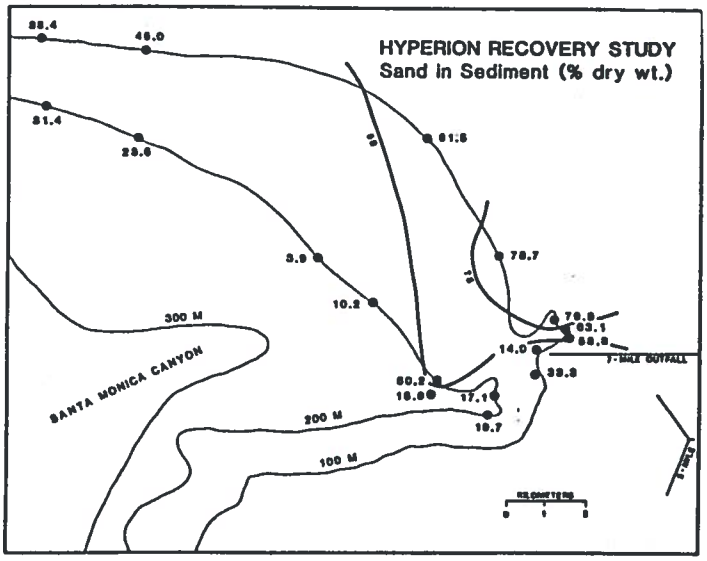

Figure 39

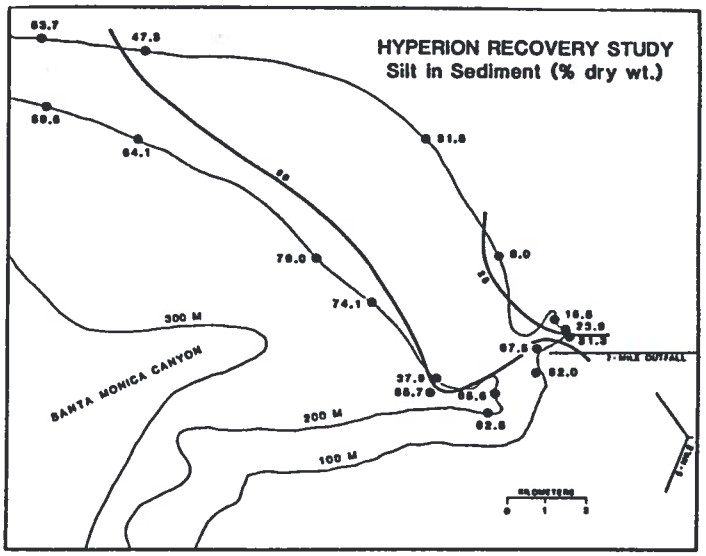

Figure 40

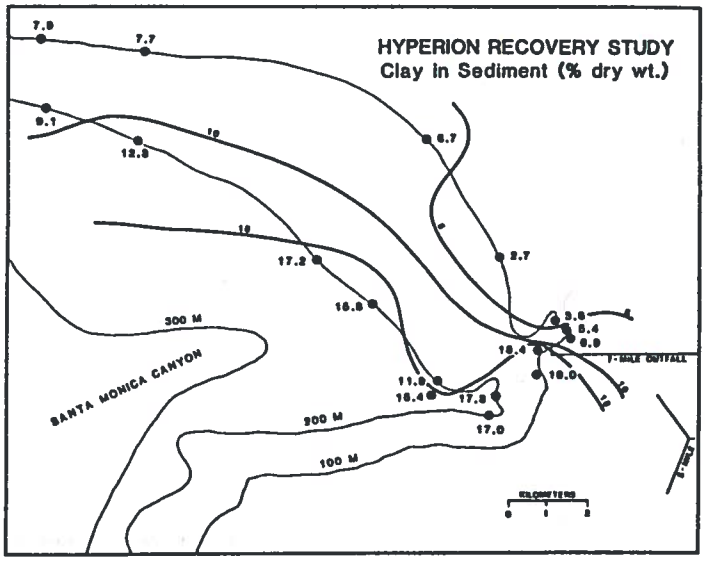

Figure 41

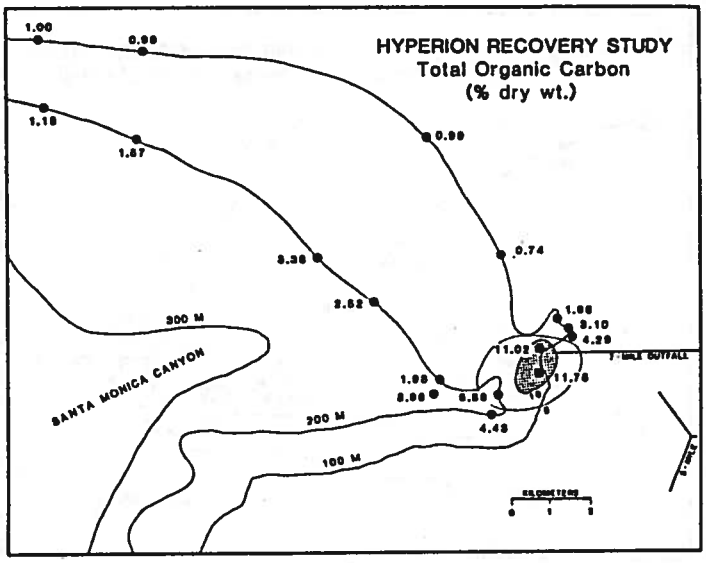

Figure 42

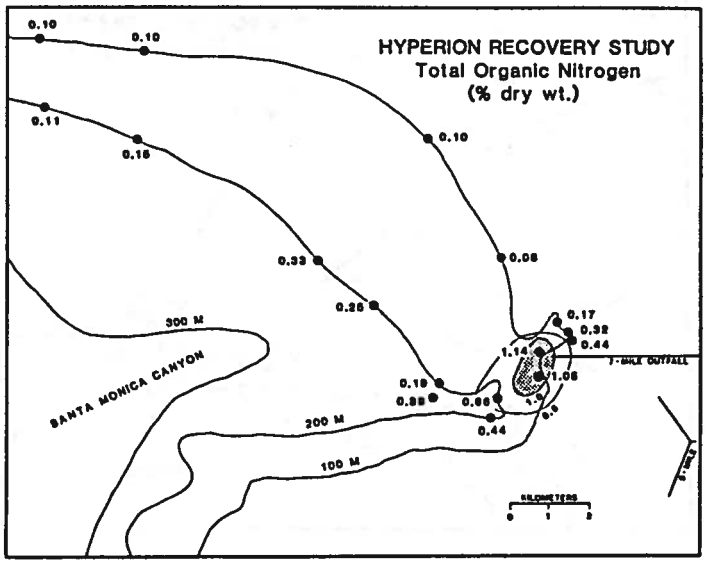

Figure 43

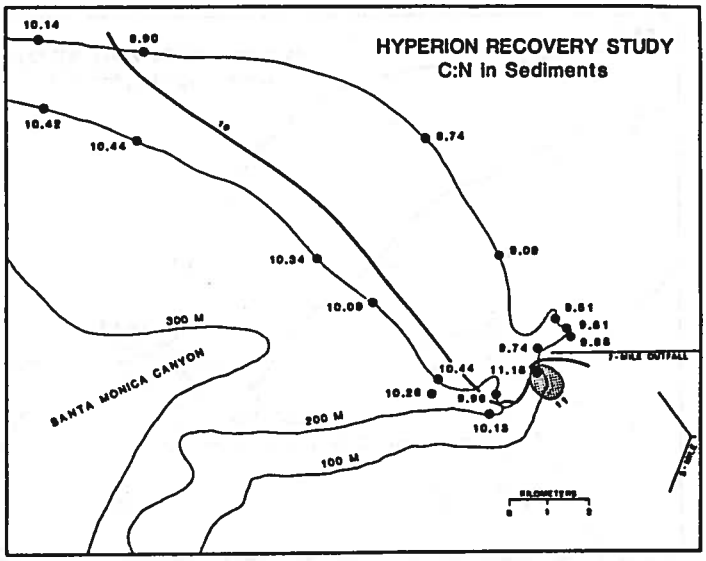

Figure 44

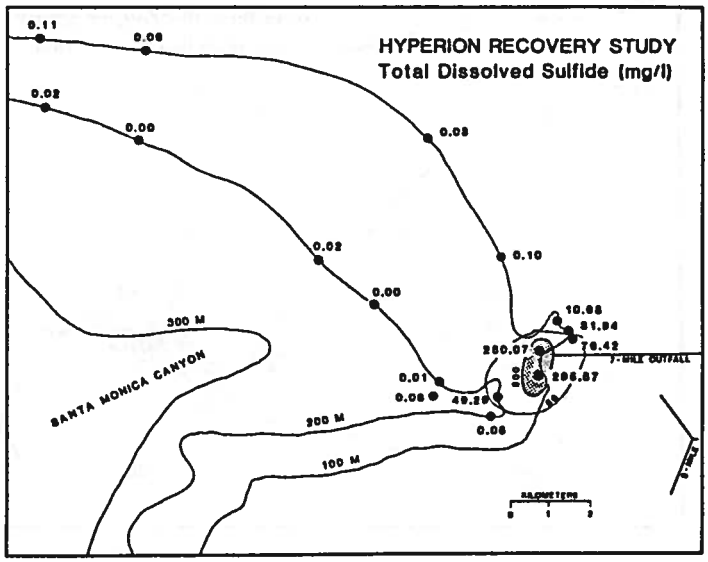

Figure 45

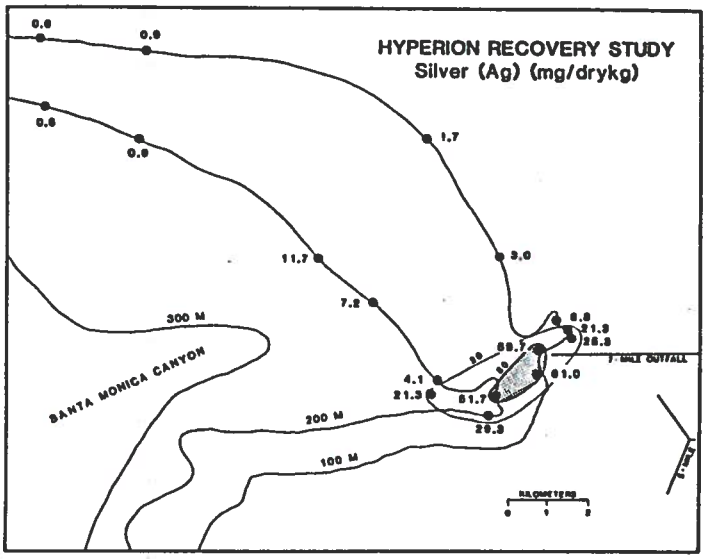

Figure 46

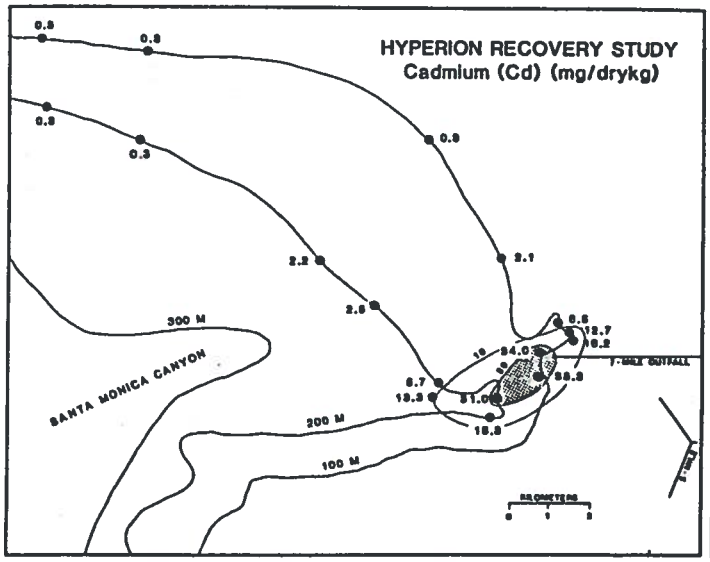

Figure 47

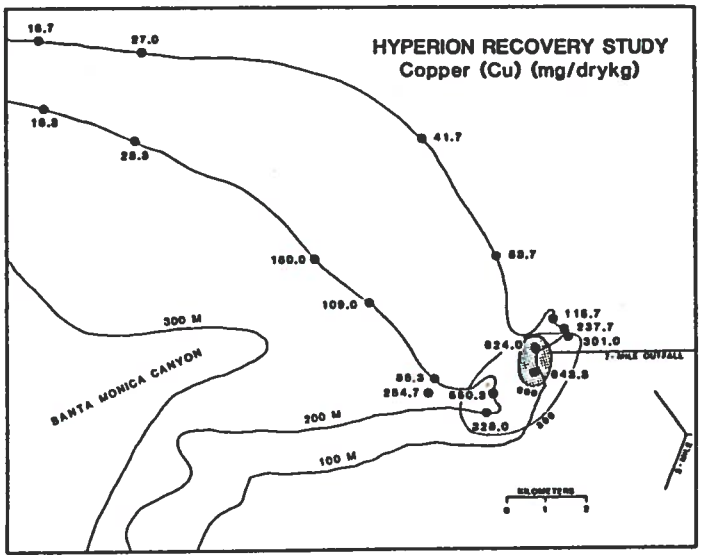

Figure 48

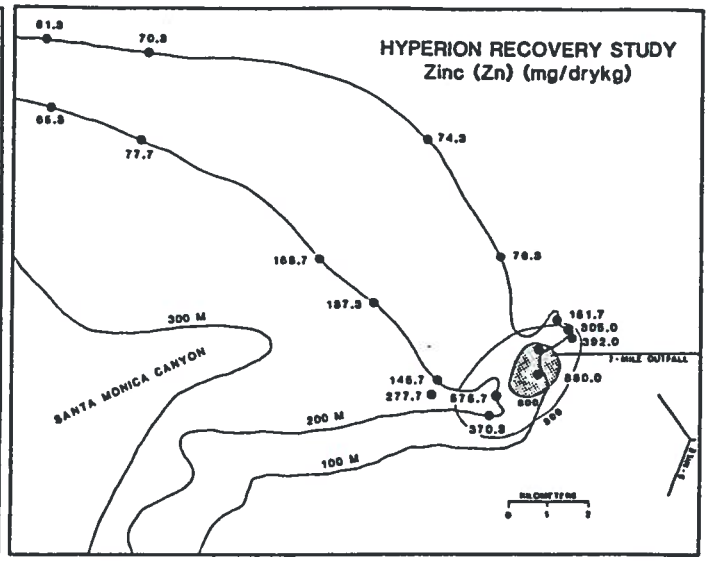

Figure 49

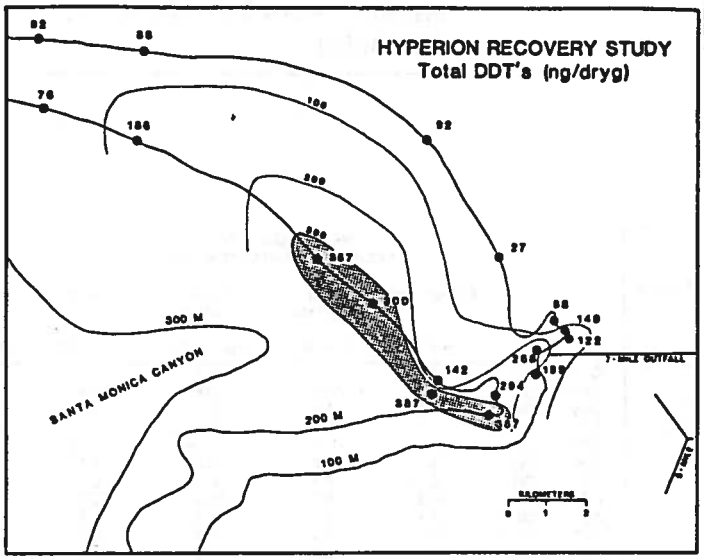

Figure 51

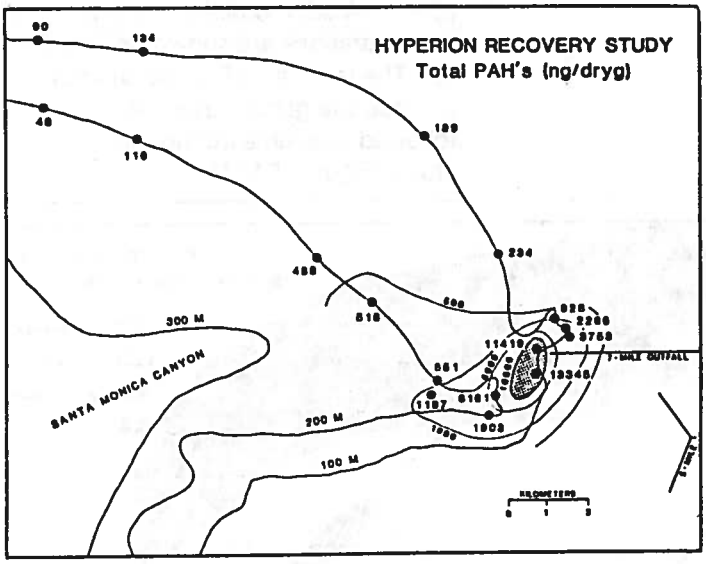

Figure 50

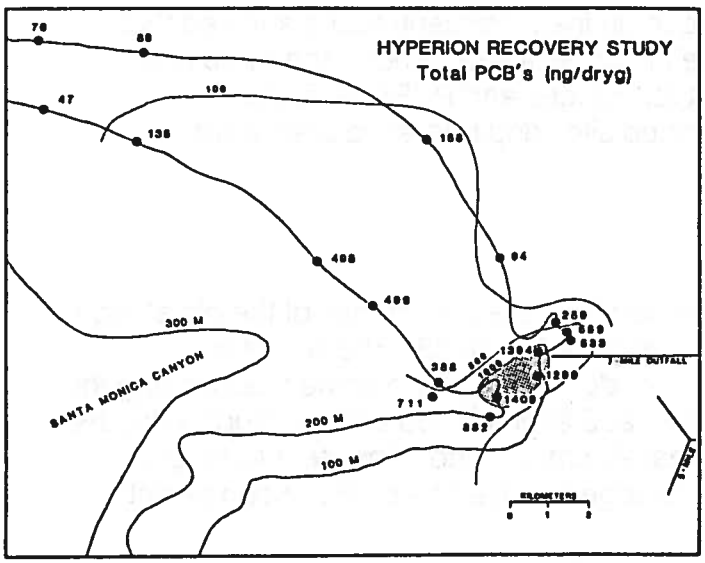

Taken all together, the sediment organic material and contaminant concentrations existed in recognizable zones (Figure 52). Cluster analysis of nine parameters (Table 12) showed four groups of sites with similar concentrations.

This analysis identified patterns similar to those shown in the contour plots of individual sediment parameters (Figures 37-51). The sludge field (Stations HR50, 51, and 52) contained the highest concentrations of most contaminants, and the reference sites had the lowest concentrations. Six sites were identified as reference stations (HR3, 4, 5, 6, 11, and 12) as they had similar concentrations of contaminants. This group included sites at both 100 and 200 m.

Figure 52 Sites with similar sediment contaminant concentrations formed four zones with similar concentrations from full sludge discharge. The groupings were based on cluster analysis of three pre-termination cruises, average concentrations are shown on Table 12. The recovery of the sediments in these site groupings were followed over time during this study (Figures 54-68).

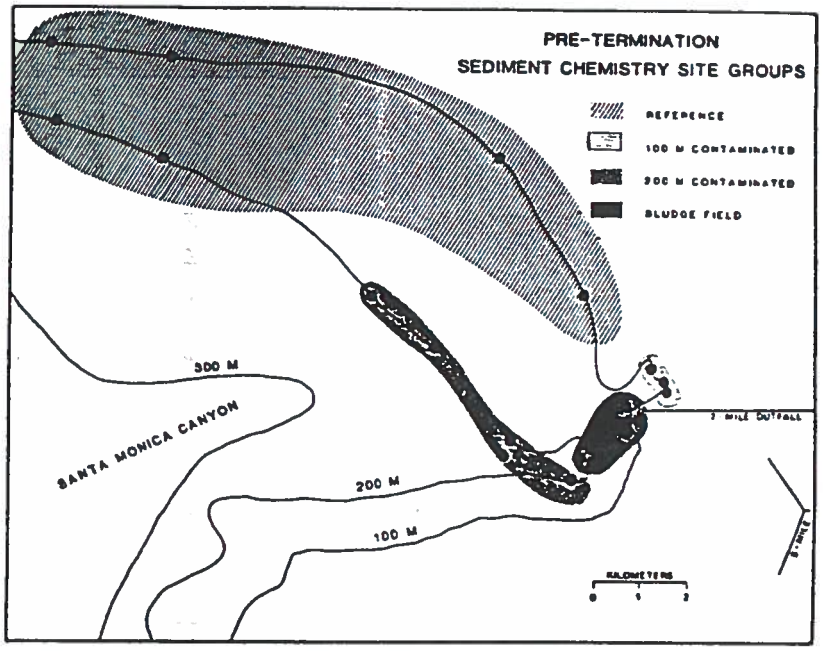

Table 12 Averages of sediment parameters measured in each zone of impact during full sludge discharge (three pre-termination cruises). Zones of impact were identified by cluster analysis (Figure 52). Average reference values from Thompson *et al.* (1987).

PRE-TERMINATION SEDIMENT CHARACTERISTICS

		Sludge field (n = 9)	100 m Contamin. (n = 9)	200 m Contamin. (n = 15)	Reference (n = 18)	1985 Ref. Survey 150 m
Gravel	(%)	0.0	5.7	0.1	2.7	-
Sand	(%)	21.5	67.2	20.6	46.4	37.2
Clay	(%)	17.2	5.4	15.4	7.7	13.0
Silt	(%)	61.7	23.6	63.9	44.1	49.8
Sulfide*	mg/l	198.3	39.7	0.04	0.05	-
TOC*	(%)	9.8	3.0	3.3	1.1	0.85
TON	(%)	0.95	0.31	0.32	0.11	-
C:N*		10.3	9.7	10.3	10.0	-
Ag*	(ppm)	57.4	18.5	14.7	1.3	0.04
Cd*	(ppm)	34.4	11.8	8.4	0.6	0.2
Cu*	(ppm)	605.9	218.1	185.6	31.3	13.1
Zn*	(ppm)	736.2	282.9	217.9	70.9	52.3
PAHs*	(ppb)	10467.0	2316.0	960.0	134.0	37.0
DDTs*	(ppb)	254.0	110.0	305.0	95.0	30.0
PCBs*	(ppb)	1367.0	460.0	602.0	103.0	23.0

* = Used in cluster analysis

Analysis of variance of individual contaminant concentrations showed that there was no significant difference in concentration among the three pre-termination times sampled except for sulfides and PCBs, and that the differences between the contaminated sites and reference sites were statistically significant ($\alpha < 0.05$).

2. Recovery of sediments

a. Deep Sediment Cores. The approximate boundaries of the old sludge field between 1988 and 1990 are shown on Figure 53. There was a considerable amount of variation in sludge depth at the same sites among the four sampling periods. For example, at Stations HR50 and 51, sludge depths ranged from over 100 cm to less that 20 cm, with no consistent temporal trends. Sites near the edge of the sludge field had much more consistent depths over time.

Figure 53 Approximate boundary of the sludge field between 1988 and 1990. Contours show approximate depth of sludge deposits overlaying natural sediment in the Santa Monica Canyon.

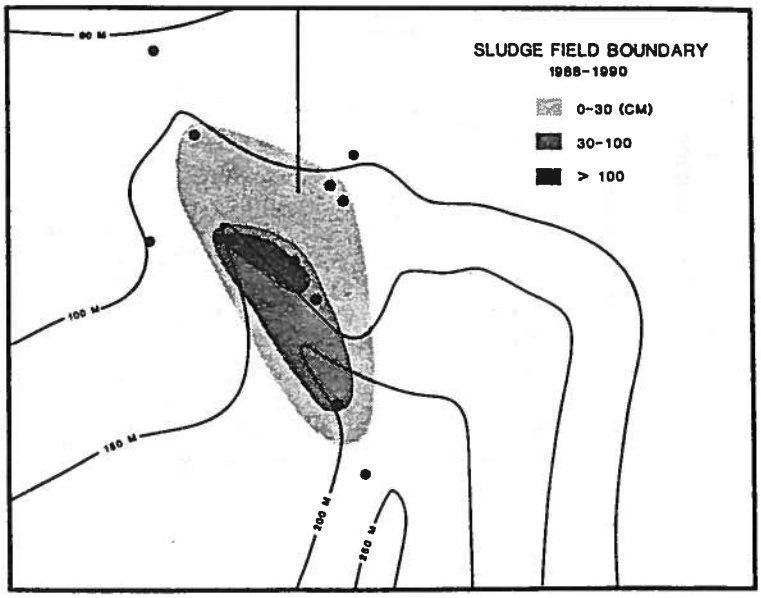

It is presumed that the variation we measured was due to small scale physical features in the floor of Santa Monica Canyon. The corer would land in a depression fill with sludge one time, then land on a ridge and collect much less sludge the next time.

During the last three sampling periods a thin veneer (~1 cm) of lighter colored sediment was observed on the surface of the cores indicating cleaner sediment was being deposited there, presumably from the adjacent Santa Monica Bay shelf. However, below that layer, at Stations HR50 and 51 there remains a large reservoir of sludge with elevated contaminant levels.

b. Sediment Contaminants. All of the contaminant concentrations have decreased in the sludge field except DDT which has increased. Despite these decreases, recovery of the sludge field has not yet occurred. Even after three years, there are still elevated concentrations of organic material, sulfide, and contaminants there.

One unexpected result was changes in sediment grain-sizes. The percentages of sand increased and clay decreased in the sludge field (Figures 54-57). This probably represents dilution of the sludge by sediments that have been entrained into the canyon from the adjacent shelf.

Organic material has also decreased in the sludge field. Carbon has decreased by 23% and nitrogen by 29% (Figures 58 and 59). Nitrogen has decreased at a faster rate than carbon as it is more biologically useful, consequently the C:N ratio has increased (Figure 60).

Sulfides decreased dramatically nine months after discharge termination. One year following discharge termination sulfide levels were very near reference levels. Sulfide concentrations have remained elevated in the sludge field probably because the sludge layer was so thick, temperature and pressure has not allowed diffusion and oxidation to occur.

Trace metals in the sediments have decreased by approximately 55% in the sludge field (Figures 62-65). All metals have decreased by about the same amount there, but they have not decreased significantly in the other adjacent contaminated sites. Trace metals concentrations in the sludge field measured in April 1988 were much lower than before or after that time because the sample from Station HR52 was contained unusually coarse sediment (69% sand compared to about 22% usually collected there).

Consequently the sludge field average (n=3 sites) was also much lower. This heterogeneity in the sludge field demonstrates the patchy nature of the sediments there.

DDTs have not decreased in the sludge field, but they were not very high there even under full discharge (Figure 66). However, DDTs at the 200 m contaminated site have decreased considerably. PCBs have decreased by approximately 49% in the old sludge field, and have also decreased in the 100 and 200 m contaminated sites (Figure 67). PAHs have also decreased in the old sludge field (49%), but there is a considerable amount of temporal variation at these sites (Figure 68). PAHs are also still elevated at the contaminated sites.

In summary, most of the sediment contaminants have decreased in concentration since sludge discharge termination, but none has reached reference concentrations.

Figure 54 Recoverygraphs for sediment parameters:

——— Sludge field (n = 3)
----- 100 m Contaminated sites (n = 3)
-·-·- 200 m Contaminated sites (n = 5)
- - - Reference sites (n = 6)

95% Confidence intervals based on all reference site samples (n = 66). (Figures 54-68)

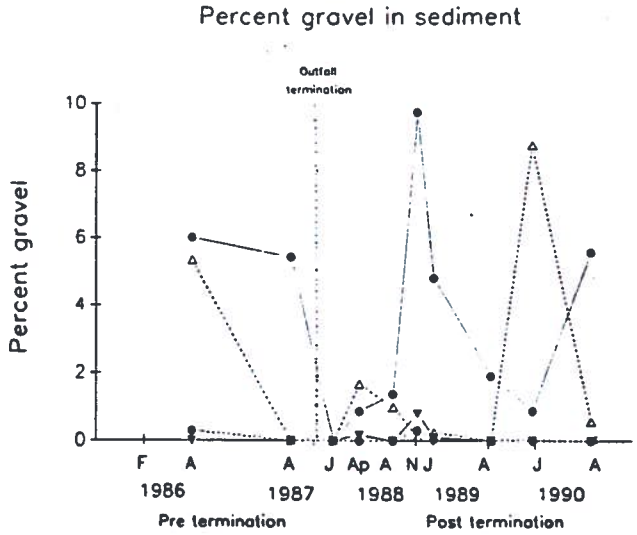

Figure 55

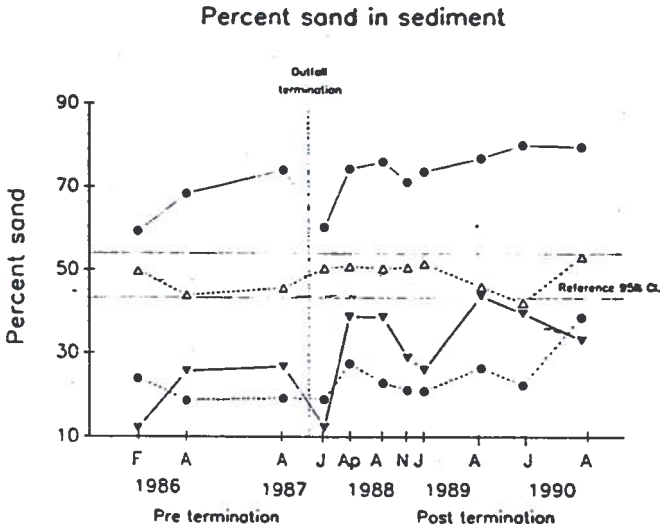

Figure 56

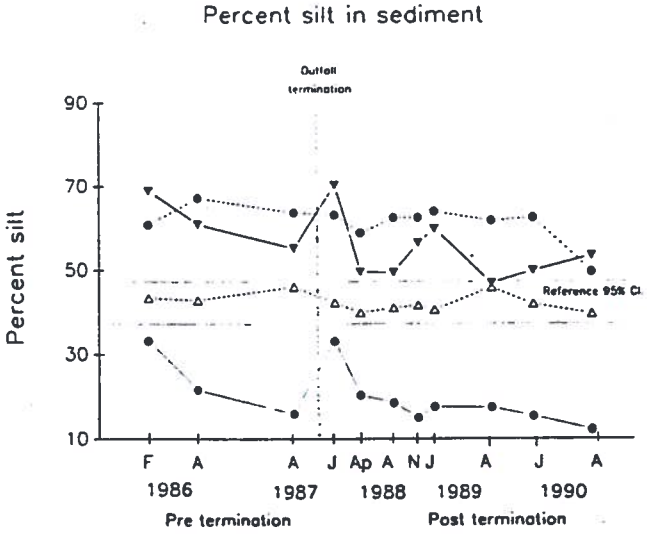

Figure 57

Percent clay in sediment

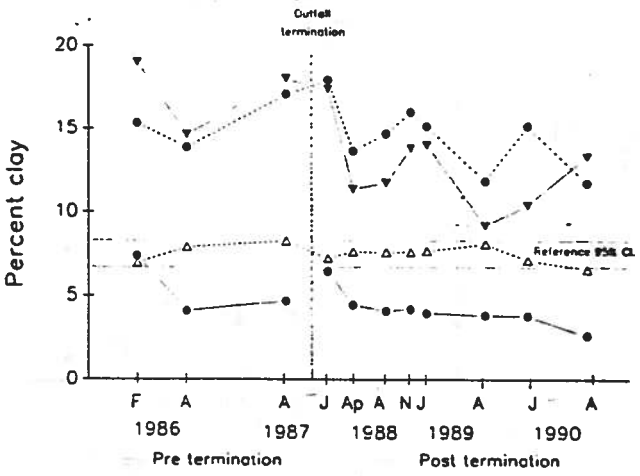

Figure 58

Total Organic Carbon

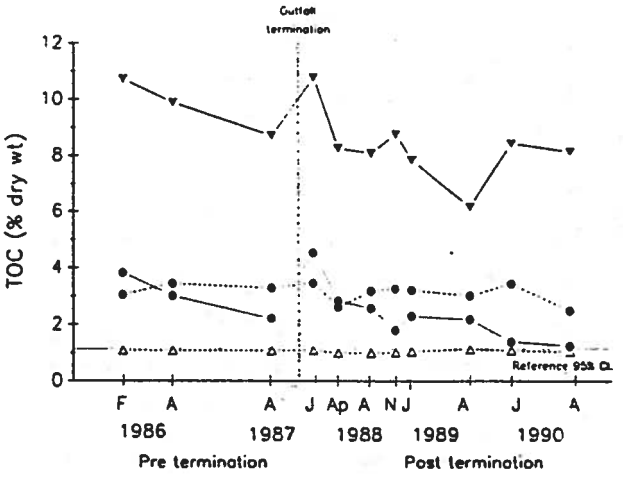

Figure 59

Total Organic Nitrogen

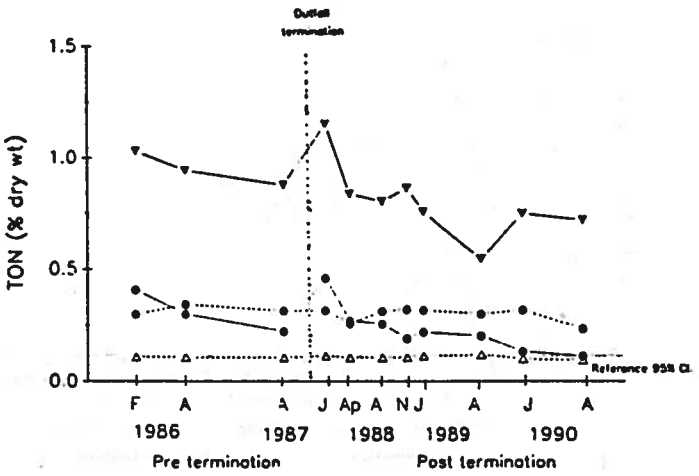

Figure 60

C:N Ratio

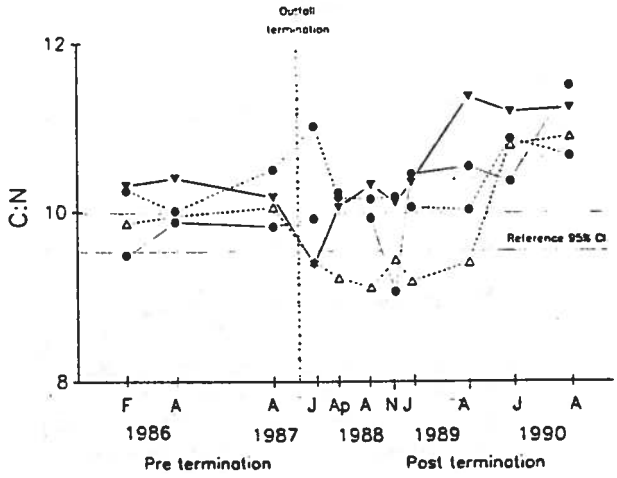

Figure 61

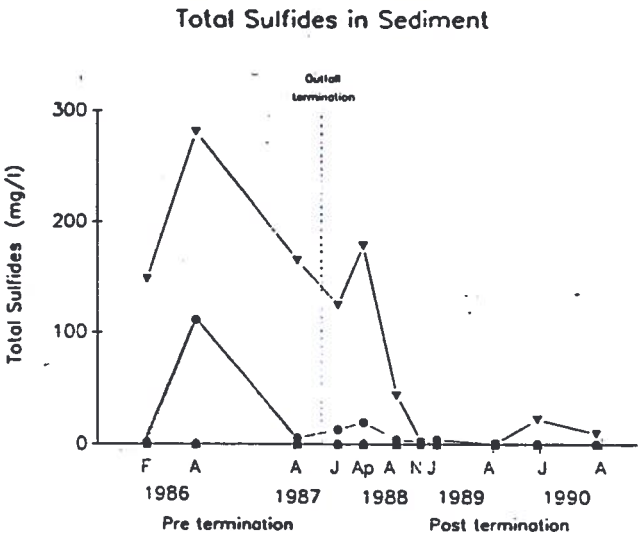

Figure 62

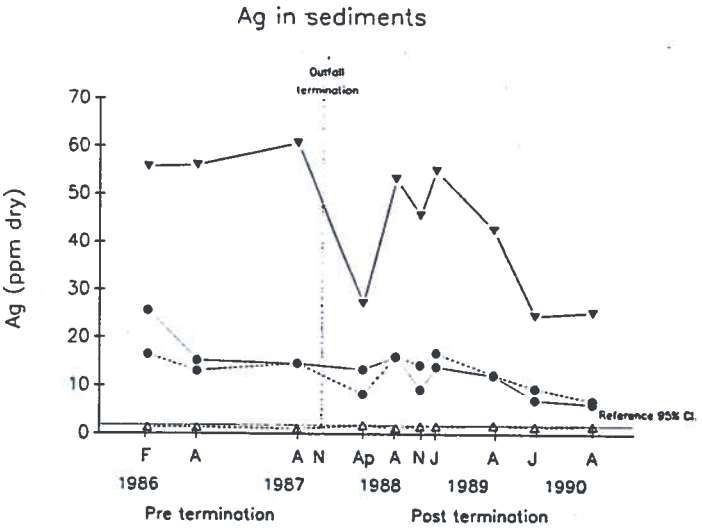

Figure 63

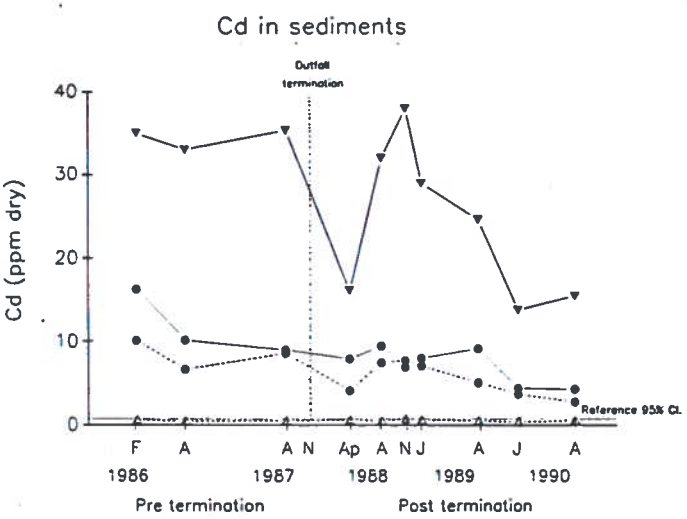

Figure 64

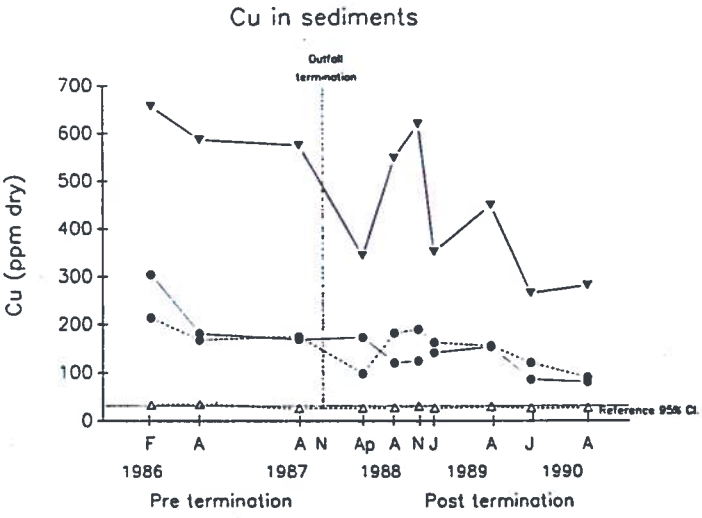

Figure 65

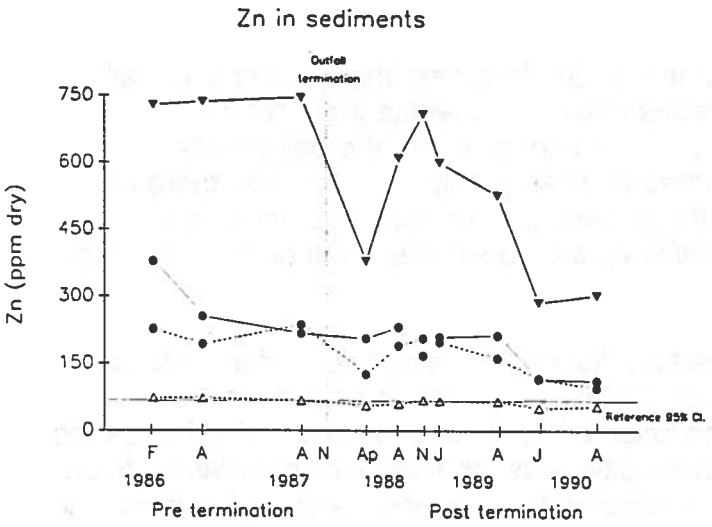

Figure 66

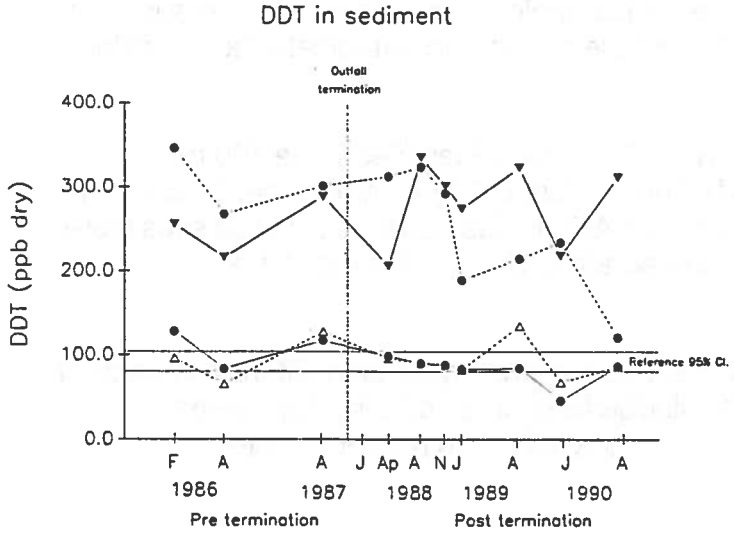

Figure 67

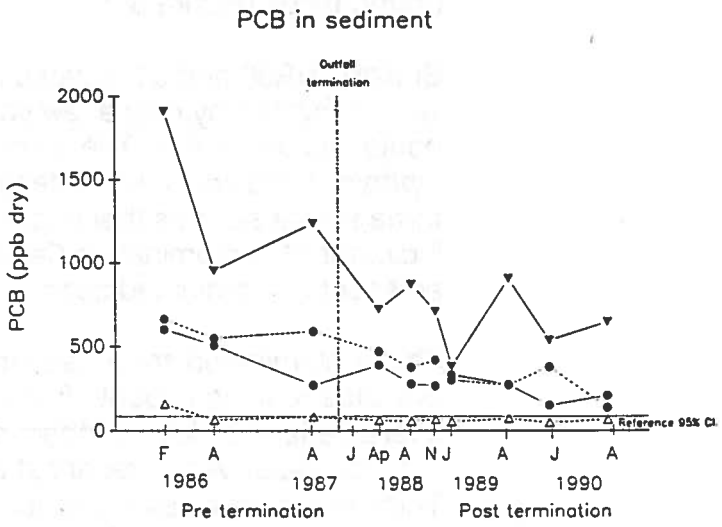

Figure 68

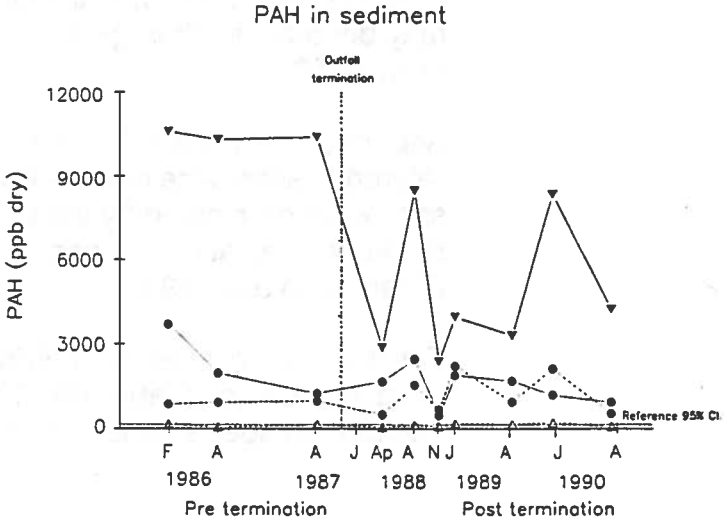

C. Biology

1 Benthic Macrofauna

a. Pre-Termination Assemblages. The benthos collected in the 1.0 mm fraction of the grab samples during full sludge discharge were classified into five groups of sites, or assemblages with different species composition and abundances (Figure 69).

Stations HR50 and 51, located in the sludge field near the end of the outfall were inhabited by only a few species that could tolerate the extreme contamination there. The most abundant species was the polychaete *Ophryotrocha sp. C,* an undescribed species (Table 13). Actually, there are three similar species that occur there. Also present was cosmopolitan indicator of contamination *Capitella capitata*, but it was most abundant in the adjacent contaminated zone.

The contaminated zone was located adjacent to the sludge field and included five sites ranging in depth from 100-200 m deep. These sites were also characterized by low numbers pollution tolerant species, except for thousands of *C. capitata*. Also present at these sites was the sludge clam *Solemya reidi*. This unusual species is especially adapted to life in areas with high sulfide levels. It utilizes an endosymbiotic bacterium which it harbors on its gill tissues, to oxidize sulfide in the sediment and provide energy to the clam. As a result these clams have evolved without a digestive tract, obtaining all of their nutrition from their symbiotic relationship (Powell and Somero 1985). However, clams were not collected in the sludge field as some component(s) of the sediments there were apparently intolerable.

The transition zone was located adjacent to the contaminated zone. Four sites ranging from 100-246 m were classified in this zone which represents a transition between the contaminated and reference sites. These sites were dominated by the clam *Parvilucina tenuisculpta*. This species may become facultatively infected with the same endosymbionts as *S. reidi*. As a result they may become much larger than those collected in uncontaminated areas (Word *et al.* 1977).

Separate reference areas at 100 and 200 m were identified. The 100 m reference sites were dominated by the ophiuroid *Amphiodia urtica*. The 200 m sites were dominated by the small clam *Axinopsida serricata*. These sites were similar to sites at other uncontaminated areas in southern California (Thompson *et al.* 1987).

The numbers of species, individuals, and biomass were also different in each of the assemblages (Table 13). The sludge field sites had very depressed numbers of species and individuals compared to the reference sites.

Figure 69 Sites with similar macrobenthic species composition and abundances formed five zones of impact, or assemblages during full sludge discharge. The recovery of the benthos at these assemblages were followed over time during this study (Figures 70-77). The groupings were based on ordination and classification analyses of the three pre-termination cruises. Average abundances of the dominant species in each assemblage are shown on Table 13.

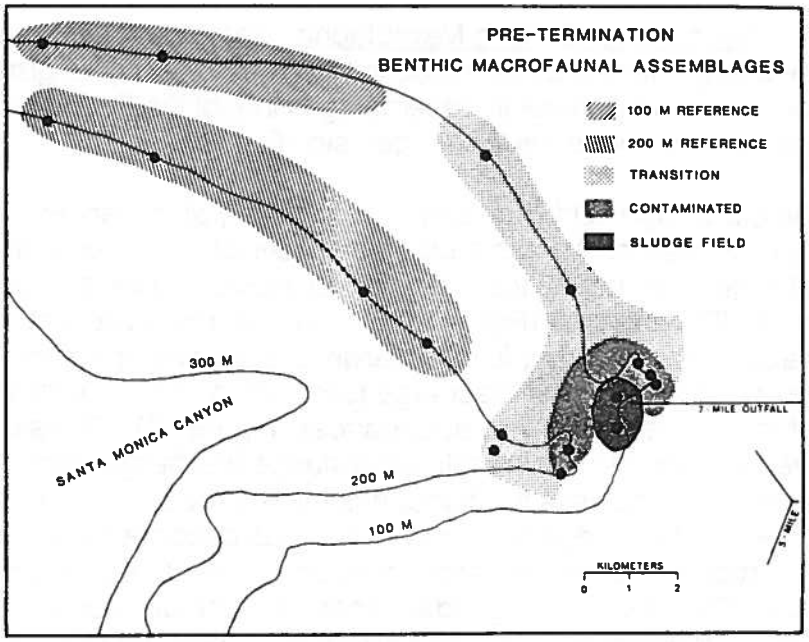

Table 13 Average abundances of the most common and abundant benthic macrofauna collected in each zone of impact, or assemblage, as identified by classification analysis; based on three pre-termination cruises.

PRE-TERMINATION
MACROFAUNAL ABUNDANCES
(Mean number/m^2)

Species	Taxon	100 m Ref. (n = 7)	Trans. (n = 13)	200 m Ref. (n = 12)	Contamin. (n = 13)	Sludge Field (n = 6)
Amphiodia urtica	e	640	3	0	5	0
Spiophanes missionensis	p	366	165	5	0	0
Mediomastus sp.	p	163	62	7	2	2
Spiophanes fimbriata	p	437	203	78	0	0
Melinna heterodonta	p	0	8	48	0	0
Axinopsida serricata	m	151	3481	309	3	0
Decamastus gracilis	p	6	847	5	0	0
Paraprionospio pinnata	p	23	93	67	4	0
Parvilucina tenuisculpta	m	76	3996	62	349	0
Tellina carpenteri	m	43	975	20	81	2
Capitella capitata	p	6	47	0	2818	28
Sigambra tentaculata	p	0	3	0	158	3
Solemya reidi	m	0	0	0	64	0
Ophryotrocha sp. B	p	0	0	0	25	8
Ophryotrocha sp. A	p	0	0	0	49	223
Ophryotrocha sp. C	p	0	0	0	81	450
Orchomene anaquela	c	0	0	0	0	8
Mean No. Species per grab		84	62	27	18	6
Mean No. Individ. per m^2		1197	12808	1026	3082	760
Mean Biomass (wet g) m^2		119	369	120	200	26

e = Echinoderm c = Crustacean p = Polychaete m = Molluscan

Biomass was highest at the transition zone sites because of the large number of *P. tenuisculpta*. Depression of these assemblage parameters is well known in contaminated areas (Pearson and Rosenberg 1978; Swartz 1986), although the exact causes of the decreases are not understood. In transition zones, these parameters may be higher than in reference areas. This is known as the intermediate disturbance effect, well known in ecological communities (Connell *et al.* 1978).

b. Recovery of Benthic Macrofauna. The most obvious biological changes since sludge discharge termination have occurred in the grab collected benthic macrofauna. In particular, assemblages inhabiting the old sludge field and contaminated zones have changed significantly.

In the old sludge field (Stations HR50 and 51) abundances of the polychaete *Ophyrotrocha sp. C.* increased by an order-of-magnitude following sludge discharge termination, then decreased again, and were nearly absent in the August 1990 samples (Figure 70). *C. capitata* was present in the sludge field in low abundances during full discharge, but became the most abundant species there within a year after discharge termination. In 1990, they had decreased in all of the zones to very low abundances (Figure 71). The sludge clam *S. reidi* moved into the old sludge following sludge discharge termination (Figure 72). They should decrease in abundance there as recovery proceeds. These changes in the sludge field show that it has become more like the pre-termination contaminated and transition zones as recovery proceeds. As of August 1990, the most abundant species in the old sludge field was the clams *Tellina carpenteri* (600 m^2) and *Axinopsida serricata* (120 m^2), a dominance pattern similar to the pre-termination transition sites.

P. tenuisculpta become less abundant in the transition sites and more abundant in the contaminated sites, than before discharge termination. This suggests that the contaminated sites are also becoming more like the transition sites as the sediments recover. Eventually, the old sludge field sites should also increase in numbers of *P. tenusiculpta* as the transition and contaminated sites decrease in abundance.

The ophiuroid *A. urtica* has not become more abundant in any of the zones (Figure 74). However, a few juveniles (about 5 per grab) have been collected in the old sludge field and contaminated sites beginning in August 1989. Abundances at the sludge field sites (depths near 150 m) should average around eight individual per grab, even when fully recovered. This species is very sensitive to contamination and its absence from even the transition sites suggests that complete recovery has not occurred. It is not known how long it will take for these species to recolonize the impacted areas.

The number of macrofaunal species per grab have increased in the old sludge field and contaminated sites by an order of magnitude (Figure 75) as of the last sampling period and were within the range of the 100-200 m reference sites. Most of the species that moved into the contaminated areas are species that inhabited the transition areas before sludge discharge termination. The number of macrofaunal individuals have also increased (Figure 76).

The large increase in the sludge field in January 1989 was due to thousands of *C. capitata* that invaded those sites. Abundances at those sites should decrease to become more like the reference sites as recovery proceeds. Biomass has also increased in the sludge field and contaminated zones (Figure 77). The contaminated sites have biomasses much like those in the transition sites because of the influx of *Parvilucina*. Biomass at all sites should decrease to reference levels as recovery proceeds.

Not only have abundances of some of the individual species changed in the impacted zones, but the entire macrobenthic assemblage has changed as well. Ordination analysis of the macrobenthic data using all of the pre- and post-termination data shows how the macrobenthic assemblages in the old sludge field and contaminated sites have changed in species composition and abundances over time. Those site groups have moved through the ordination space to positions closer to the reference site assemblages, demonstrating that those assemblages are recovering (Figure 78).

The old sludge field sites (HR 50 and 51) were located at depths of 153 and 136 m. Since there were no reference sites at these depths, it is presumed that they will eventually recover to conditions intermediate between those at the 100 and 200 m reference sites. However, as shown on Figure 78 the old sludge field sites are becoming more like the 100 m sites than the 200 m reference site. This may be due to a canyon effect. In canyons, depth ranges of benthic assemblages are often extended deeper (Hartman 1963 and Thompson *et al.* 1984).

The contaminated zone sites have also moved closer to the 100 m sites. This group included sites at 100 and 200 m depths, yet it too is moving closer to the 100 m sites than the 200 m sites. Ordination scores at the transition sites have not changed much since sludge discharge termination.

Figure 79 shows the benthic macrofaunal ordination scores plotted over time in recoverygraph format. This plot shows that the rates of recovery for each of the zones decreases farther away from the sludge field. The old sludge field has recovered the fastest so far, but the transition sites have not recovered much at all.

In summary, as of August 1990, the benthic macrofauna in the old sludge field had recovered to be like those in the contaminated and transition zones. Complete recovery to reference-like assemblages has not yet occurred. As the old sludge field becomes more like transition zone assemblages, the slower recovery will proceed. Forecasts for full recovery are considered in the Discussion and Conclusions section of this report.

Figure 70 Recoverygraphs of benthic macrofaunal indicator species and community parameters:

- ——— Sludge field (n = 2)
- ····· Contaminated (n = 5)
- ----- Transition (n = 4)
- ----- 100 m Reference (n = 2)
- ----- 200 m Reference (n = 4)

95% Confidence intervals based on all means of all 100 + 200 m reference sites (n = 66). (Figures 70-77)

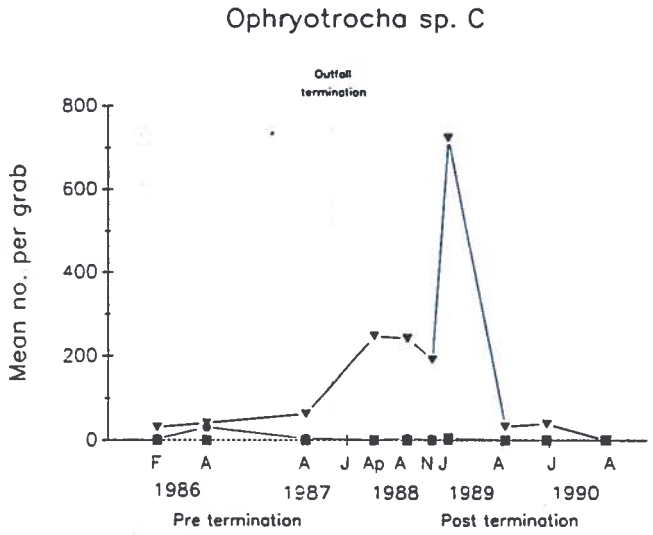

Figure 71

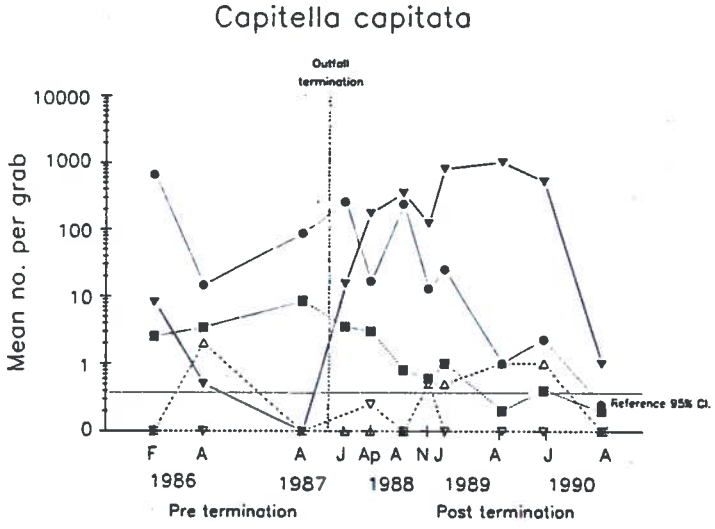

Figure 72

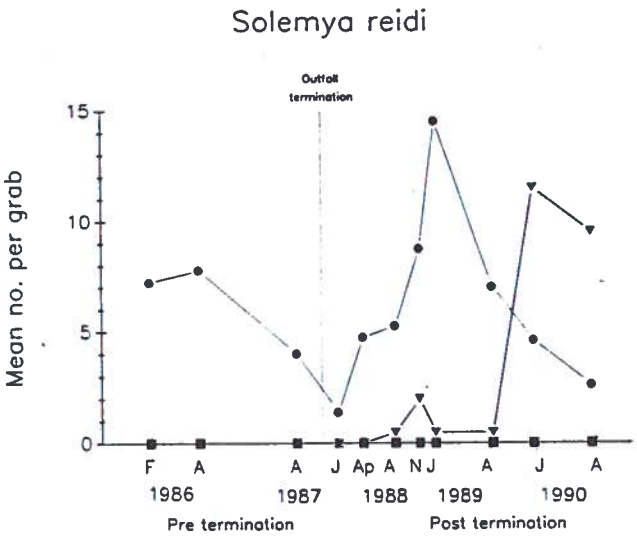

Figure 73

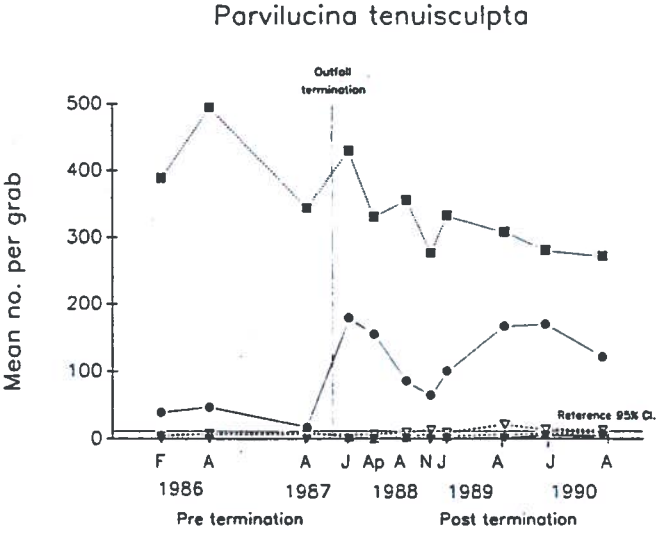

Figure 74

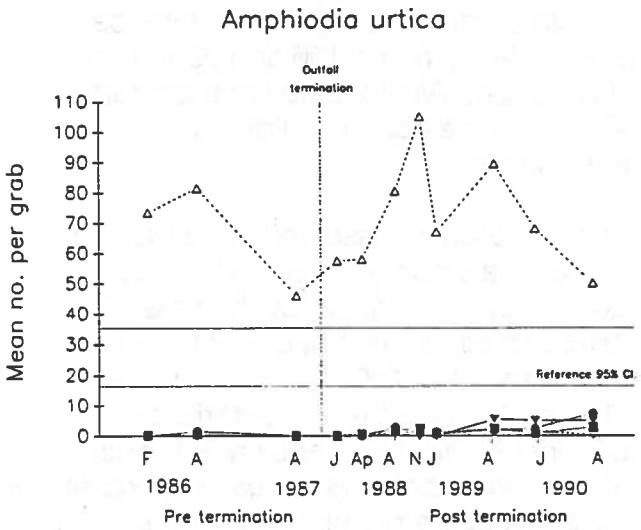

Figure 75

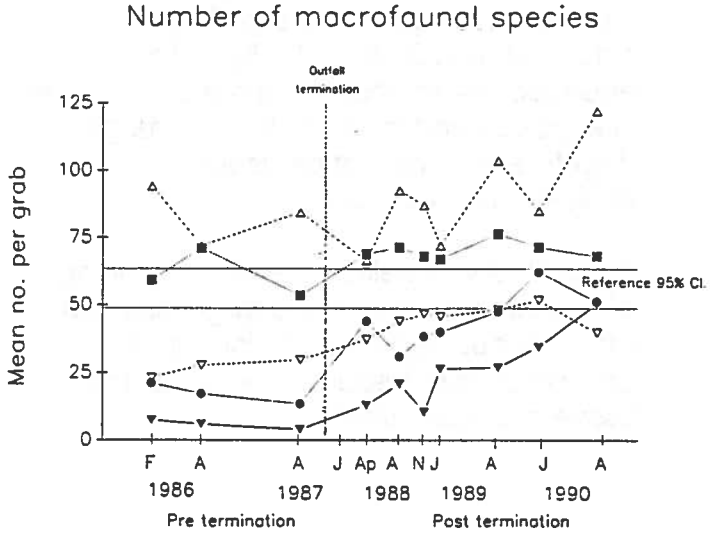

Figure 76

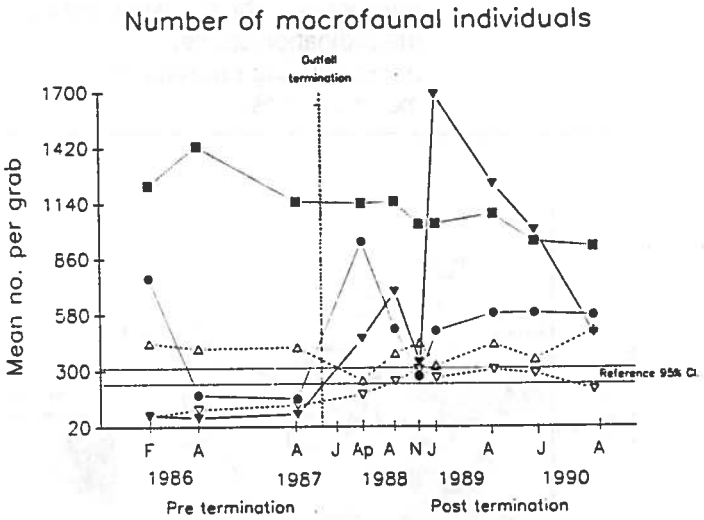

Figure 77

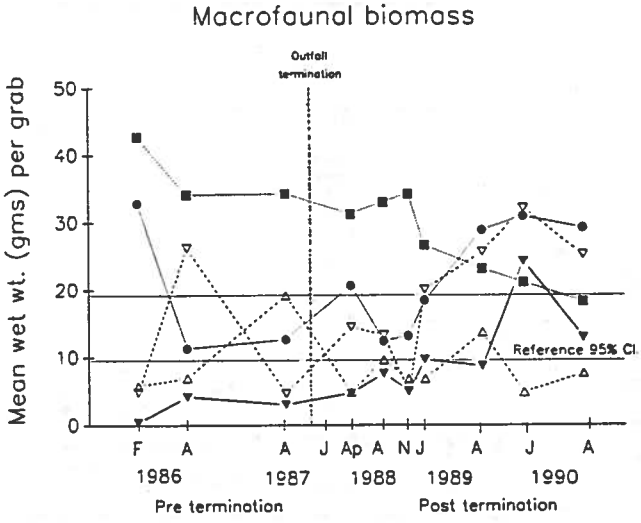

Figure 78 Recovery of benthic macrofaunal assemblages. Ordination analysis was used to compare the scores of the pre-termination assemblages with scores of post-termination cruises. Scores of the old sludge field sites have 'moved' towards the scores of the reference sites in the ordination space, demonstrating recovery of the macrobenthos.

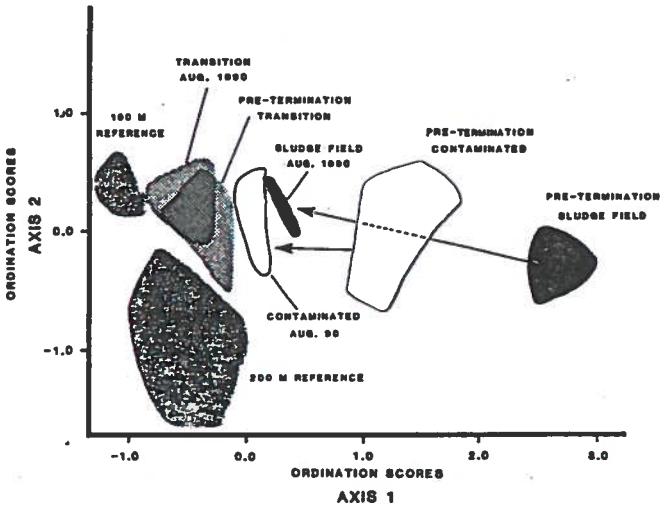

Figure 79 Plot of macrobenthic ordination scores over time (symbols - same as Figure 70)

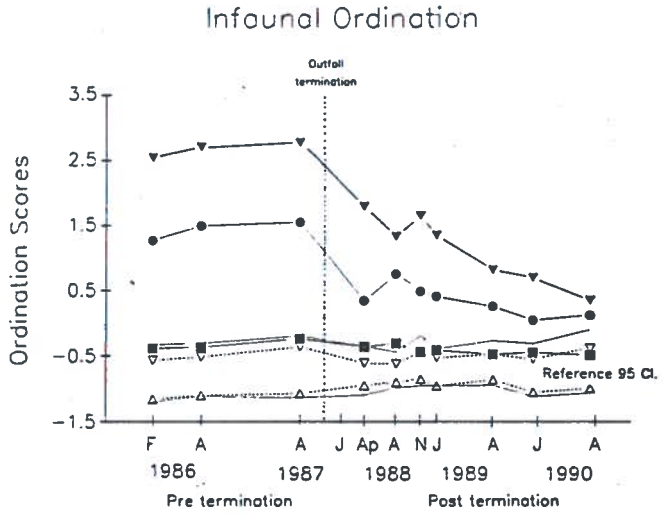

2. Benthic Megafauna

a. Pre-Termination Assemblages.
Classification analysis of the pre-termination trawl data showed the existence of three megabenthic assemblages: a contaminated zone assemblage at Stations HR1 and 2 near the old outfall, and separate reference assemblages at the 100 and 200 m sites (Figure 80). All of the 200 m sites had similar species composition and abundances.

The megafaunal assemblage at the two contaminated sites (HR1 and 2) was dominated numerically by the asteroid *Astropecten verrilli*, but only a few were collected at the 100 m reference sites (Table 14). Species characteristic of uncontaminated reference areas, such as the urchin *Lytechinus pictus*, were rarely collected at the contaminated sites.

The 100 m reference sites were dominated by the ridgeback prawn *Sicyonia ingentis* and *L. pictus*. These species are characteristic of uncontaminated areas all along the southern California shelf (Thompson *et al.* 1987; submitted ms). Although *S. ingentis* was, on the average, more abundant in the reference sites than in the contaminated sites, due to temporal variations, there was no significant difference (ANOVA, $p<0.05$) in their abundances among any of the megafaunal site groups under full sludge discharge, therefore they will not be useful in evaluation of recovery.

S. ingentis was selected at the beginning of this study as one of the target species for more detailed analysis, including population size-frequency analysis and tissue chemistry analyses.

Figure 80 Sites with similar trawl-caught megabenthic species composition and abundances formed three zones of impact, or assemblages during full sludge discharge. The groupings were based on ordination and classification analyses of the three pre-termination cruises. Average abundances of the dominant species in each assemblage are shown on Table 14.

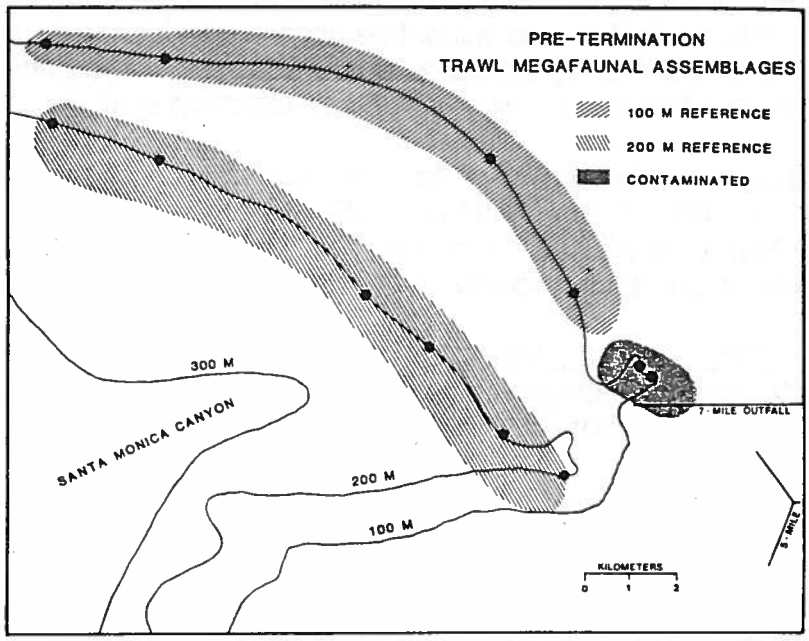

Table 14 Average abundances of the most common and abundant trawl-caught megafaunal invertebrates collected in each zone of impact, or assemblage, as identified by classification analysis; based on three pre-termination cruises.

PRE-TERMINATION TRAWL MEGAFAUNA (Mean number/trawl)

Species	Taxon	200 m Ref. (n = 17)	100 m Contamin. (n = 7)	100 m Ref. (n = 12)
Pandalus jordani	c	61	+	+
Brisaster latifrons	e	47	0	0
Spirontocaris holmesi	c	72	1	0
Neocrangon zacae	c	79	+	1
Allocentrotus fragilis	e	130	2	3
Metridium senile	cn	2	4	+
Sicyonia ingentis	c	157	51	1472
Pleurobranchaea calif.	m	2	4	1
Ophiopholis bakeri	e	+	+	5
Calanatacina oldroydii	m	+	3	0
Astropecten verrilli	e	+	154	4
Parastichopis calif.	e	+	1	63
Lytechinus pictus	e	1	1	822
Acanthoptilium sp.	cn	0	0	6
Mean No. Species per trawl		13.7	8.9	14.3
No. Individ. per trawl		587	235	2389
Mean Biomass (wet kg) per trawl		16.9	8.9	42.1

+ = <0.5/trawl

c = Crustacean e = Echinoderm Cn = Cnidarian m = Molluscan

However, since this species did not show any outfall related changes in its abundances or any toxic reaction to the sediment (SCCWRP unpublished), the size-frequency data has not been analyzed. Tissue chemistry data are reported below.

All of the 200 m sites were classified together, indicating no effects of sludge discharge on the 200 m assemblage, even under full sludge discharge. Therefore, the 200 m sites will not be useful in evaluation of recovery. Those sites were inhabited by typical outer shelf-upper slope organisms such as *S. ingentis* and the pink urchin *A. fragilis* (Thompson *et al.* ms).

There were significantly fewer species, individuals, and biomass per trawl at the two contaminated sites than in the 100 m reference sites (ANOVA, $p=0.05$; Table 14). As explained for the macrofauna, depression of these parameters is common in contaminated environments.

b. Recovery of the Megafauna. There has been very little change in the megafaunal assemblages at the two contaminated sites at 100 m since sludge discharge termination.

The only obvious change has been in abundances of *A. verrilli* at the contaminated sites (Figure 81). During full sludge discharge this species was the most abundant megafaunal animal at those sites, averaging 154 per trawl. Abundances of this species did not decrease for more than one year after sludge discharge termination. However, beginning in January 1989, abundances decreased over the next year to none collected during 1990. Decreases in *A. verrilli* abundances were expected during recovery, however they should remain at reference site abundances, not disappear completely. The cause of their disappearance is not known. In photographs of the area, this species was closely associated with the white bacterial mats that existed on the periphery of the sludge field (Undersea Graphics 1987). The mats have also disappeared suggesting some connection. Perhaps the asteroid eats the bacteria, or another organism that does.

Abundances of *S. ingentis* decreased significantly in both the contaminated and 100 m reference sites during the study (Figure 82) This decrease is part of a natural response to the 1982-83 El Niño, when *S. ingentis* abundances averaged thousands per trawl throughout the southern California region (Thompson *et al.* ms). Since 1988, this species has been present throughout the Bay in averaging about 25 per trawl.

The urchin *L. pictus*, representative of 100 m reference sites, has not emigrated to the contaminated sites (Figure 83). This species has been shown to avoid contaminated species in several previous studies (Thompson *et al.* 1989; Anderson *et al.* 1989; Thompson *et al.* in press). It is not known when this species will begin to recolonize in the Santa Monica Canyon area.

Numbers of species, individuals, and biomass per trawl have not changed significantly since discharge termination.

The contaminated sites still have reduced counts in all of those parameters. However, trawl biomass has increased by approximately 52% since sludge discharge termination (Figures 84-86).

Ordination analysis of the megabenthic invertebrate data, including all pre- and post-termination cruises, shows that megabenthic assemblages in the Santa Monica Canyon have not changed in species composition and abundances since sludge discharge (Figure 87). Ordination scores for the contaminated sites (Stations HR1 and 2) from August 1990 overlap with scores from the pre-termination samples and have not moved towards the 100 m reference sites.

The ordination scores from the contaminated sites are plotted in recoverygraph format on Figure 88. This plot shows that the scores for the contaminated sites do not fall within the confidence limits of the reference sites. Forecasts for complete recovery based on these plots are considered in the Discussions and Conclusions section.

3. Epibenthic and Demersal Fish

a. Pre-Termination Assemblages. Four fish assemblages were identified during full sludge discharge (Figure 89). These site groupings were not as distinctive as with benthic invertebrates. Fish are much more motile and have more natural seasonal fluctuations in their abundances, thus trawl abundances are more variable. Additionally, the presence of rocks at some sites provides a different type of habitat, thus different fish.

Fish catches at the contaminated sites (HR1 and 2) were dominated by Dover sole and white croakers (Table 15). Both of these fish were significantly more abundant at these stations than at the 100 m reference sites (ANOVA, $p < 0.17$).

Dover sole were selected as one of the target species for more detailed analysis. Size-frequency distributions, disease incidence, and tissue chemistry in this species were also measured and are reported below.

Figure 81 Recoverygraphs of trawl megabenthos indicator species and assemblage parameters:
..... Contaminated sites (n = 2)
---- 100 m Reference sites (n = 4)
---- 200 m Reference sites (n = 6)
95% Confidence intervals based on all 100 m reference sites (n = 36). (Figures 81-86)

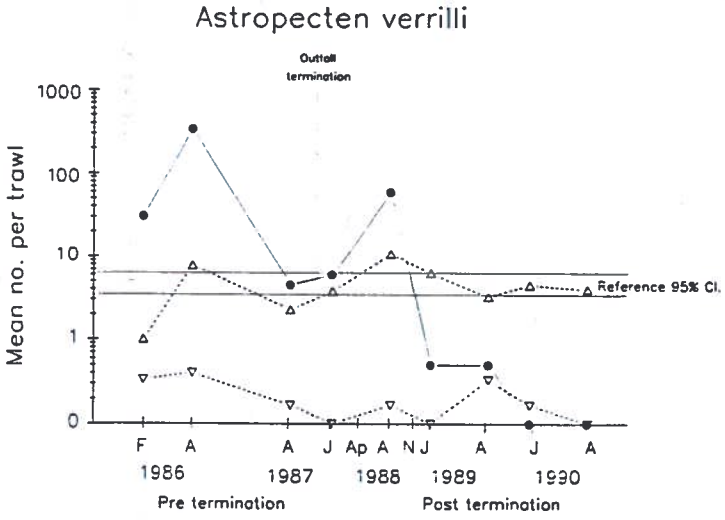

Figure 82

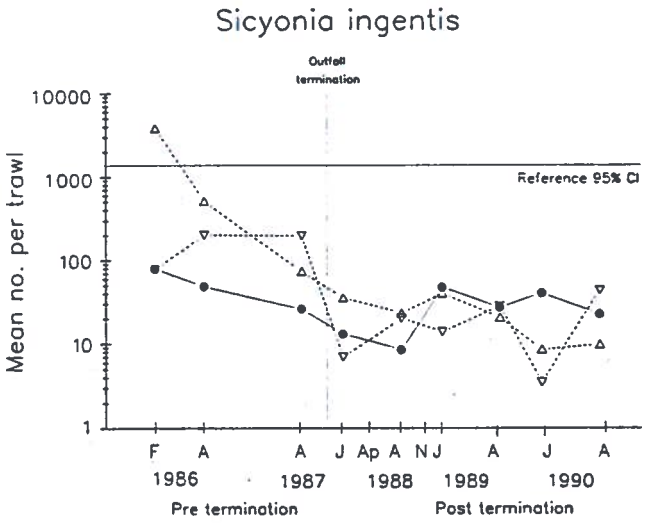

Figure 83

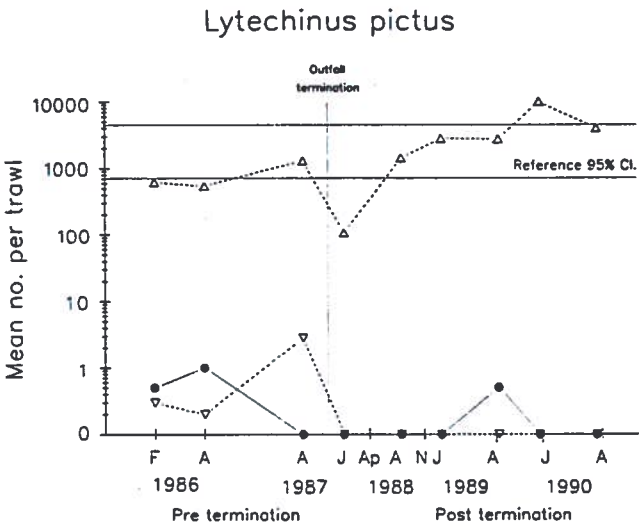

Figure 84

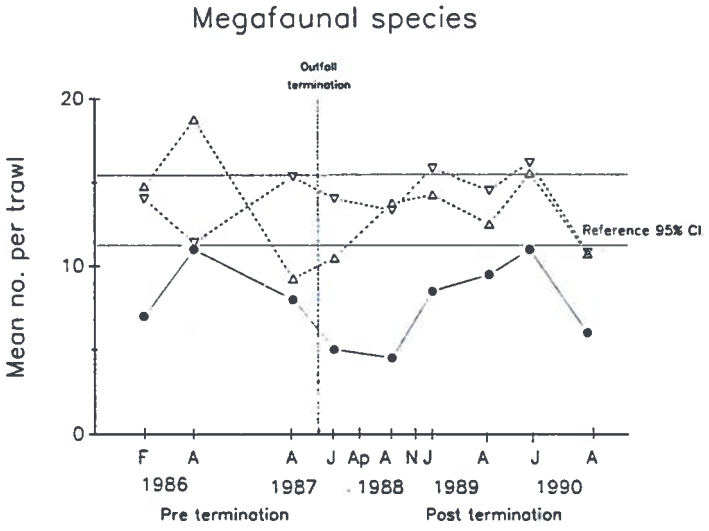

Figure 85

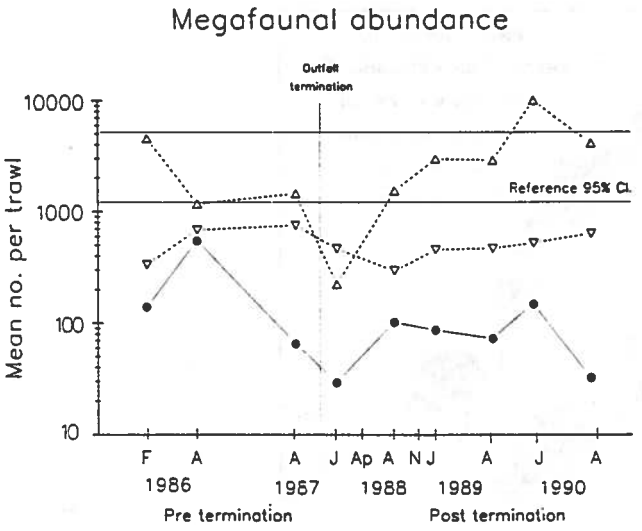

Figure 86

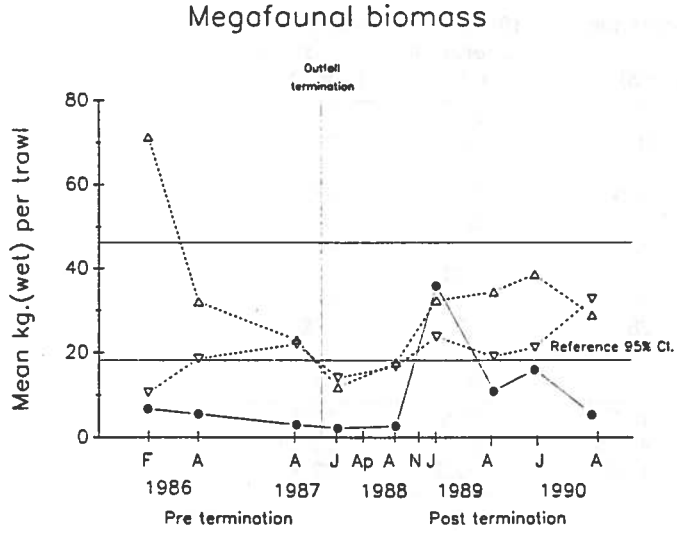

Figure 87 Ordination analysis of trawl-caught megabenthic invertebrates

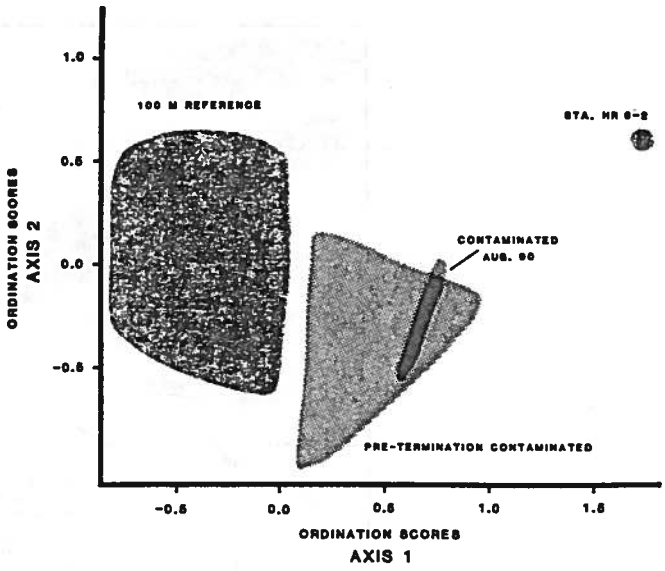

Figure 88 Plot of megabenthic ordination scores over time (symbols - same as Figure 81)

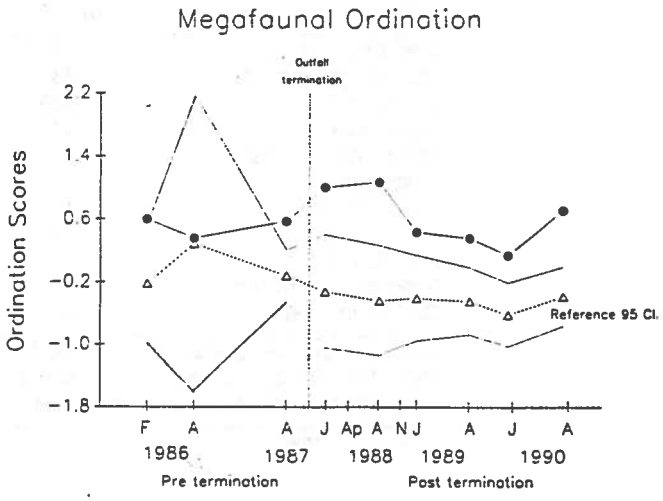

Figure 89 Sites with similar trawl-caught fish species composition and abundances formed four zones of impact, or assemblages during full sludge discharge. The groupings were based on ordination and classification analysis of the three pre-termination cruises. Average abundances of the dominant species in each assemblage are shown on Table 15.

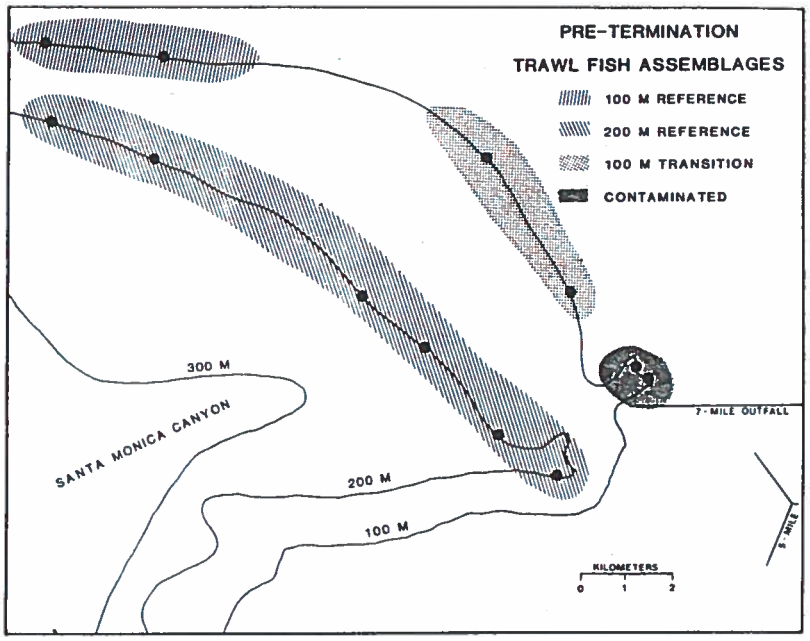

Table 15 Average abundances of the most common and abundant trawl-caught fish collected in each zone of impact, or assemblage, as identified by classification analysis; based on three pre-termination cruises.

	PRE-TERMINATION TRAWL FISH (Mean number/trawl)			
Species	All 200 m Sites (n = 18)	Contamin. (n = 5)	100 m Reference (n = 4)	100 m Transition (n = 8)
Splitnose rock fish	12	0	0	0
Black-edge poacher	23	0	<1	0
Slender sole	289	0	17	19
Dover sole	47	118	7	27
Plainfin midshipman	41	50	57	62
White croaker	1	78	0	6
Pacific sanddab	1	58	110	71
Half-banded r.f.	<1	6	19	2
Stripetail r.f.	4	28	36	280
Longspine combfish	0	4	3	53
Calif. tonguefish	0	<1	0	23
Mean No. Species per trawl	12.3	13.2	15.7	17.2
Mean No. Individ. per trawl	454.0	406.5	317.7	591.8
Mean Biomass per trawl (wet kg)	19.1	40.8	10.3	22.1

+ = <0.5/trawl

A transition assemblage was observed at Stations HR3 and 4. These sites were dominated by stripetail rockfish and Pacific sanddabs. The latter was the most abundant fish at the 100 m reference sites.

The 100 m reference sites, HR5 and 6, were dominated by Pacific sanddabs averaging 110 per trawl. All of the 200 m sites, including those near the Santa Monica Canyon were classified together. These sites were dominated by slender sole and may be considered reference sites. Since the 200 m sites showed no outfall effects during full sludge discharge, they will not be useful in following recovery. The fish inhabiting the reference sites in Santa Monica Bay also inhabit uncontaminated areas throughout the southern California mainland shelf (Allen and Voglin 1976 and Thompson *et al.* 1987).

Other fish assemblage parameters were also measured. However, there was no significant difference in the numbers of fish species or individuals caught per trawl at any of the sites under full sludge discharge. Regardless of where or when trawling occurred, an average of 15 fish species were collected, although as shown on Table 15, the species caught were somewhat different. These two parameters will not be useful in evaluation of recovery. Fish biomass was about four times greater at the contaminated sites than at the reference sites mostly due to the presence of increased numbers of white croakers and Dover sole.

b. Recovery of Fish Assemblages. The most obvious changes in trawl-caught fish at the contaminated sites are in decreased abundances of Dover sole and white croakers. White croakers have decreased, on the average, by 92% (Figure 90). There was a significant amount of variation in white croaker abundances among pre-termination samples: abundances up to 331 per trawl were collected in August 1986, but none were collected in February 1986. Immediately following sludge discharge termination their abundances consistently decreased to low levels, and only in January 1990 where they again caught in abundances above 25 per trawl.

This species feeds by picking food particles from the water column, probably including sludge particles. They may have decreased in number because their food supply (as sludge) was no longer available.

Dover sole abundances have also decreased, on the average, but there is considerable variation in these values. During the last trawl sampling cruise (August 1990) more Dover sole were collected than ever before (Figure 91). Seasonality is apparent; the summer months usually have more Dover sole than the winter months (Figures 91 and 92). Detailed analysis of Dover sole fluctuations are included in the next section.

Pacific sanddabs have increased by an order of magnitude at the contaminated sites. However, they have also increased at all of the other sites (Figure 93). Seasonality is also apparent in the abundances of this species, it is usually most abundant in the winter.

Slender sole have also increased in the contaminated sites. None were collected in the pre-termination samples, but an average of 247 per trawl were collected in the August 1990 samples. This species was most abundant at the 200 m sites.

The number of fish species and individuals have remained rather constant at all of the sites (Figures 94-96). Fish biomass is still elevated at the contaminated sites.

Ordination analysis of the trawl-caught fish assemblages shows that there has been little change in the species composition and abundances of the fish at the contaminated sites (Figure 97). The scores of the fish collected in August 1990 have not moved towards the reference assemblage. Rather they have moved up on ordination axis 2 which represents seasonal differences more than actual recovery.

Neither the contaminated or transition sites have recovered to reference conditions (Figure 98). Scores from the transition and contaminated sites were variable over time, and fell within the reference confidence interval in August 1989, but have since moved outside that interval. The scores should consistently fall within the reference confidence interval before recovery can be considered to occur. Forecasts for recovery are considered in the Discussion and Conclusions section.

Figure 90 Recoverygraphs of fish indicator species and assemblage parameters:

·····	Contaminated sites	(n = 2)
·····	Transition sites	(n = 2)
----	100 m reference sites	(n = 2)
----	200 m reference sites	(n = 6)

95% Confidence intervals based on 100 m reference sites (n = 18). (Figures 90-96)

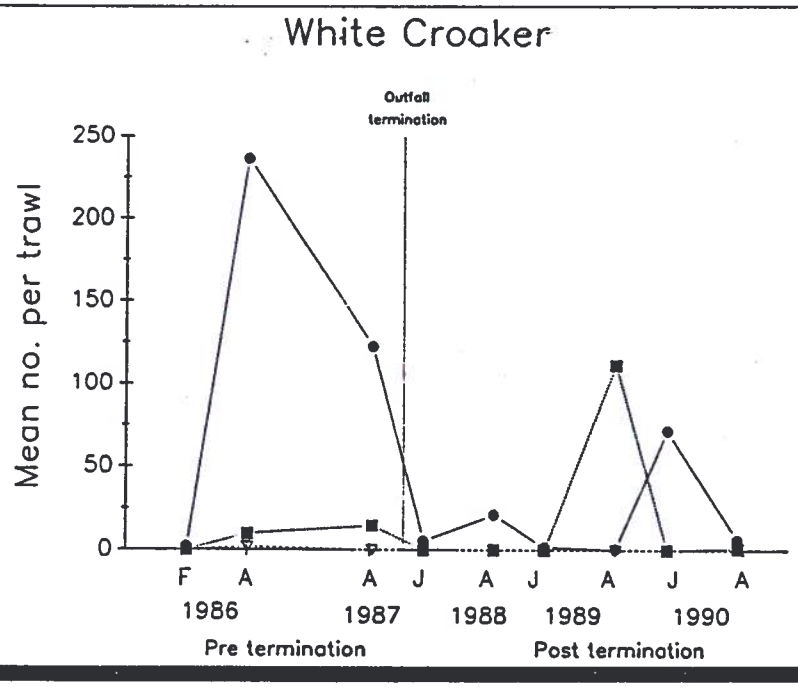

Figure 91

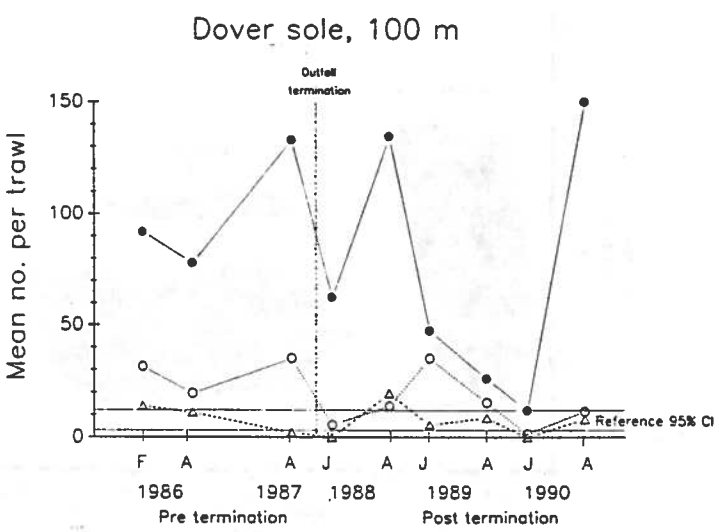

Figure 92

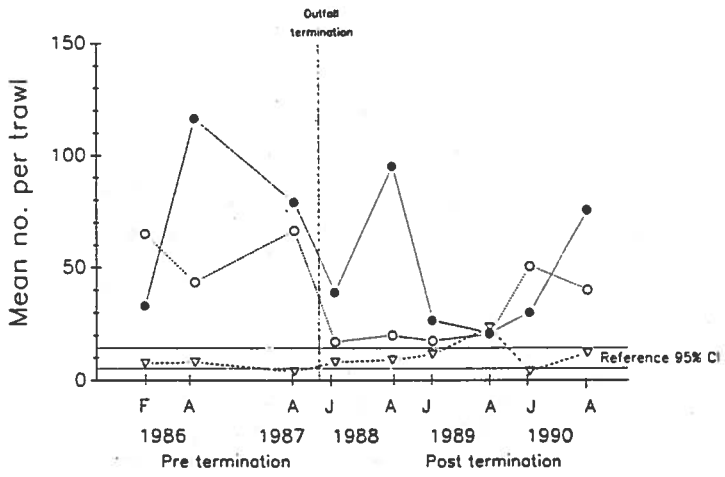

Figure 93

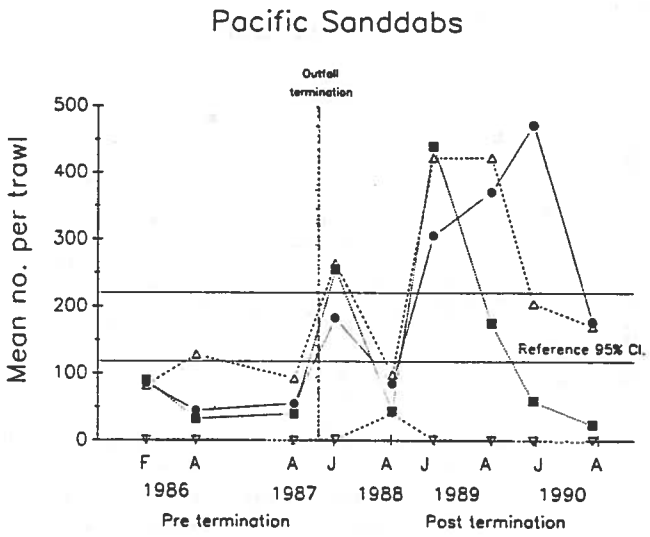

Figure 94

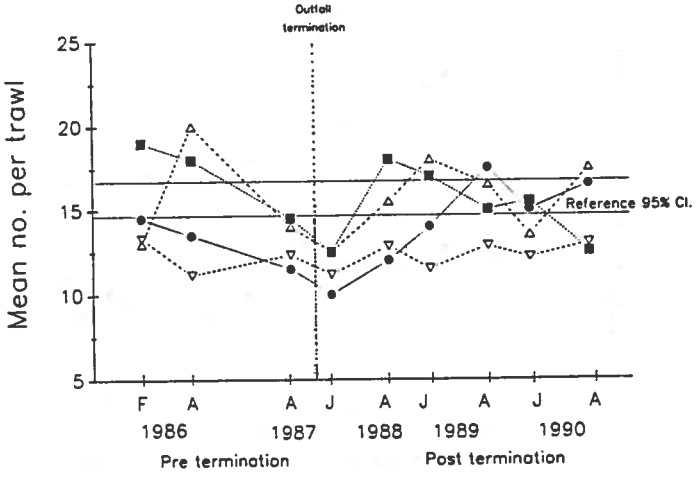

Figure 95

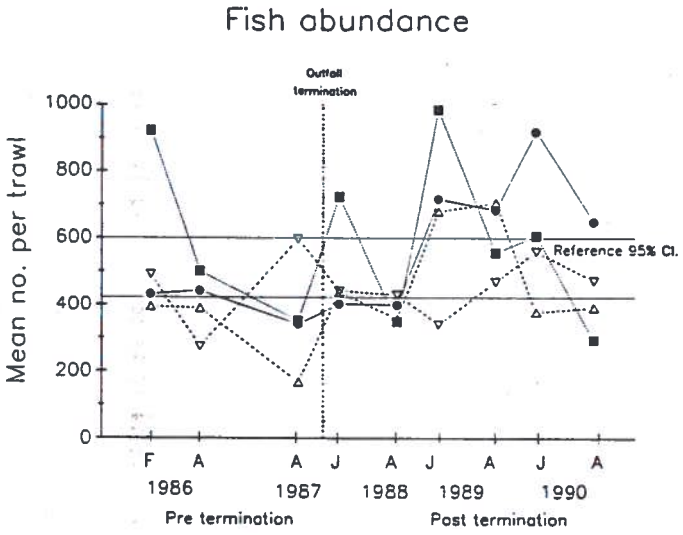

Figure 96

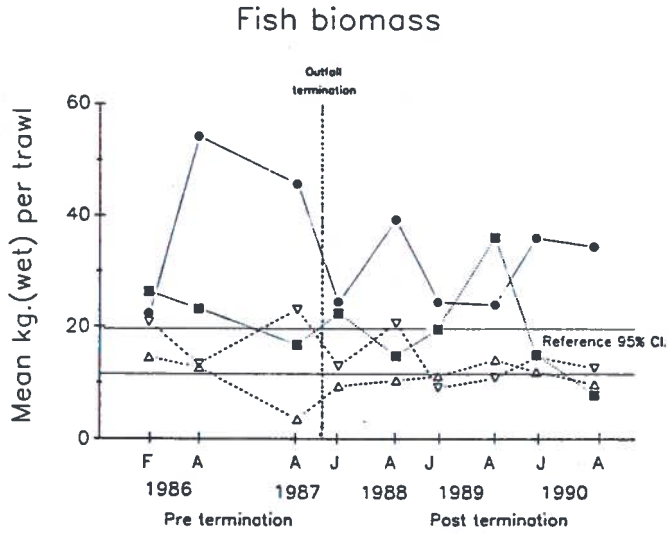

Figure 97 Ordination analysis of fish data

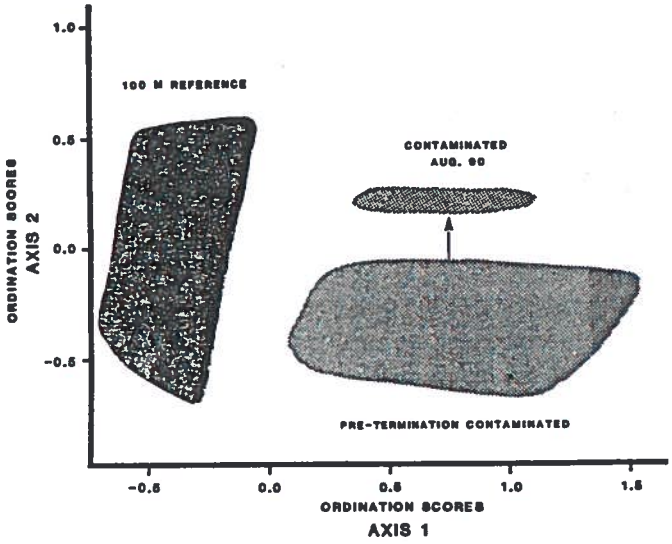

Figure 98 Plot of fish ordination scores over time (symbols - same as Figure 90)

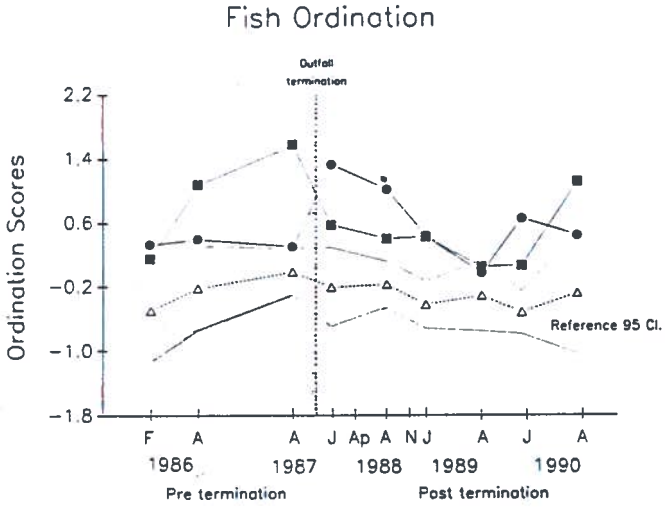

4. **Dover Sole** (Larry Cooper and Dr. Jeff Cross)

Introduction

Dover sole (*Microstomus pacificus*) are commonly found on the upper slope off Southern California at depths up to 1006 m (Hunter, Butler, Kimbrell, and Lynn 1990). Most of the fish migrate to shallow depths in summer and deep water in the winter (Hunter *et al.* 1990).

Abundance of these fish is higher near municipal waste water outfalls and disease incidence is also higher in these areas (Cross 1985). Fish near the outfalls are often afflicted with fin rot and or epidermal tumors. Fish in contaminated areas may be more susceptible to these diseases due to elevated body burdens of contaminants. The contaminants may interfere with the fish's immune system.

Dover sole appear to prefer substrata with high total organic carbon (TOC) content. This may be related to the abundance of deposit feeding polychaetes found in these areas. These polychaetes are the prey of preference for Dover sole. The high levels of TOC around the outfalls gives rise to higher abundances of deposit feeding polychaetes which may be a factor in the higher abundance in these areas.

This section examines the changes in the biology of Dover sole that are related to the termination of discharge.

Fish abundance was log transformed to normalize the distribution of abundances and to ensure homogeneity of the variances. TOC and proportion of incidence of disease were arcsine transformed to normalize the distribution and homogenize the variances.

Analysis of variance was performed on the log of fish abundance by station with regard to depth, season, location in proximity to the outfall, and pre/post sludge discharge. Analysis of variance was performed for arcsin percent TOC and arcsin proportional disease using the same parameters.

Results

Dover sole in this study showed seasonal migration patterns. The fish are more abundant at the deep sites in the winter and shallow sites in the summer. There was no significant difference in abundance of fish collected at 100 m and 200 m. The fish migrate to deeper water in the winter to spawn and back to shallow water in the summer to feed.

The fish were more abundant near the outfalls in the contaminated zone than any other zone. Abundance was significantly different between the contaminated zone and the transition zone. The transition zone was significantly different in fish abundance form the reference zone (Table 16). This distribution of abundance is correlated with elevated levels of TOC.

The distribution of fish during summer of 1989 demonstrates an anomaly in the pattern of abundance seen during the period of the study. Low fish abundances were

seen in the canyon contaminated stations during the summer of 1989. Correlated with this pattern is a general decrease in the level of TOC at these stations. In 1990, the distribution patterns of the fish returned to the levels prior to summer of 1989. In November 1987, the discharge of solid waste was terminated. In the contaminated canyon areas the levels of TOC in the sediment demonstrate a decreasing trend after the termination of solid waste discharge.

The transition zone and the reference zone were both significantly different from each other and from the contaminated zone in TOC concentration, Dover sole abundance, and incidence of disease (see next section).

Analysis of variance for TOC shows significant differences in the levels of TOC with regard to location but not with regard to season. The levels are generally higher near the outfall (Table 17).

Unusually high currents were measured in the winter of 1989 in the canyon. This was the only remarkable current related event during the course of the study.

Physical oceanography showed the normal temperature stratification in the summer and uniform decline in temperature with depth during the winter months.

Discussion

Dover sole migrate up and down the slope seasonally. Their abundance may be controlled by prey availability. The fish move to deeper water in the winter to spawn and move back to shallow water in the summer to feed. The relative abundance at each station demonstrates these seasonal patterns with the exception of 1989.

Dover sole are the most susceptible species to tumors and fin rot of all the fish commonly collected in the Santa Monica Bay (Cross 1985). The pattern of disease incidence near the 7 mile outfall is similar to the patterns reported around the outfall at Palos Verdes (Cross 1986). Incidence of disease was highest close to the outfall and low or non-existent in the transition and reference sites.

The abundance of Dover sole seems to be most closely related to elevated levels of TOC. These areas support large populations of deposit feeders such as polychaetes which are Dover sole's main prey item. The abundance of these fish decreased dramatically in 1989. This decrease was seen in the canyon stations where the levels of TOC are generally the highest. The elevated levels of TOC may be responsible for a greater abundance of deposit feeding polychaetes in these areas.

In 1989, unusually high canyon currents were measured. During this period, the stations in the canyon showed an increase in the percent of sand composition and a general decrease in TOC and polychaete abundance. This strong current condition seems to be responsible for the decrease in Dover sole abundance during 1989. Resuspension of the organic material in the sediment or burial by shelf sediments entrained in the high currents, down the canyon may be responsible for decreasing the number of polychaetes in the sediment grabs. This may have in turn reduced the number of fish because of the limited prey availability.

Table 16 Mean ± SD, (n) Dover sole abundances in each zone of impact

	CONTAMINATED	TRANSITION	REFERENCE
PRE WINTER	62.5 ± 70.1 (4)	48.3 ± 40.4 (4)	10.8 ± 11.8 (4)
SUMMER	101.6 ± 66.7 (8)	41.1 ± 31.5 (8)	6.3 ± 4.6 (8)
POST WINTER	36.2 ± 29.0 (12)	21.2 ± 23.4 (12)	4.8 ± 5.1 (12)
SUMMER	83.7 ± 74.6 (12)	25.8 ± 24.6 (12)	13.3 ± 10.8 (12)

Table 17 Mean percent, ± SD, (n) TOC in each zone of impact

	CONTAMINATED	TRANSITION	REFERENCE
PRE WINTER	2.9 ± 1.4 (4)	1.9 ± 1.1 (4)	1.2 ± 0.3 (4)
SUMMER	2.7 ± 1.1 (8)	1.9 ± 1.2 (8)	1.2 ± 0.2 (8)
POST WINTER	2.8 ± 1.4 (12)	1.8 ± 1.1 (12)	1.1 ± 0.4 (12)
SUMMER	2.2 ± 1.2 (12)	1.7 ± 1.2 (12)	1.2 ± 0.2 (12)

In the winter of 1990, conditions returned to normal and the relative abundances of Dover sole and their prey species increased to previous levels consistent with the seasonal patterns of distribution.

The prevalence of fish disease should decrease after the termination of solid waste discharge. The incidence of disease in the contaminated zone was significantly lower after the termination. This may be an indicator of improving conditions in the vicinity of the outfall. Perhaps with time incidence of disease will decrease to very low levels as the body burdens of contamination in the fish decreases.

5. Fish Disease

Visual evidence of fin erosion and epidermal tumors in Dover sole were recorded at each site trawled. During full sludge discharge between 5-13% of the Dover sole caught at the contaminated sites had fin erosion, and between 2-11% had epidermal tumors (Table 18). Low percentages of Dover sole from the 200 m reference sites had fin erosion.

Both of these diseases are know to be associated with waste water discharge in the region (Cross 1988) and occur in similar proportions near other outfalls.

Following sludge discharge termination, the incidence of fin erosion and epidermal tumors has decreased. Except for a relapse in January 1989, epidermal tumors have nearly disappeared (Figure 99). Fin erosion has not been observed in any fish caught in the contaminated zone at 100 m near the outfall since January 1989 (Figure 100).

Table 18 Percentages of Dover sole with epidermal tumors and fin erosion collected at 100 m (A), and 200 m (B) sites during full sludge discharge. Based on three pre-termination cruises.

A.

Area (100 m)	n	Epidermal tumors %	Fin erosion %
Contaminated	613	5.1	9.5
Transition	161	0	0
Reference	54	0	0

B.

Area (200 m)	n	Epidermal tumors %	Fin erosion %
Contaminated	396	2.3	5.3
Transition	340	0	0.6
Reference	39	0	2.6

Figures 99-100 Recoverygraphs for epidermal tumors and fin erosion in Dover sole:
..... 100 m Contaminated sites (n = 2)
---- 200 m Contaminated sites (n = 2)

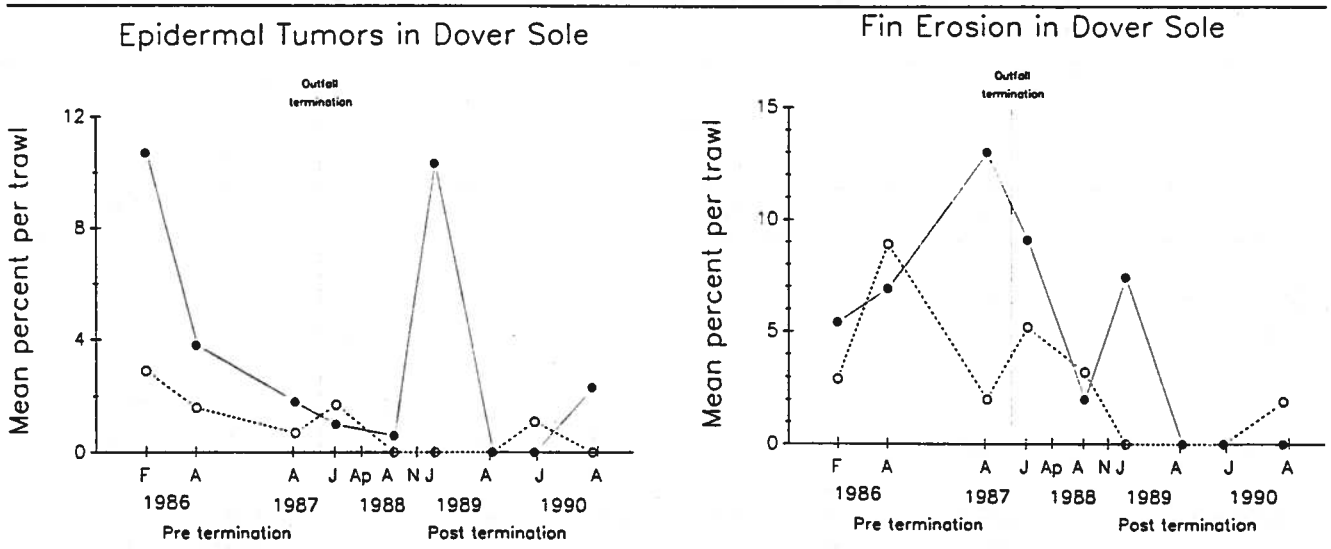

6. Tissue Contamination

Contaminant concentrations in Dover sole liver and muscle, and in *Sicyonia* (prawn) hepatopancreas and muscle were measured at the 100 m sites each summer.

Analyses of trace metals in muscle tissues are incomplete. The results of these analyses will be provided in an addendum upon completion.

Due to the potential for human consumption, contaminant concentrations in edible tissues, or muscle, are of the greatest interest. Under full sludge discharge, DDTs and PCBs in Dover sole and *Sicyonia* muscle tissue was extremely variable in all areas and was not statistically different from the reference sites in the contaminated zone (ANOVA, $p>0.05$). DDT concentrations in Dover sole muscles in the contaminated zone averaged 289 ppb, but were actually higher at the transition sites (Table 19). DDTs in *Sicyonia* muscle were much lower (19.3 ppb) than in Dover sole livers. PCBs in Dover sole muscles averaged 1265 ppb, and in *Sicyonia* muscles averaged 492 ppb in the contaminated zone under full sludge discharge.

Liver and hepatopancreas tissues contained orders-of-magnitude higher concentrations of DDTs and PCBs than muscle because livers and hepatopancreas have proportionally higher fat contents. These concentrations were also highly variable among the zones and except for PCBs in *Sicyonia* hepatopancreas, were not significantly different among the zones (ANOVA, $p<0.05$). DDTs were higher in livers (1297 ppb) and hepatopancreas (697 ppb) from the reference sites than in the contaminated sites. This non-gradient pattern reflects the ambiguous pattern of DDTs present in the sediments.

PCBs in tissues were always higher at the contaminated sites than in the reference sites. Moderate concentration up to 1714 ppb were measured in livers and hepatopancreas.

Table 19 Concentrations of contaminants (ng/wet kg) in Dover sole (A), and *Sicyonia* tissues (B), collected during full sludge discharge. Based on two pre-termination cruises. Values without error estimates represent composite samples. Average reference site values from Thompson *et al.* (1987).

A.

	Dover sole							
	liver						muscle	
	DDT	PCB	Ag	Cd	Cu	Zn	DDT	PCB
Contaminated	633	1379	.09	.17	.73	22	289	1265
(sd)	(330)	(815)	(.05)	(.12)	(.44)	(1.5)	(320)	(1264)
Transition	1197	1714	.33	.35	1.0	22	344	692
(sd)	(452)	(1013)	(.02)	(.23)	(.54)	(8.7)	(443)	(652)
Reference	1297	561	.10	.28	.78	27	143	26.5
(sd)	(363)	(462)					(119)	(202.0)
So. Cal. average of mainland shelf (1985)	440	368	.08	1.2	4.0	22		

B.

	Sicyonia ingentis hepatopancreas						muscle	
	DDT	PCB	Ag	Cd	Cu	Zn	DDT	PCB
Contaminated	659	1576*	61	2.1	262	129	19.3	492
(sd)	(332)	(1117)	(15)	(1.5)	(15)	(38)	(17.9)	(775)
Transition	892	1144	48	3.2	333	72	20	363
(sd)			(23)				(19.8)	(38.2)
Reference	697	318	30	2.6	268	63	21	246
(sd)	(387)	(90)		(1.0)	(128)	(15)	(9.2)	(19.8)
So. Cal. average of mainland shelf (1985)	655	568	25	1.8	357	120		

* Significant difference from reference sites.

Ag and Zn in *Sicyonia* hepatopancreas were the only trace metals that were significantly elevated at the contaminated sites compared to the reference sites (Table 19). Cd and Cu in *Sicyonia*, and all four metals in Dover sole livers showed no significant sludge field related concentrations under full sludge discharge, therefore will not be useful in determination of recovery.

The tissue contaminant concentrations measured at the reference sites in Santa Monica Bay (HR5 and 6) under full sludge discharge are generally similar to those measured at other reference sites off southern California (Table 19).

Recovery of tissue contamination

Since sludge discharge termination, PCBs in all tissues has decreased considerably. In particular, PCBs in Dover sole and *Sicyonia* muscle, and in *Sicyonia* hepatopancreas have decreased to below 89 ppb (86-99%), near reference levels (Figure 102, 106, 108). Concentrations in Dover sole livers remain elevated at about 1092 ppb in the contaminated zone (Figure 104).

DDTs in tissues have changed only moderately or remained the same. DDTs in Dover sole muscle tissue have decreased in all areas, by about 86% at the contaminated sites, since sludge discharge termination (Figure 101). During August 1988, DDT concentrations in *Sicyonia* hepatopancreas averaged 13,521 ppb at the reference sites (Figure 102). On the average, DDTs in Dover sole livers have increased at the contaminated sites (Figure 107).

Only two trace metals in *Sicyonia* hepatopancreas have responded to sludge discharge termination. Ag has decreased to reference level, but Zn has not (Figure 110). Cd and Zn in *Sicyonia*, and all four trace metals in Dover sole were equal to or less than reference levels during full discharge and were not useful in evaluating recovery (Figures 109 and 110).

Figure 101 Recoverygraphs of contaminants in Dover sole and *Sicyonia* tissues - 100 m sites in summer collections only:

..... Contaminated sites (n = 2)

. . . Transition sites (n = 2)

----- Reference sites (n = 2). (Figures 101-110)

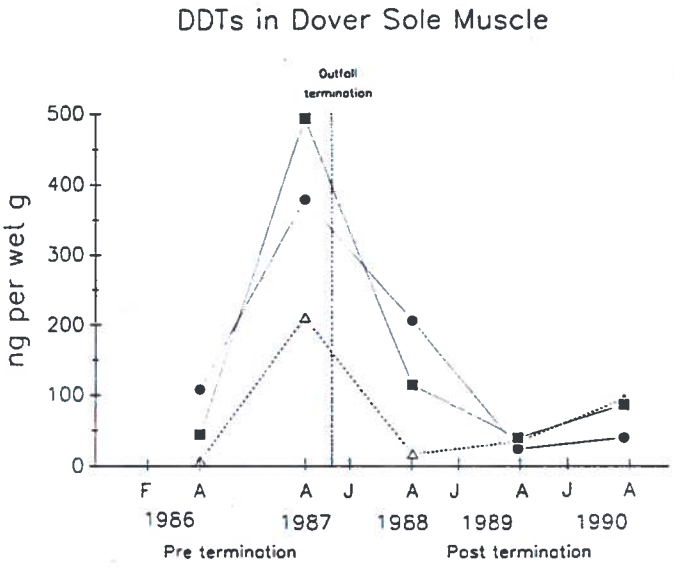

Figure 102

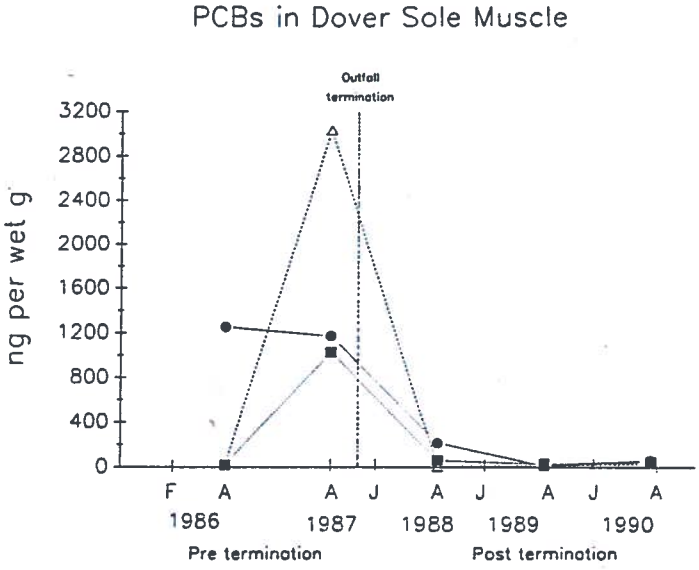

Figure 103

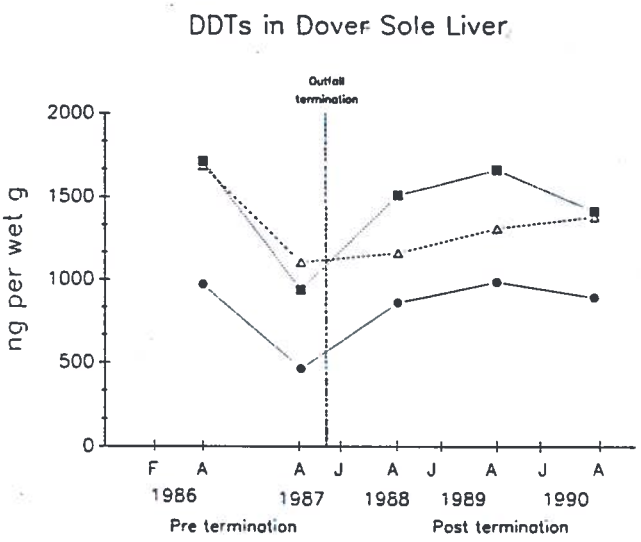

Figure 104

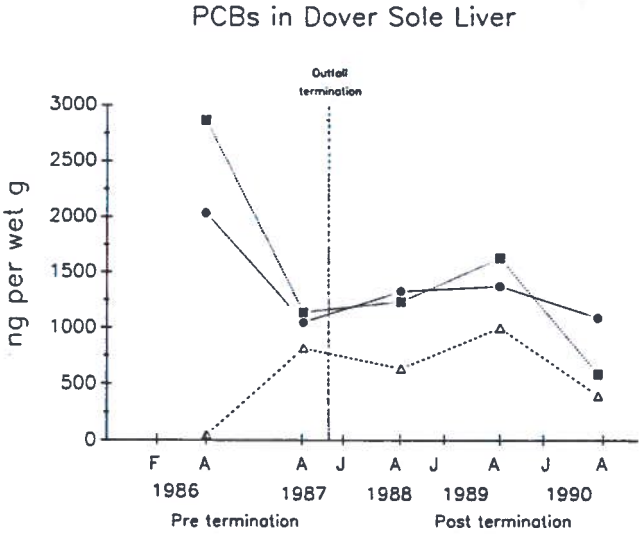

Figure 105

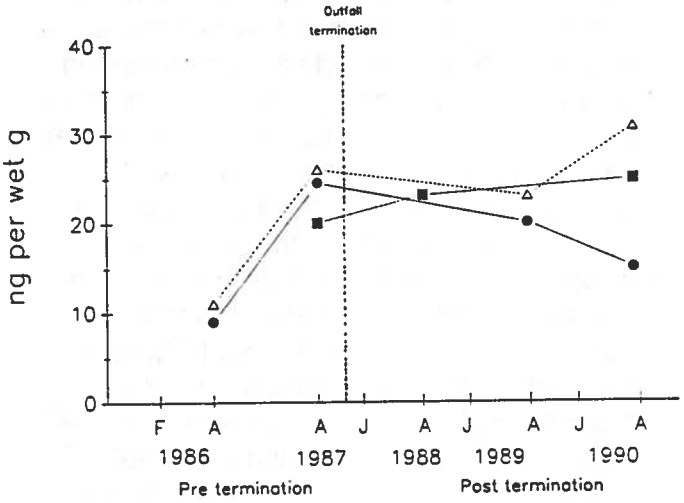

Figure 106

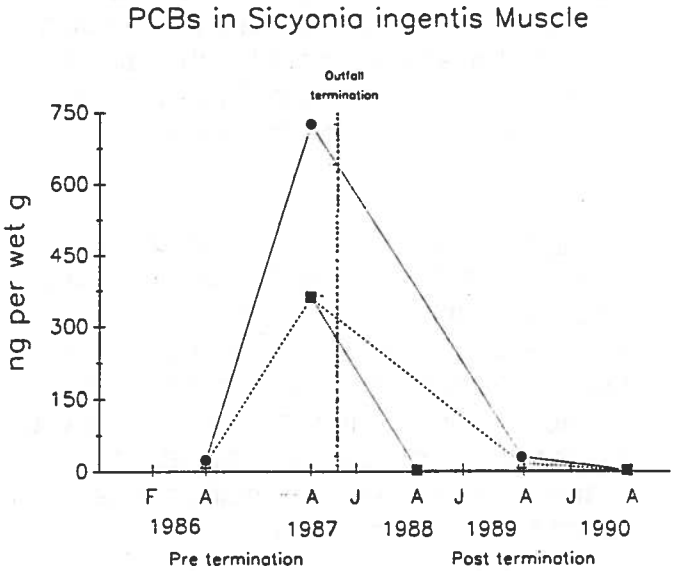

Figure 107

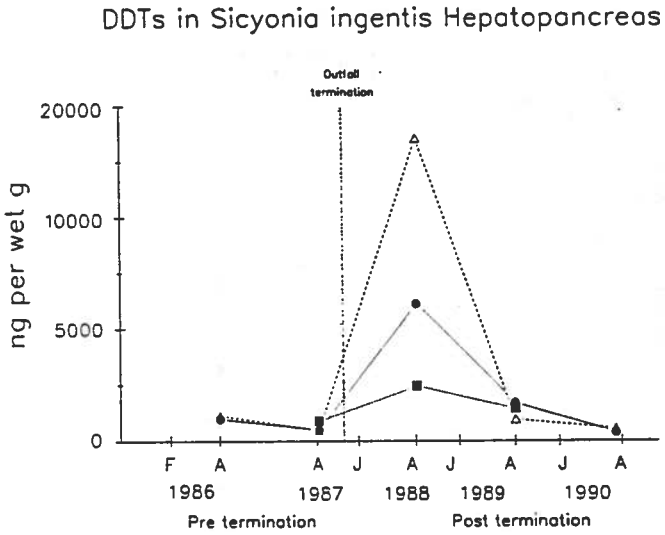

Figure 108

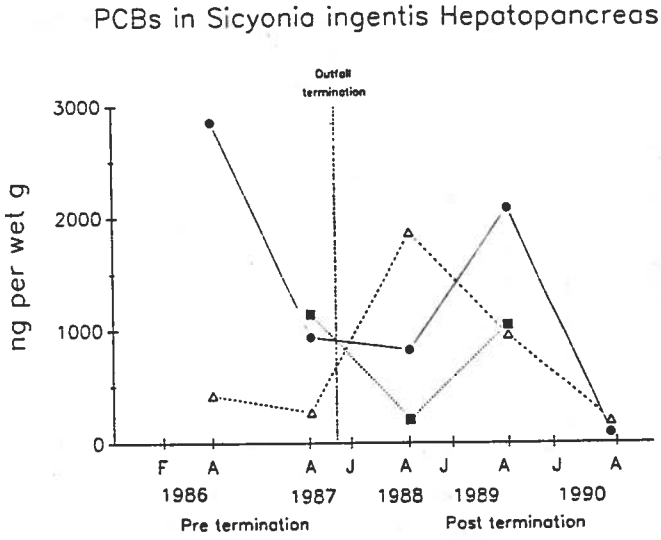

Figure 109

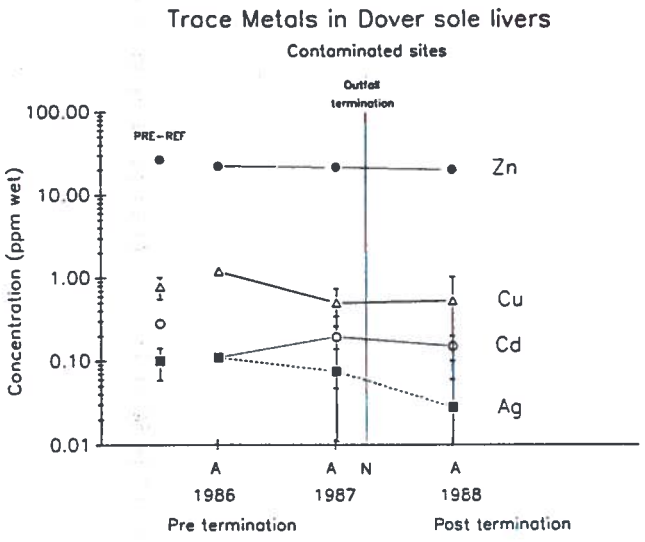

Figure 110

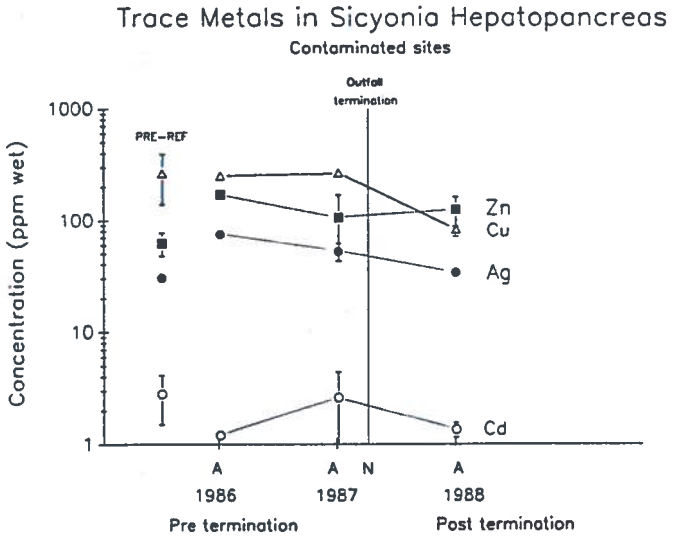

7. **Sediment Toxicity** (Steve Bay)

Short-term toxicity: The ten day amphipod survival test results are shown in Table 20. Survival of the amphipods in the lab control sediment collected from Newport Bay was high for all tests except those conducted in February 1990. This variability in lab control survival influenced amphipod survival in the test sediments and was compensated for by expressing survival as a percentage of the lab control value (Figure 111). This figure shows that a large reduction in short-term toxicity of canyon sediment occurred between the 1988-89 experiments. *Grandidierella* survival increased from less than 40% of the lab control value in 1987-88 to over 90% of the lab control in 1989 (Figure 111). Survival in canyon sediment remained relatively high in the subsequent two 1990 experiments, although survival in the August 1990 experiment was significantly less than the lab control.

The toxicity of sediment from the control zone (Stations HR5 and 6) was also measured in 1989 and 1990. *Grandidierella* survival in these sediments was high and similar to that of the lab control sediment, except in the February 1990 test. The cause of the reduced survival observed in February is unknown but may have been related to the use of poor quality test organisms, as suggested by their low survival in lab control sediment.

Long-term toxicity: The survival of juvenile *Grandidierella* following 28-day exposure to Santa Monica Bay sediments is summarized in Table 22. Survival in the lab control sediment was relatively low and variable. This situation has been observed in other experiments and may reflect a natural rate of juvenile mortality that is not related to sediment quality.

Survival results for contaminated sediments from Santa Monica Bay were compared to sediment from the control zone in order to minimize the influence of variations in sediment grain size on the test results. There were no statistically significant differences observed for the 28-day survival exposures between sediment collected from the control, transition, contaminated, and canyon zones.

Results of the amphipod growth measurements obtained from the 28-day experiments are shown in Table 21. The growth rates have been expressed as a percentage of the lab control value to compensate for variations between experiments (Figure 112). Statistical tests of the data from the two August experiments indicated that the growth of amphipods exposed to sediment from the transition, contaminated, or canyon stations was not significantly different from that of amphipods exposed to control zone sediment. A comparison of the growth rate data for the February experiments was not made since sediment from the control and canyon zones were not tested simultaneously.

Amphipods surviving the August 1990, 28-day toxicity test were examined to determine their degree of sexual maturity. Those animals possessing key morphological sex characteristics were classified as either males or females while the remainder were counted as undifferentiated. The results of this analysis are presented in Table 23. The greatest proportion of identifiable males and females were found in the lab control sediment, reflecting the rapid growth rate of amphipods in this sediment. Ten percent of the animals in the control and contaminated sediments were females, while no females could be distinguished among the amphipods exposed to sediment from the transition and canyon zones. A trend indicating a reduction in the proportion of males found in the transition and contaminated sediment samples was also observed. Neither of these trends represented statistically significant changes relative to sediment from the control zone, however.

In summary, sediment toxicity test results indicate that a large reduction in the toxicity of sediment from the canyon sludge field occurred between April 1988 and August 1989. The results of recent tests indicate that the quality of sediment from the transition, contaminated, and canyon zones is similar to that of control zone sediment. Evidence of impaired amphipod sexual maturation was found at some stations, but additional data need to be collected before these effects can be attributed to the presence of contaminated sediment.

Table 20 Summary of 10-day survival of exposure of *Grandidierella* to sediments from Santa Monica Bay. Asterisks indicate means that are significantly different from the lab control (ANOVA; $p<0.05$).

		10-Day Percent Survival (mean + SE)		
Date	N	Control[a]	Canyon[b]	Lab Control
Nov. 1987	3	NA[c]	35 ± 20*	92 ± 4
Apr. 1988	4	NA	8 ± 8*	88 ± 4
Aug. 1989	2	90 ± 5	90 ± 0	98 ± 3
Feb. 1990 A	4	40 ± 5	NA	79 ± 2
Feb. 1990 B	4	NA	53 ± 5	65 ± 3
Aug. 1990	4	80 ± 2	72 ± 10*	94 ± 3

a Samples were replicates from Stations HR5 and 6.

b Canyon samples for November 1987 and April 1988 were composites for Station HR50 only. All other time points used replicates from Stations HR50 and 51.

c Sample not analyzed at this time-point.

Table 21 Summary of 28-day growth data for *Grandidierella* exposed to sediments from Santa Monica Bay.

		28-Day Length Change (mm; mean + SE)			
Date	Control	Transition	Contaminated	Canyon	Lab Control
Aug. 1989	2.2 ± 0.3	2.3[a]	2.9 ± 0.1	1.8 ± 0.2	3.4 ± 0.1
Feb. 1990 A	3.2 ± 0.1	NA	NA	NA	2.7 ± 0.2
Feb. 1990 B	NA[b]	NA	NA	0.8 ± 0.1	1.7 ± 0.3
Aug. 1990	2.0 ± 0.4	1.6 ± 0.2	1.9 ± 0.2	1.8 ± 0.2	2.8 ± 0.1

a N for this sample equaled 1. For all other samples and time-points the N value was two, three, or four.

b Sample not analyzed at this time-point.

Table 22 Summary of 28-day survival data for *Grandidierella* exposed to sediments from Santa Monica Bay.

	28-Day Percent Survival (mean + SE)				
Date	Control	Transition	Contaminated	Canyon	Lab Control
Aug. 1989	50 ± 4	20[a]	22 ± 4	25 ± 4	42 ± 6
Feb. 1990 A	46 ± 1	NA[b]	NA	NA	74 ± 7
Feb. 1990 B	NA	NA	NA	30 ± 14	44 ± 14
Aug. 1990	26 ± 10	31 ± 15	47 ± 6	44 ± 2	74 ± 3

a N for this sample equaled 1. For all other samples and time-points the N value was two, three, or four.

b Sample not analyzed at this time-point.

Table 23 Effect of sediment exposure on maturation rate of *Grandidierella* juveniles. Values are mean ± SE.

	% attaining sexual differentiation	
Zone	Female	Male
Lab control	26 ± 8	30 ± 4
Control	10 ± 6	22 ± 13
Transition	0	8 ± 5
Contaminated	10 ± 4	8 ± 5
Canyon	0	14 ± 6

Figure 111

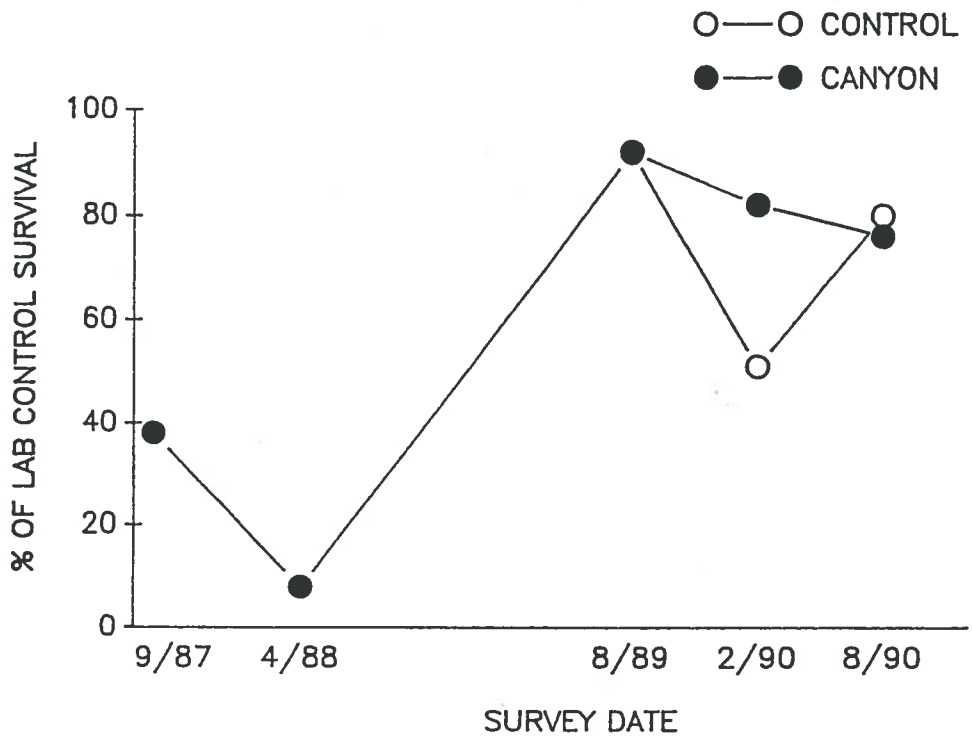

Survival of *Grandidierella* following 10-day sediment exposure.

Figure 112

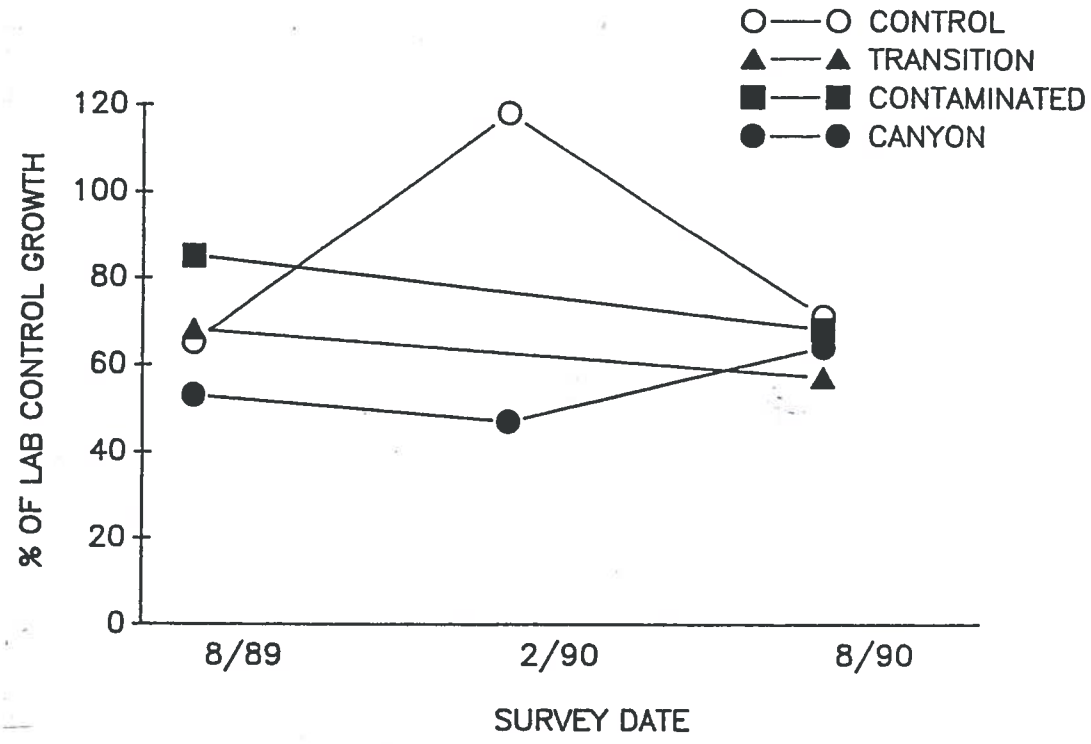

Change in *Grandidierella* length during 28-day sediment exposure.

VII. DISCUSSION AND CONCLUSIONS

Since sludge discharge was terminated in November 1987, concentrations of all contaminants in the old sludge field sediments have decreased. Fish disease and sediment toxicity are significantly reduced or absent in the sludge field and the benthic macrofauna have shown a significant amount of recovery.

Using the trends observed on the recoverygraphs, a forecast for recovery of the Bay is shown on Table 24. While sediment contaminant levels are decreasing, only total nitrogen has shown a significant trend in recovery over time. Except for sulfides, estimates for sediment contaminants to reach reference levels exceed ten years.

The benthic macrofauna are recovering most rapidly and show significant trends over time. Recovery of the number of individuals and biomass is non-linear because they increase to transition site phases before they decrease to reference site values. Numbers of macrofaunal individuals reached reference levels in February 1988, then increased to transition site levels; they should now begin to decrease back to reference levels as recovery proceeds. However, the number of macrofaunal species are showing significant, constant recovery rates.

As of August 1990, the sludge field macrobenthos was similar to contaminated and transition assemblages under full sludge discharge. However, none of the most abundant species found in reference areas had recolonized the sludge field.

Benthic macrofaunal species composition and abundances, as reflected by ordination scores, provide the best indicator of benthic recovery. Recovery in each zone of impact (sludge field, contaminated, and transition zones) proceeds at different rates. Thus, it would not be accurate to predict sludge field recovery from regressions of only sludge field data since that assemblage must become like contaminated, then transition sites, each with different recovery rates, before they recover to reference conditions. Therefore, recovery was predicted by lagging the recovery rates in each successive recovery stage to create a recovery curve. The resulting prediction for recovery of the benthos in the sludge field is in spring 2002.

Similar predictions for trawl-caught megabenthos and fish recovery were not very precise. None of the recovery trends for trawl parameters were significant over time. Forecasts are presented based on regression solutions (Table 24).

These forecasts are based on trends observed in the data through August 1990. As recovery proceeds, the rates may change and invalidate the estimates. Therefore, these estimates for recovery should be verified and modified as recovery proceeds.

Some of the parameters measured during this study did not show any effects of full sludge discharge, thus they were not useful in evaluation of recovery. Trawl-caught fish and invertebrates at the 200 m sites were all similar. Numbers of fish species and individuals, and abundances of *Sicyonia ingentis* were not good sludge field indicators. Cd, Cu, and DDTs in tissues were not any higher near the sludge field than at the reference sites.

In our original proposal (1985) we predicted that recovery would be rapid, with most of the recovery occurring within the first year. Our prediction was based on previous studies of recovery in shallower water summarized in the introduction of this report. Probably because of the deeper water depth, the confined nature of the Santa Monica Canyon, and the large amount of sludge in the canyon, recovery is taking much longer than we expected. Based on the results presented in this report, complete recovery from 30 years of sludge discharge into Santa Monica Bay will take at least 15 years.

It is not clear exactly which processes are operating to make recovery occur. Much more extensive oceanographic measurements of currents in the canyon, more extensive deep coring of the sludge field, and more sedimentological studies would have been very informative. The data that we did collect suggests that a combination of erosion by sediment resuspension and down-canyon transport, and burial by clean shelf sediments is probably responsible for the recovery seen so far. More sensitive animals can recolonize the cleaner sediment and bioturbation mixes and dilutes the deeper layers of the old sludge field. This erosion, burial, and mixing should eventually disperse the sludge, transport it down-canyon, or bury it.

Although this report completes the contractual portion of the study of recovery, sampling should continue until full recovery can be demonstrated. The Environmental Monitoring Division at the Hyperion Treatment Plant is currently sampling a sub-set of the stations used in this study and their continuation is strongly encouraged.

Table 24 Forecast for recovery of sludge field based on trends in data collected during this study. Univariate and macrofaunal ordination score regressions were log 10-log 10 transformed; megafaunal and fish ordination regressions were x-axis (time) transformed. * = significant trend of recovery over time, $\alpha = 0.05$; ** = $\alpha = 0.01$. 1. Trend is opposite to what it should be for recovery to occur. 2. This parameter increased to transition values. 3. There was no significant difference in contaminated and reference values under full sludge discharge, thus not useful in evaluating recovery.

Parameter		(n=)	Correlation with time (r)	Forecast for Time of Recovery
Sulfides		9	-0.59	Nov. 1994
TOC		9	-0.61	> 10 Years
TON		9	-0.74*	> 10 Years
Ag		8	-0.57	> 10 Years
Cd		8	-0.56	> 10 Years
Cu		8	-0.67	> 10 Years
Zn		8	-0.66	> 10 Years
DDTs		8	0.27	Opposite[1]
PCBs		8	-0.54	> 10 Years
PAHs		8	-0.20	> 10 Years
Macrofaunal ordination		8	0.998**	Apr. 2002
Macrofaunal	Species	7	0.88**	Aug. 1990
Macrofaunal	Individ.	7	0.81*	Feb. 1988[2]
Megafaunal ordination		7	0.45	Jul. 2001
Megafaunal	Species	7	0.31	Nov. 1997
Megafaunal	Individ.	7	-0.26	Opposite
Fish ordination		7	0.421	Jan. 1998
Fish	Species	7	NSD[3]	
Fish	Individ.	7	NSD	

VIII. REFERENCES CITED

American Public Health Association (APHA), American Water Works Association & Water Pollution Control Federation. 1985. Standard Methods for the Examination of Water and Wastewater, 16th ed. Amer. Public Health Assoc. Washington, D.C.

Anderson, J.W., S.M. Bay, and B.E. Thompson. 1988. Characteristics and effects of contaminated sediments from southern California. Final report to California State Water Resources Control Board. 120 p.

Anderson, J.W. and R. W. Gossett. 1987. Polynuclear Aromatic Hydrocarbon Contamination in Sediments from Coastal Waters of Southern California. Final Report to the California State Water Resources Control Board. 51 p.

Allen, M.J. and R. Voglin. 1976. Regional and local variation in bottom fish and invertebrate populations. Annual report, of the Southern California Coastal Water Research Project, El Segundo, CA. p. 217-221.

Ballschmiter, K. and M. Zell. 1980. Analysis of polychlorinated biphenyls (PCB) by glass capillary gas chromatography. *Fresen. Z. Anal. Chem.* 302:20-31.

Bascom, W. 1978. Life in the bottom. Annual report, of the Southern California Coastal Water Research Project, El Segundo, CA. p. 57-80.

Bascom, W., J. Mardesich, and H. Stubbs. 1982. An improved corer for soft sediments. Biennial Annual Report of the Southern California Coastal Water Research Project. p. 267-271.

Bernstein, B.B. and J. Zalinski. 1983. An optimum sampling design and power tests for environmental biologists. *J. Env. Mgt.* 16:35-43.

Boesch, D.F. 1977. Application of numerical classification in ecological investigations of water pollution. U.S.E.P.A., Ecological Research Series. EPA-600/3-77-033.

Bradfield, G.E. and N.C. Kenkel. 1987. Nonlinear ordination using shortest path adjustment of ecological distances. Ecology 68(3): 750-753.

Byers, S., E. Mills, and P. Stewart. 1978. A comparison of methods of determining organic carbon in marine sediments with suggestions for standard method. Hydrobiologia. 58(1):43-47.

Clifford, H.T. and W. Stephenson. 1975. An Introduction to Numerical Classification. Academic Press, New York. 229 p.

Connell, J.H. 1978. Diversity in tropical rain forests and coral reefs. *Science*. 199:1302-1310.

Cross, J.N. 1988. Fin erosion and epidermal tumors in demersal fish from southern California. Ocean Processes in Marine Pollution. D. Wolfe and T. O'Connor, editors. Krieger Publishing. 5:57-64.

Cross, J.N. 1986. Epidermal tumors in Microstomus pacificus (Pleuronectidae) collected near a municipal wastewater outfall in the coastal waters off Los Angeles (1971-1983). Calif. Fish and Game. 72(2):68-77.

Cross, J.N. 1985. Fin erosion among fishes collected near a southern California municipal wastewater outfall Fishery Bulletin. Vol. 83, No. 2.

Digby, P.G.N. and R.A. Kempton. 1987. Multivariate Analysis of Ecological Communities. Chapman and Hall, New York. 206 p.

Eganhouse, R.P. and R.W. Gossett. 1991a. Sources and magnitude of bias associated with determination of polychlorinated biphenyls in environmental samples. *Anal. Chem.* (in press).

Eganhouse, R., R.W. Gossett, and G.P. Hershelman. 1990. Congener-specific Characterization and Source Identification of PCB Input to Los Angeles Harbor. Final Report to the Los Angeles Regional Water Quality Control Board. September 20, 1990. 34 p.

Eganhouse, R.P. and R.W. Gossett. 1991b. Historical deposition and biogeochemical fate of polycyclic aromatic hydrocarbons in sediments near a major submarine wastewater outfall in southern California. *In:* Organic Substances and Sediments in Waters. Ch. 10. R.A. Baker, ed., Lewis Publishers, Boca Raton, FL. p. 191-220.

Eleftheriou, A. and D.C. Moore *et al.* 1982. Underwater experiments on the effects of sewage sludge on a marine ecosystem. *Neth. J. Sea Res.* 16:465-473.

Emery, K.O. 1960. The sea off southern California, a modern habitat of petroleum. J. Wiley and Sons, New York, NY. 366 p.

Farley, K.J. and A.P. Castro. 1990. Effects of stratification on the deposition of organic material near marine sewage outfalls. *Final report to:* Southern California Coastal Water Research Project. Long Beach, CA.

Gordon, R.L. and N.F. Marshall. 1976. Submarine canyons: Internal Wave Traps. Geophys. Res. Letters. Vol. 3, No.10.

Green, R.H. 1979. Sampling design and statistical methods for environmental biologist. Wiley-Interscience. 257 p.

Greene, C.S. 1976a. Response and recovery of benthos at Orange County. Annual report, of the Southern California Coastal Water Research Project, Long Beach, CA. p. 197-204.

Greene, C.S. 1976b. Partial recovery of the benthos at Palos Verdes. Annual report, of the Southern California Coastal Water Research Project, Long Beach, CA. p. 211-216.

Hagerman, F.B. 1952. The Biology of Dover sole, Microstomus pacificus (Lockington). Calif. Dep. Fish Game, Fish Bull. No. 85. 48 p.

Hartman, O. 1963. Submarine canyons of southern California. Part II, Biology. Allan Hancock Pacific Exped. University of Southern California of Los Angeles, CA. 424 p.

Hedges, J.I. and J.H. Stern. 1984. Carbon and nitrogen determinations of carbonate-containing solids. *Limnol. Oceanogr.* 29:657-663.

Hendricks, T.J. and R. Eganhouse. 1990. Modification and verification of sediment deposition models - Phase 1 Modeling Component. Progress report to: California State Water Resources Control Board. Contract #7-192-250-0. SWRCB, Sacramento, CA.

Hume, N.B. *et al.* 1962. Characteristics and effects of Hyperion effluent. *J. Water Pollution Control Federation.* 34:15-35.

Hunter, J.R., J.L. Butler, C. Kimbrell, and E.A. Lynn. 1990. Bathymetric patterns in size, age, Sexual maturity, water content, and caloric density of Dover sole, Microstomus pacificus. CalCOFI Rep. Vol. 31.

Jones, G.F. and B.E. Thompson. 1984. The ecology of *Parvilucina tenuisculpta* (Carpenter 1865) on the southern California borderland. Veliger. 26:188-198.

Kalil, E. and M. Goldhaber. 1973. A sediment squeezer for removal of pore waters without air contact. *J. Sed. Petrol.* 43:553-557.

Kruskal, J.B. 1964a. Multidimensional scaling by optimizing goodness of fit to a nonmetric hypothesis. Psychometrika. 29:1-27.

Kruskal, J.B. 1964b. Nonmetric multidimensional scaling: a numerical method. Psychometrika. 29:115-129.

Kruskal, J.B. and M. Wish. 1978. Multidimensional Scaling. Sage University Papers on Quantitative Applications in the Social Sciences, series no. 07-011. Beverly Hills and London: Sage Publications. 93 p.

Ludwig, J.A. and J.F. Reynolds. 1988. Statistical Ecology. John Wiley & Sons. New York. 263 p.

Mitchell, F.K. and H.A. Schafer. 1975. Effects of ocean sludge disposal. Annual report, of the Southern California Coastal Water Research Project, Long Beach, CA. p. 153-162.

Oviatt, C.A., M.E. Pilson, and S.W. Nixon *et al.* 1984. Recovery of a polluted estuarine system: A mesocosm experiment. *Marine Ecol. Prog. Sec.* 16:203-217.

Pearson, T.H. and R. Rosenberg. 1978. Macrobenthic succession in relation to organic enrichment and pollution of the marine environment. *Oceanography Marine Bio. Ann. Rev.* 16:229-311.

Pielou, E.C. 1984. The Interpretation of Ecological Data. John Wiley and Sons. New York. 337 p.

Plumb, R. 1981. Procedures for handling and chemical analysis of sediment and water samples. Technical Report EPA/CE-81-1, U.S. Army Corps of Engineers. Vicksburg.

Powell, M.A. and G.N. Somero. 1985. Sulfide oxidation occurs in the animal tissue of the gutless clam, *Solemya reidi*. *Biol. Bull.* 169:164-181.

Prentice, I.C. 1977. Non-metric ordination methods in ecology. J. Ecol. 65:85-94.

Prentice. I.C. 1980. Vegetation analysis and order invariant gradient models. Vetetatio. 42:27-34.

Reish, D.J. 1971. Effects of pollution abatement in Los Angeles harbors. *Mar. Poll. Bull.* 2:71-74.

Rosenberg, R. 1976. Benthic faunal dynamics during succession following pollution abatement in a Swedish estuary. OIKOS 27:414-427.

Sanders, H.L., J.F. Grassle, and G.R. Hampson *et al.* 1980. Anatomy of an oil spill: long-term effects from the grounding of the barge Florida off West Falmouth, Massachusetts. *J. Mar. Res.* 38:265-380.

SCCWRP. 1986. Sedimentation, resuspension, and transport of particulates. In: Southern California Coastal Water Research Project-1986. Long Beach, CA.

SCCWRP. 1987. Seasonal and spatial variations in sediment resuspension. In: Southern California Coastal Water Research Project-1987. Long Beach, CA.

Sibson, R. 1972. Order invariant methods for data analysis. J. Royal Stat. Soc. B, 34(3):311-349.

Smith, G.B. 1974. Some effects of sewage discharge to the marine environment. Ph.D. Dissertation, U.C. San Diego.

Smith, R.W., B.B. Bernstein, and R.L. Cimberg. 1988. Community-Environmental Relationships in the Benthos: Applications of Multivariate Analytical Techniques. Chapter 11 *In:* Marine Organisms as Indicators. Springer-Verlag. New York. p. 247-326.

Swartz, R.C., F.A. Cole, D.W. Schultz, and W.A. Deben. 1986. Ecological changes in the southern California Bight near a large sewage outfall: Benthic Conditions in 1980 and 1983. *Marine Ecol. Prog. Ser.* 31:1-13.

Thompson, B.E., S.M. Bay, and J.D. Anderson *et al.* 1989. Chronic effects of contaminated sediment on the urchin *Lytechinus pictus. Environ. Toxicol. Chem.* 8:629-637.

Thompson, B.E. and S.M. Bay *et al.* 1991. Sublethal effects of hydrogen sulfide in sediment on the urchin *Lytechinus pictus. Mar. Env. Research.* 31:309-321.

Thompson, B.E. and J.N. Cross *et al.* 1984. Sediment and Biological Conditions on Coastal Slopes. *Biennial report*: Southern California Coastal Water Research Project. Long Beach, CA. p. 37-68.

Thompson, B.E., J. Laughlin, and D. Tsukada. 1987. 1985 Reference site survey. *Technical report*: Southern California Coastal Water Research Project. Long Beach, CA. 50 p.

Thompson, B.E., J.D. Laughlin, and D. Tsukada. In revision. Megabenthic assemblages of southern California mainland shelf, slope, and basins. Submitted to Bulletin of Southern California Academy of Science.

Undersea Graphics Inc. 1987. Advance 7-mile Results. July 1987.

Williamson, M.H. 1978. The ordination of incidence data. *J. Ecol.* 66:911-920.

Word, J.Q., B.C. Myers, and A.J. Mearns. 1977. Animals that are indicators of marine pollution. *Annual report*: Southern California Coastal Water Research. Long Beach, CA. p. 199-206.

X. APPENDICES

Appendix 1

Station depths and locations

Station	Depth	Latitude	Longitude
HR-1	100 m	33° 55.76	118° 32.83
HR-2	100 m	33° 55.91	118° 33.08
HR-3	100 m	33° 56.66	118° 33.78
HR-4	100 m	33° 57.83	118° 34.75
HR-5	100 m	33° 58.65	118° 38.53
HR-6	100 m	33° 59.00	118° 39.91
HR-7	200 m	33° 54.08	118° 33.90
HR-8	200 m	33° 55.33	118° 34.33
HR-9	200 m	33° 56.10	118° 35.41
HR-10	200 m	33° 56.66	118° 36.16
HR-11	200 m	33° 57.90	118° 37.58
HR-12	200 m	33° 58.28	118° 39.80
HR-49	111 m	33° 55.75	118° 32.80
HR-50	153 m	33° 55.66	118° 33.21
HR-51	136 m	33° 55.41	118° 33.31
HR-52	198 m	33° 55.23	118° 33.83
HR-53	246 m	33° 55.16	118° 34.61

Appendix 2

Collection dates for grab and trawl samples
(no trawls were collected in Cruises 5 and 7)

Cruise	Dates
1	February 18-24, 1986
2	August 2 - September 4, 1986
3	September 3-9, 1987
Discharge Termination	November 1987
4	January 13-29, 1988
5	April 22-23, 1988
6	July 28 - August 4, 1988
7	November 7-10, 1988
8	January 26 - February 2, 1989
9	August 14-21, 1989
10	January 25 - February 16, 1990
11	August 8-13, 1990

Appendix 3

Methods of sampling and analysis

1. Current Meters

The current measurements were made at a single mooring (Station HR2), located within the canyon in a water depth of 100-108 m (Figure 2). This site is approximately 900 m up-canyon from the terminus of the 7-mile outfall and in a region of complex bathymetry.

Current speeds and directions of flow were recorded at 15-minute intervals, but analyzed at 45-minute intervals. The deployment periods varied in length from 21-38 days.

Analysis consisted of transcribing the film-recorded data into a digital format. The latter was stored on a floppy diskette and combined with current meter calibration information to convert current meter "tilt" into flow speed. A suite of computer programs were used to extract basic statistical information on the properties of the currents.

These include single and joint probabilities of speed and direction, average speed by direction, net flow during the deployment period, the variance about the mean, and the principal axes of variation.

The speed-direction time-series were also converted into velocity (Vx,Vy) time-series, with the two velocity components selected to be aligned with the major and minor principal axes of variation, respectively. A digital fast Fourier transform was used to examine the temporal properties of these velocity time-series. Running-average filters (25-hour, 6-hour) were applied to the original time-series to decompose them into time-series representative of the tidal frequency band, and fluctuations of supertidal and subtidal frequency. Cross-correlations were computed among the various current meter elevations and directions to examine relationships between the flows at the various depths and directions.

2. Sediment Traps

The sediment traps consist of cylindrical PVC tubes with an aspect ratio of 2.5:1, a diameter of 10 cm, and a collection area of 79 cm^2.

At the end of each deployment period, the contents of each trap were analyzed for total dry mass and total volatile solids (TVS). Previous studies by SCCWRP with these traps on the coastal shelf have shown that the distribution of total dry mass collected by the trap often varies with elevation above the bottom according to an equation of the form:

$$F(z) = F(z=0) \exp(-z/h_0)$$

where: $F(z)$ = flux at the elevation z above the bottom
h_0 = characteristic height

Estimates of the sedimentation flux at the sea-surface interface, and the "characteristic thickness" of the depositional flux were obtained from the measured fluxes at the three elevations by a least-squares best fit for the constants $F(z=0)$ and h_0 in the linearized form of equation (1):

$$\ln F(z) = \ln F(0) + (1/h_0)\, z$$

3. C.T.D.-DO

Information on the distribution of salinity, temperature, density, light transmissivity and dissolved oxygen was obtained from hydrocast data collected with a SeaBird or EGG Smart CTD. Data obtained from the CTD casts were examined for the basic properties of the ambient water column, the presence of discharged wastewater, and evidence of the resuspension or transport of particles from the sediments. Parameters measured include water temperature, conductivity, light transmissivity, and dissolved oxygen.

4. Deep Sediment Cores

The approximate boundaries and depth of the sludge field was measured using the SCCWRP sediment corer (Bascom *et al.* 1982). The corer has a 12.5 cm diameter and a 1 m long barrel. The sampling activity was added to the program after the project had begun. Only three exploratory cores were taken in the Santa Monica Canyon prior to discharge termination.

Ten cores were collected during each of the four post-termination sampling periods. The core samples were extruded and longitudinally halved to expose the strata in the sediment. The depth of the sludge layer was measured and the core was photographed. Single composite samples were collected from the sludge layer and below the sludge layer. However, these samples have not been analyzed.

5. Van Veen Grabs

Grab samples were collected with a 0.10 m^2 chain-rigged Van Veen grab. Two separate grab samples were collected at each site. For sediment analyses, subsamples were taken from the grab sample: one for trace metals, grain-size, and organic material, and the second for chlorinated and petroleum hydrocarbons. To collect the subsamples, five small subcores were taken from the top 2 cm of the sample using an open barreled syringe (26 mm diameter), composited, and immediately frozen.

Macrobenthic infauna were collected from the Van Veen grab sample by sieving through a 1.0 mm and 0.5 mm screens. The animals and debris were fixed in 10% borax buffered formalin in sea water. Upon return to the laboratory, the samples were transferred to 70% ethanol for preservation, sorted to major taxa and identified to the lowest taxon practical.

6. Otter Trawls

Megafaunal invertebrates and fishes were collected at each site using an otter trawl, with a 7.6 m headrope 4.2 cm mesh (stretched) net with a 1.3 cm mesh cod-end liner. Trawls were made along the depth contours for 10 min. (estimated time on bottom) and at a speed of 2 kts using a scope of between 2.5:1 and 4.5:1, covering an estimated 0.5 km along the bottom. All organisms collected in the trawls were identified and counted. Total biomass (wet weight) and biomass of the most abundant species were measured. Size measurements were made of Dover sole (standard length) and *Sicyonia ingentis* (carapace length) and samples of both were collected at the 100 m sites, during summer months, for tissue chemistry. The individuals chosen for tissue analysis were frozen whole and transported to the lab.

7. Taxonomy

The following taxonomists identified the animals collected during this study: Polychaetes - Leslie Harris, Larry Lovell, and Diane O'Donohue; Crustaceans and echinoderms - Jim Laughlin David Tsukada; Molluscans - David Tsukada, Don Cadien; others - David Tsukada and Bruce Thompson, and Fish - Dario Diehl.

8. Sediment Grain Size

The sample was thoroughly homogenized by stirring or shaking. Approximately 20-40 g was subsampled and placed in a 1000 ml beaker or flask. For sandy sediments, more was used (~40 g): for finer sediments less was used (~20 g). Twenty-five ml 10% hydrogen peroxide was added to digest organic material. When frothing ceased, an additional 10 ml hydrogen peroxide was added and the sample was boiled to remove any excess hydrogen peroxide. Care was taken to avoid boiling over the sample.

The sample was separated into sand and silt/clay fractions by wet sieving through a 63 um stainless steel sieve. The silt/clay fraction that passed through the sieve was collected and the sand fraction was retained on the sieve. The bottom of the sieve was wrapped with foil to prevent loss of sample, and the sample was dried at 40-50°C.

The silt/clay fraction was transferred to a 1000 ml graduated cylinder and allowed to stand until most of the particles had settled (over night). The water was decanted into 500 ml polypropylene bottles and centrifuged for 20 minutes at 1000 RPM. The clear water from the centrifuged bottles was siphoned off and the remaining fine residue was washed back into the graduated cylinder. Twenty-five ml of 1% Calgon solution was added to the silt/clay fraction to prevent flocculation of the sediment particles.

The sample was then adjusted to 1000 ml with distilled H_2O and observed for flocculation. The sample was vigorously mixed and a 25 ml sample was withdrawn from a depth of 20 cm, 20 seconds after the stirring was stopped (silt fraction). The sample and pipet were rinsed with distilled water into the aluminum weighing dish. A 25 ml sample was taken from a depth of 5 cm at the times tabulated by Plumb (1981) and transferred to a pre-weighed aluminum dish (clay fraction). Twenty-five mls of 1% Calgon solution was also dried in a pre-weighed dish to act as a correction factor in the pipette analysis calculations.

After the sand fraction were dried, a sieve was placed over a smooth sheet of paper. A 1-inch soft bristle paint brush was used to brush the particles across the screen until no fine particles continued to pass through the sieve. The fine particles that passed through the 63 um sieve were dried in a pre-weighed aluminum dish and the dried weight added to the silt fraction. The sieve was inverted and the screen brushed to remove additional sand particles caught in the sieve and added to the sand dish.

Aluminum dishes containing the samples were dried at 50°C and weighed to the nearest 0.0001 g. Calculations were as follows:

Silt weight = ([Net weight sample - Calgon correction factor] X 40) + Additional silt

Clay weight = (net weight sample - Calgon correction factor) X 40

Calgon correction factor = (net weight of 25 ml Calgon) X .025 (ml of Calgon in sample)

9. Total Organic Carbon, Nitrogen, Volatile Solids

Total Volatile Solids (TVS) or total organic material was measured using the methods of Byers *et al.* (1978). Approximately 4 grams of the top 2 cm of surface sediment is dried at 60°C, weighed, then ashed at 500°C for five hours and placed in a desiccator until cool. The ash weight is measured and % TVS calculated using the following formula:

$$\% \text{ TVS} = \frac{\text{Dry Wt. - Ash Wt.}}{\text{Dry Wt.}} \times 100$$

Total Organic Carbon, Nitrogen

Elemental analyses (total organic carbon-TOC, total nitrogen-TN) were carried out on sediments by high temperature (flash) combustion using a Carlo Erba EA1108 elemental analyzer. The sediments were ground with a mortar and pestle, weighed into silver combustion boats, treated for carbonate removal by a modification of the vapor acidification technique of Hedges and Stern (1984) and heated to drive off excess HCl and water. The carbonate-free sediments were then wrapped in tin combustion boats and analyzed on the Carlo Erba elemental analyzer.

Data were acquired with a Carlo Erba EAGER 100 data system which utilizes an IBM-compatible microcomputer. The instrument was calibrated with acetanilide daily. The precision of the sediment analyses for TOC and TN are estimated at < 2% and < 5%, respectively, based on replicate determinations of carbonate-free sediments and sludges. Analysis of acetanilide showed that the instrument yields results within 0.5, 05. and 3.3% of the actual amounts of carbon, nitrogen and hydrogen, respectively. Analysis of National Research Council of Canada standard reference sediments, PACS-1, for total carbon yielded results that agreed with the certified value to within 5.7%. All concentrations presented here are relative to total sediment weight (i.e. including carbonate carbon).

10. Total Sulfides

Total dissolved sulfides were measured at each station by collecting pore water as described by Kalil and Goldhaber (1973). Approximately 25 cc of sediment was squeezed in a specially designed syringe which forced the pore water into a plastic syringe containing approximately .5 cc in acetate, which fixed the sample. Upon returning to the lab total dissolved solids were measured using the methylene blue colormetric method (APHA 1985).

11. Trace Organics Contaminants

Biological tissues were analyzed for chlorinated hydrocarbons (DDT isomers, hexachlorobenzene, polychlorinated biphenyls), whereas sediments were analyzed for chlorinated hydrocarbons **and** polycyclic aromatic hydrocarbons. During the course of this study, a number of changes in methodology occurred as a result of the implementation of new, more advanced techniques and the subcontracting of a portion of the samples for trace metal analysis. These changes are summarized in Table A1.

Because of the changes in methodologies employed during this study, the description of trace organics methods is broken into two categories: 1) *old methods* and 2) *new methods*. In the case of the chlorinated hydrocarbons, the *new method* differs from the *old method* by the use of recovery surrogates and a new internal standard as well as a revised chromatographic cleanup technique. For the PAH analyses, the changes were similar. However, an entirely new calibration standard was prepared and different internal standards were used for given PAH compounds. These differences are elaborated below.

Old method. Frozen sediments were allowed to warm to room temperature and manually homogenized using a clean glass rod. Aliquots of wet sediment were then transferred to a pre-weighed aluminum pan.

The wet sediments were placed in an oven at 60°C overnight after which they were removed, and the pan + sediments were reweighed. The weight difference was used to compute the water content. Subsamples of the oven-dried sediments were placed into glass vials for later analysis (CHN).

A separate aliquot of wet sediment (ca. 40 g) was weighed into a centrifuge bottle. After the sediments had been centrifuged, the supernatant was decanted and the sample was amended with the PAH surrogate spike solution containing naphthalene-d_8, acenapthene-d_{10}, phenanthrene-d_{10}, chrysene-d_{12} and perylene-d_{12}. Then 100 ml of methylene chloride and 50 g anhydrous sodium sulfate were added, the bottle was sealed and placed on a roller table for 16 hours. The sediments were allowed to settle, and the supernatant was decanted into a boiling flask. The centrifuge bottle was then recharged with 100 ml of methylene chloride and the bottle rolled again. After the solvent was combined with the first extract, the procedure was repeated a third time. The combined extract was then reduced in volume by rotary evaporation and dehydrated by passage through a filter paper containing anhydrous sodium sulfate. The extract was then brought to a volume of 50 ml and divided into three fractions: 1) PAH-20 ml; 2) CHC-20 ml; 3) archive-10 ml. These were placed into vials sealed with Teflon liners and stored in a freezer until further processing could be carried out.

Table A1 Summary of the methodologies employed for samples collected during the Hyperion Recovery Study[1]

Cruise: / Analyte[2]	1	2	3	5	6	7	8	9	10	11
Sediments										
CHC	O	O	N	N	N	N	N	N	N	N
PAH	O	O	N	N	N	N	N	N	N	N
TMs	S	S	S	W	S	S	S	S	W	W
Tissues										
CHC	NC	O	N	NC	N	NC	NC	N	NC	N
PAH	NC	NA	NA	NC	NA	NC	NC	NA	NC	NA
TMs:										
DS-liver	NC	S	S	NC	S	NC	NC	L	NC	L
DS-musc	NC	L	L	NC	L	NC	NC	L	NC	L
Syc-hep	NC	S	S	NC	S	NC	NC	L	NC	L
Syc-musc	NC	L	L	NC	L	NC	NC	L	NC	L

1 O-old method; N-new method; S-SCCWRP trace metal analysis (AAS); W-West Coast Analytical Services trace metal analysis (ICP-MS); NC-no collection; L-Los Angeles County Sanitation Districts trace metals analysis (AAS).

2 CHC-chlorinated hydrocarbons (DDTs, PCBs); PAH (polycyclic aromatic hydrocarbons); TMs (trace metals); DV-liver-Dover sole liver; DV-musc-Dover sole muscle; Syc-hep-*Sycionia ingentis* hepatopancreas; Syc-musc-*Sycionia ingentis* muscle.

Each fraction was rotovaped to dryness and taken up in hexane. The PAH fraction was fractionated on activated silica gel as described in Anderson and Gossett (1987) and Thompson *et al.* (1987). The CHC fraction was cleaned up on Florisil as described in Thompson *et al.* (1987). In the case of the PAH fraction, analyses were performed by GC/MS on a Hewlett-Packard 5970B with quantitation by the internal standard method (anthracene-d_{10}: internal standard). The DDT compounds (*o,p'*-DDE, *p,p'*-DDE, *o,p'*-DDD, *p,p'*-DDD, *o,p'*-DDT, *p,p'*-DDT), hexachlorobenzene and the Aroclors (1242, 1254) were quantified by the internal standard method using mirex. In the case of the PCBs, quantitation was referred to the respective Aroclors with one peak being used for quantitation of 1242 and two peaks for 1254. The concentrations of 1254 reported here represent the average of the concentrations determined by the two peaks (cf. Eganhouse and Gossett 1991a). Details of the instrumental analysis can be found in Thompson *et al.* (1987).

Tissues were extracted by procedures also outlined in Thompson *et al.* (1987). The final extract was transferred to hexane and fractionated on Florisil as described therein. Instrumental analyses were carried out in the same fashion as described above.

New method. Sediments were extracted as described for the *old method*. However, in addition to amending the sediments with PAH recovery surrogates, each sample was spiked with a solution containing three PCBs (congeners 30, 112 and 198; cf. Ballschmiter and Zell 1980). Details of the extraction and subsequent cleanup steps are given in Eganhouse *et al.* (1990). The combined extract was concentrated to a small volume, treated for water and sulfur removal and analyzed gravimetrically on a Cahn 31 microbalance to determine the concentration of total extractable organics (TEO). These data provided a basis for using an aliquot of final extract corresponding to $\leq$ 25 mg of TEO for adsorption chromatography. The aliquot was transferred to hexane and fractionated on a 1:2 alumina/silica gel column (each deactivated with 3% water). A fraction corresponding to the PAH + chlorinated hydrocarbons was isolated. This fraction was concentrated by rotary evaporation, transferred to a vial. After being amended with internal standard solutions containing hexamethylbenzene and benzo[b]fluoranthene-d_{12} (PAH) and PCB congener 207 (chlorinated hydrocarbons), this fraction was subjected to instrumental analysis.

The PAH were quantified on a Hewlett Packard 5790B benchtop GC/MS in the full scan, electron impact mode. Gas chromatographic and mass spectral acquisition conditions can be found in Eganhouse and Gossett (1991b). The internal standard method was used, and no correction for recovery has been made. The chlorinated hydrocarbon analyses were performed as described for the *old method* with the exception that PCB congener 207 was used in place of mirex. Moreover, recoveries for the three PCB recovery surrogates were determined (although no correction for recovery was made).

12. Trace Metal Contaminants

During the course of this study SCCWRP lost its ability to perform trace metals measurements. As indicated in Table A2 most of the sediment analyses (70%) and a small portion of the tissue analyses (24%) had been completed by the time this occurred. After consulting with Sam Cheng at Hyperion, we decided to have these analyses carried out under sub-contract by a separate laboratory. After investigating laboratories capable of meeting rather rigorous detection limit specifications, we selected West Coast Analytical Services, Inc. (WCAS).

As a preliminary attempt to guarantee intercomparability between the existing dataset generated at SCCWRP and the remaining analyses we carried out an intercalibration with WCAS using standard reference materials (SRMs) from the National Research Council of Canada and one sediment from Santa Monica Bay previously analyzed by SCCWRP. The intercalibration for tissues was unsuccessful and will not be discussed here. What follows is a brief recapitulation of the sediment analysis intercalibration.

Table A3 shows the results of the intercalibration using two separate standard reference materials, PACS-1 and MESS-1 and the Santa Monica Bay sediment, HR-9-2. These materials come from the National Research Council of Canada and have previously been used in a SCECS (Southern California Environmental Chemistry Society) intercalibration among wastewater treatment plant laboratories in southern California. These SRMs are estuarine sediments delivered as a dry powder. It should be noted that the methodologies used by the SCCWRP and WCAS laboratories, described below, differ. WCAS uses ICP-MS (inductively coupled plasma-mass spectrometery), whereas SCCWRP uses AAS (atomic absorption spectrophotometry). The data provided by the Canadian NRC is based on *total dissolution* of the sediment. This contrasts with procedures employed by SCCWRP and WCAS which rely upon acid digestion using HNO_3 and HCl or HNO_3 alone. In such digestions, silicate minerals are not dissolved, and some fraction of certain metals, trapped within the crystal lattice, is not extracted. The difference in digestion procedures employed by the NRC and SCCWRP/WCAS is believed to account for the sometimes higher concentrations reported by the NRC.

These variations in technique notwithstanding, the data produced by SCCWRP and the WCAS generally show acceptable agreement. The only obvious differences are for Cr (not of concern in this study) and possibly Cd. WCAS obtained higher concentrations for Cr for both of the reference materials. Given the fact that the concentrations obtained by the NRC for Cr exceed those of WCAS and SCCWRP to a greater extent than for any other metal, the discrepancy between the SCCWRP and WCAS measurements may reflect some difference in extraction efficiency during the digestion step. The only other apparent discrepancy is for the Cd results obtained with the PACS-1 reference material. It is difficult to explain why agreement was found for MESS-1 and not for PACS-1 in the case of Cd.

Table A2 Results of intercomparison exercise between West Coast Analytical Services and SCCWRP using National Research Council of Canada Standard Reference Materials

Metal	Concentrations (μg dry g^{-1}) Certified value	SCCWRP	WCAS
	MESS-1		
Cr	71.	34.	27.4
Ni	29.5	21.	21
Cu	25.1	23.	20.9
Zn	191.	165.	150.
Ag	--	--	0.1
Cd	0.59	0.55	0.52
Pb	34.0	23.	29.7
	PACS-1		
Cr	113.	77.	54.5
Ni	44.1	32.	29.
Cu	452.	459.	328.
Zn	824.	792.	650.
Ag	--	--	1.08
Cd	2.38	2.6	1.44
Pb	404.	384.	396.
	HR-9-2		
Cr	--	--	151.
Ni	--	--	27.3
Cu	--	90.0	81.7
Zn	--	127.	93.5
Ag	--	3.20	2.79
Cd	--	1.90	2.42
Pb	--	--	37.0

Table A3 Results of analyses of NIST standard reference materials by the Los Angeles County Sanitation Districts' San Jose Creek laboratory.

Element	Concentration ($\mu g\ g^{-1}$) Bovine liver Cert. value	LACSD	Oyster Tissue Cert. value	LACSD
Cd	0.44 $\pm$ 0.06	0.39	4.15 $\pm$ 0.38	3.83
Cu	158. $\pm$ 7.	168.	66.3 $\pm$ 4.3	79.2
Ag	0.04 $\pm$ 0.01	<0.13	1.68 $\pm$ 0.15	1.41
Zn	123. $\pm$ 8.	113.	830. $\pm$ 57.	768.

Results obtained for the Santa Monica Bay sediment, HR-9-2, show no obvious systematic difference. Concentrations reported by WCAS for Cu, Zn, and Ag are all lower by $\leq$ 27% than the SCCWRP results. By contrast, the concentration of Cd is 27% higher. Although these data are limited in number, the degree of intercomparability would appear to be acceptable relative to the magnitude of changes expected in the field over time.

As noted earlier, the intercomparison exercise for tissue samples was not successful with WCAS. Therefore, we approached the Los Angeles County Sanitation Districts' (LACSD) laboratory in San Jose Creek, California, because of their experience with the analysis of tissues for trace metals. Although SCCWRP's most recent intercalibration (within SCECS) involved liver and muscle tissues of dogfish supplied by the Canadian NRC, these materials do not have certified concentrations for Ag. Consequently, the LACSD laboratory chose to use NIST (National Institute for Standards and Technology) reference materials which have been certified for the four metals of interest in this study. These are the bovine liver () and the oyster tissue (..) SRMs. Table A3 summarizes the results obtained by the LACSD using methods to be described later. In general, agreement between the LACSD results and the certified values is good. However, it must be recognized that the concentrations in these SRMs exceed those likely to be found in the Dover sole and prawn muscle tissues from Santa Monica Bay. On the basis of these data, however, we decided to proceed with the analyses. Presently, the results are being prepared and will be reported in a forthcoming addendum. Following are brief descriptions of the methods used to analyze sediments and tissues for trace metals by the SCCWRP, WCAS, and LACSD laboratories.

SCCWRP methods. Details of the method of sediment and tissue digestion and analysis are given in Thompson *et al.* (1987). Briefly, sediment was weighed into a glass-covered beaker and dried to constant weight at 75°C. Following homogenization of the oven-dried sediments, an aliquot (1-2 g) was wet ashed with 20 ml of a 1:1 mixture of concentrated HNO_3/deionized water. In the case of tissues, the wet sample was added directly to the beaker after which the acid was added. The contents of the beaker were heated to incipient boiling, and the liquid was reduced in volume to near dryness. The same procedure was repeated once again. Then a 20 ml solution of 1:3 HCl (conc.)/water was added to the residue and boiled for 20 minutes in order to reduce the liquid volume to about 10 ml. This material was cooled to room temperature and filtered through a Whatman # 40 filter paper. The volume of the filtrate was then adjusted to 50 ml with deionized water. The sediment digests were aspirated into an air-acetylene flame for analysis on a Varian AA6 atomic absorption spectrophotometer (simultaneous background correction). However, silver and cadmium concentrations were low enough in Dover sole livers that the analyses had to be performed by graphite furnace AAS. Concentrations were determined by direct comparison with a calibration curve developed on the same day using freshly prepared standard solutions. Precision is estimated at <5%. Information on the detection limits for the flame analysis are given in Thompson *et al.* (1987).

WCAS method. In the case of sediment samples, 0.5 grams of dry powder were placed inside a glass test tube and digested in 2 ml of concentrated HNO_3 for two hours at 120°C. The digest was cooled to room temperature, an internal standard solution containing Sc, In and Tb was added, and the volume of the sample was brought to 100 ml with redistilled water. The diluted digest was then filtered through a 0.8 μm filter as described above.

Diluted digests were analyzed on a VG Plasma Quad inductively coupled plasma-mass spectrometer (Model PQ2 Turbo Plus). The mass spectrometer was operated in the full scan mode (2-250 amu) with quantitation ions selected so as to minimize interference. Precision is estimated at 10-15%. Analysis of SRM 1646 (estuarine sediment) on 3/19/91 for Cd and Pb yielded the following results: Cd-0.4 $\mu g\ g^{-1}$, Pb-26.4 $\mu g\ g^{-1}$. The NIST certified values for Cd and Pb are 0.36 and 28.2 $\mu g\ g^{-1}$, respectively.

LACSD method. Approximately 0.5 g of homogenized tissues is weighed into a 250 ml Erlenmeyer flask to which 10 ml of concentrated HNO_3 is added. A condenser is attached to the flask, and the sample is refluxed for one hour. The flask is removed from the hot plate, and after the digest has cooled to room temperature an additional 10 ml of HNO_3 and 30% H_2O_2 are added. The sample is then refluxed for an additional 1.5 hours. The condenser is then removed, and the flask is heated to reduce the volume to approximately 15 ml. The digest is filtered through a 25 mm glass fiber filter. The filtrate is collected in a 25 ml volumetric flask and brought to volume with naopure water. The digest is then diluted such that the concentration of HNO_3 is 16% that of concentrated acid.

Cadmium, copper and silver were analyzed by graphite furnace atomic absorption spectrophotometry (GFAAS). Instrumental analysis was carried out on a Thermo Jarrel Ash, Smith-Hieftje 12 AAS equipped with a Thermo Jarrell Ash Controlled Temperature Furnace 188 accessory. Samples are injected using a FASTAC aerosol automated sample injector. Samples are dried, pyrolyzed and atomized in a cylindrical non-pyrolytically coated graphite tube. Quantitation is achieved using peak areas, comparing sample runs against a standard curve.

Zinc is analyzed using a Thermo Jarrell Ash Video 22E atomic absorption spectrophotometer with a premix burner assembly and a lean air/acetylene mix. Instrument response is measured in terms of peak height, and, again, quantitation is by comparison of sample peak heights with a standard curve.

13. Dissections of S. ingentis and Dover sole for tissue chemistry samples

Frozen specimens were allowed to partially thaw for about 1 h. The specimen was blotted and weighed whole to the nearest .1 g. The length was measured and the sex recorded.

Dissections were conducted under "clean" conditions using sterile utensils with Teflon tips and deionized water.

The hepatopancreas or liver was carefully removed and placed into a pre-weighed vial kept on ice. Samples from several individuals were composited and the incremental vial wt. was used to calculate sample wt. Similarly, samples of muscle tissue (*Sicyonia* tail; Dover sole meat) were composited. Details of the composites collected are shown in Appendix 7.

The composites of each tissue at each site were homogenized, then split into trace metals and trace organics samples. Those samples were then frozen to - 20°C to await extraction.

14. Sediment Toxicity Tests

Sediment samples were collected during three Hyperion Termination cruises between August 1989 and August 1990. Sediment from each of three zones (control, transition, and contaminated) at the 100 m and from the sludge field in Santa Monica Canyon were collected. Surface sediment (upper 2 cm) was removed from the Van Veen grab sample, placed in a plastic jar and stored under refrigeration for up to two weeks before use in toxicity tests.

The stations sampled and the degree of replication varied between collection dates because of sampling difficulties, equipment limitations, and limited availability of test specimens. A single sediment sample from Stations HR1, 2, 4, 5, 6, 50, and 51 was tested in August 1989. Duplicate grab samples from Stations 6 and 50 were tested during the February 1990 experiments. Duplicate samples from Stations HR1, 2, 3, 4, 5, 6, 50, and 51 were tested in August 1990.

Two toxicity tests using the amphipod, *Grandidierella japonica*, were conducted on each set of samples. A 10-day survival test done at 15°C was used to document short-term toxicity on samples from the control and canyon zones. Sediment from the amphipod collection site in Newport Bay was used as a laboratory control for statistical comparisons. These data were compared to toxicity test results for Station HR50 sediment samples collected during other research projects in November 1987 and April 1988.

A 28-day amphipod growth test was conducted on sediment from all of the stations sampled during each survey. This test was conducted at 20°C using juvenile amphipods (two to seven days old). The survival and increase in body length growth of amphipods during the exposure period was measured.

15. Numerical Analysis

Ordination is a technique which simultaneously uses abundances of all species to summarize the patterns of overall community change. With this technique, samples are represented as points positioned in a multidimensional space. The positions of the sample points in the space depend on the relative community composition of the corresponding samples. Samples with similar community composition will be relatively close in the space, and those with very different communities will be relatively far apart. Thus, the distance between a pair of samples in the ordination space is a relative measure of how different are the communities in the two samples.

General discussions of ordination techniques are found in Gauch (1982), Pielou (1984), Digby and Kempton (1987), Ludwig and Reynolds (1988), and Smith *et al.* (1988). The specific ordination method used in the present study is called local nonmetric multi-dimensional scaling (Sibson 1972; Prentice 1977, 1980; Kruskal 1964a, 1964b; Kruskal and Wish 1978).

The data input to the ordination technique is a matrix of intersample dissimilarity index values contrasting the communities found at all pairs of samples. A pair of samples with similar species composition and abundances will have a relatively low dissimilarity value, and vise versa for sample pairs with very different communities.

The particular index used is called the Bray-Curtis, Czekanowski, or percent (dis)similarity index (Clifford and Stephenson 1975, Boesch 1977).

Dissimilarity values were re-estimated using the step-across method (Williamson 1978, Smith 1984, Bradfield and Kenkel 1987). Here, the longer dissimilarity values are re-estimated from the shorter dissimilarity values. If one thinks of dissimilarity values as distances, the manner in which a dissimilarity value is re-estimated is analogous to computing the shortest distance between two cities on a road map by adding the distances between the cities which must be passed through on the way from one city to the other. With the present application, all dissimilarity values above .8 are re-estimated by the step-across procedure. This value (.8) is the point where the Bray-Curtis dissimilarities begin to lose sensitivity.

Before use in the dissimilarity index computations, the species abundance data for each separate impact and control area were pooled (averaged) for each survey.

The data were then transformed by a square root and standardized by the species mean (of values > 0).

Appendix 4

List of sediment parameters measured.

1. **Sediment Quality:**

Gravel
Sand
Silt
Clay
Total Organic Carbon
Total Nitrogen
Total Sulfides

2. **Trace Metals:**

Silver (Ag)
Cadmium (Cd)
Copper (Cu)
Zinc (Zn)

3. **Chlorinated Hydrocarbons:**

Hexachlorobenzene
o,p' DDE
p,p' DDE
o,p' DDD
p,p' DDD
o,p' DDT
p,p' DDT
Aroclor 1242
Aroclor 1254

4. **Polynuclear Aromatic Hydrocarbons (PAHs)**

Napthalene
C1-Napthalenes
C3-Napthalenes
Biphenyl
Phenanthrene
C1-Phenanthrenes
C2-Phenanthrenes
C3-Phenanthrenes
Anthracene
Fluoranthene
Pyrene
2,3-Benzofluorene
Benz(a)anthracene
Chrysene
Benzo(b)fluoranthene
Benzo(k)fluoranthene
Benzo(e)pyrene
Benzo(a)pyrene
Perylene
9,10-Diphenylanthracene
Dibenz(ah)anthracene
Benzo(ghi)perylene

Appendix 5

CTD profiles. Station and dates are shown on each figure
(Pages 99 - 107).

Hyperion Recovery - Cruise 2 (CD238-46,1986)

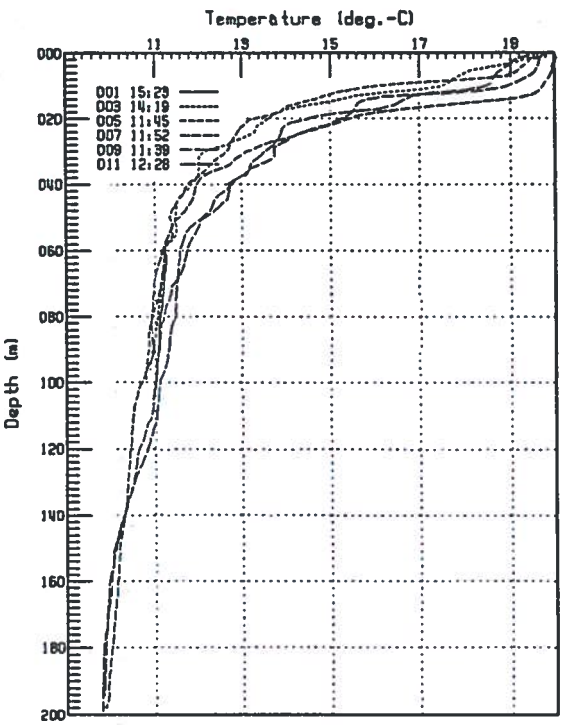

Hyperion Recovery - Cruise 4 (CD043, 1987)

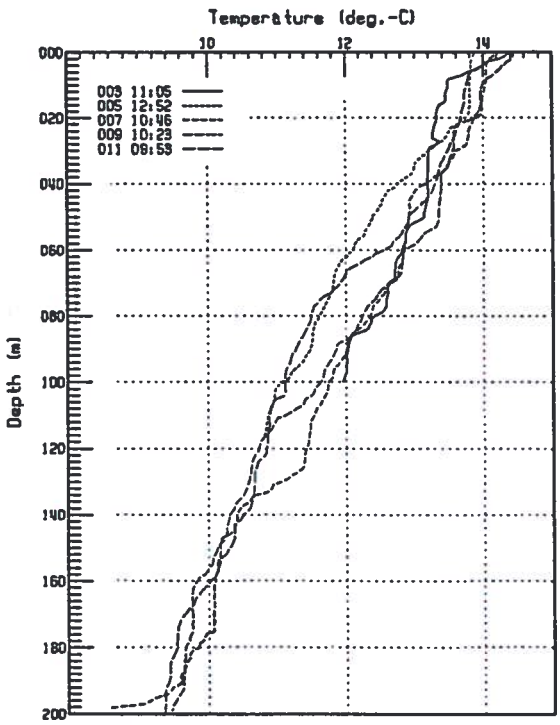

Hyperion Recovery - Cruise 6 (CD218, 1988)

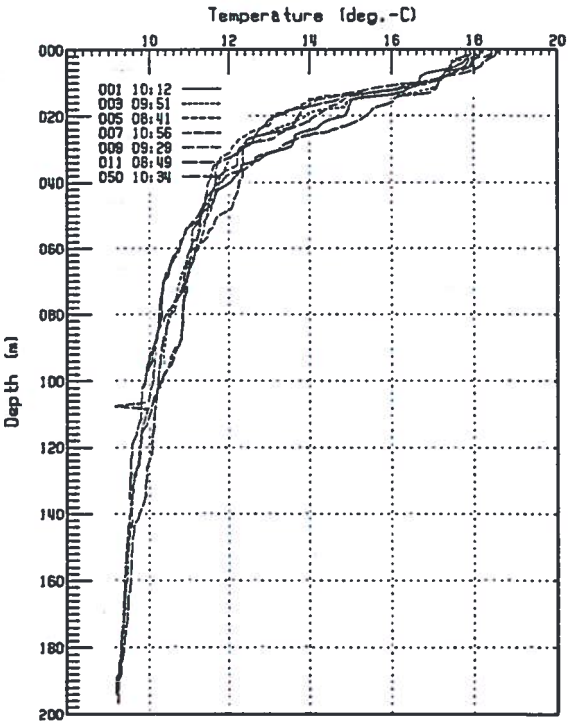

Hyperion Recovery - Cruise 8 (CD031, 1988)

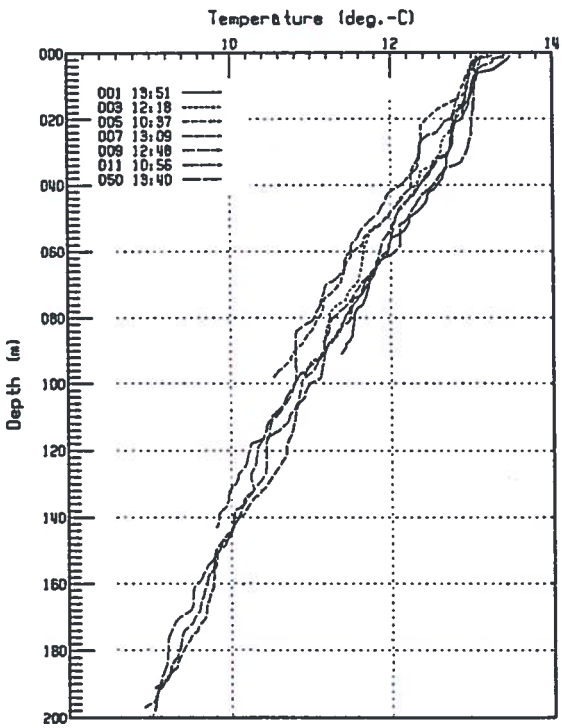

Hyperion Recovery - Cruise 9 (CD236, 1989)

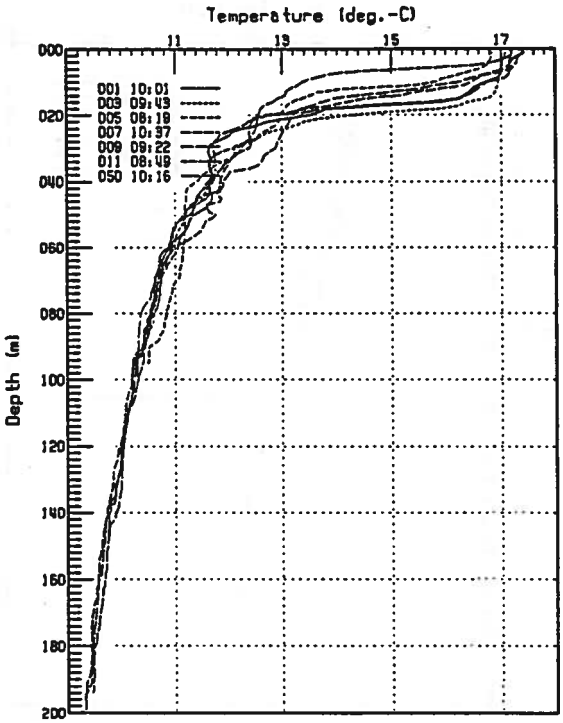

Hyperion Recovery - Cruise 10 (CD047, 1990)

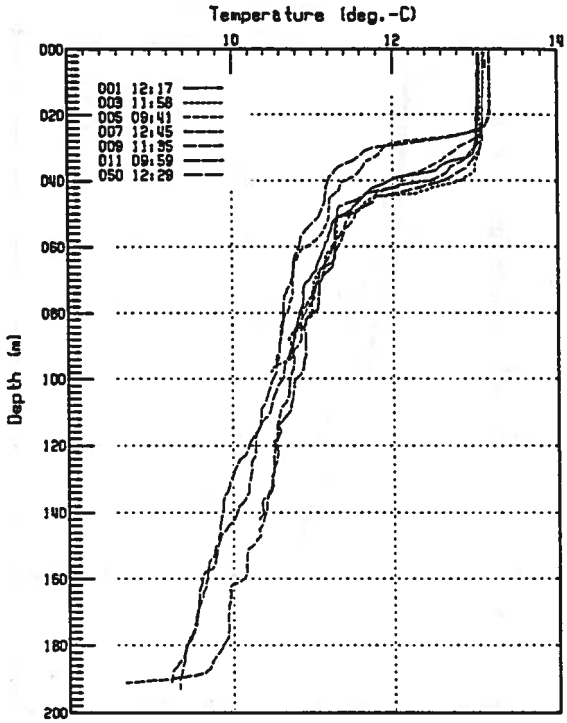

Hyperion Recovery - Cruise 11 (CD226, 1990)

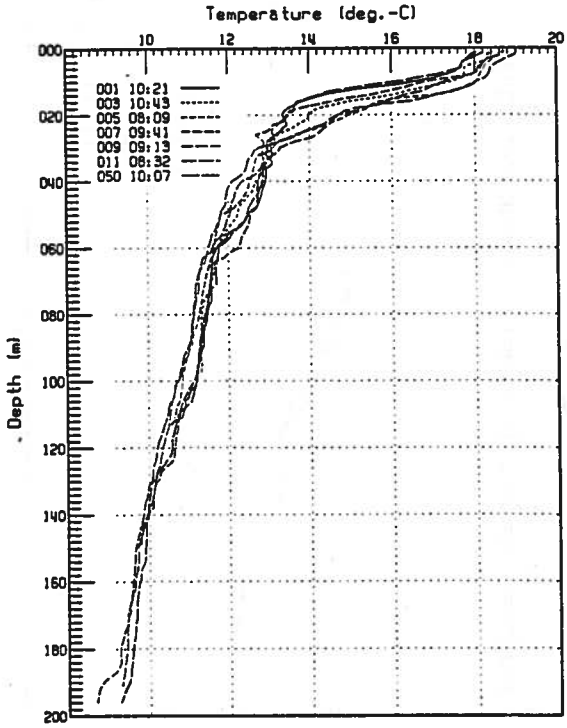

Hyperion Recovery - Cruise 2 (CD238-46, 1986)

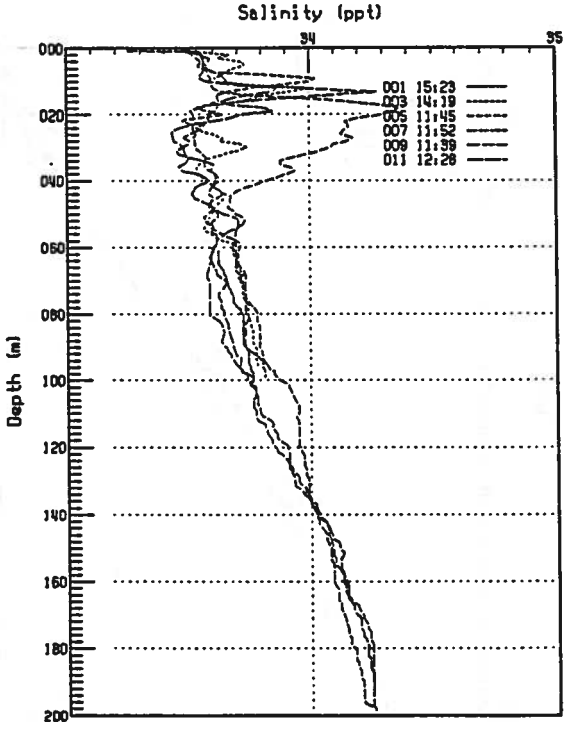

Hyperion Recovery - Cruise 4 (CD043, 1987)

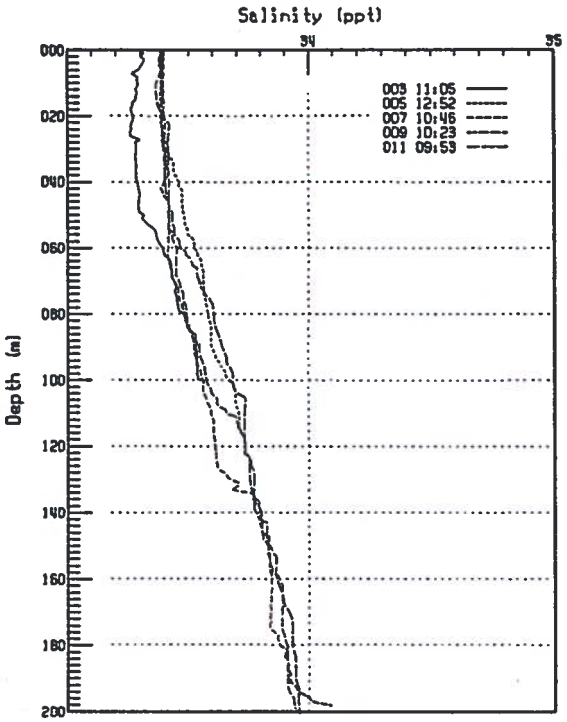

Hyperion Recovery - Cruise 6 (CD218, 1988)

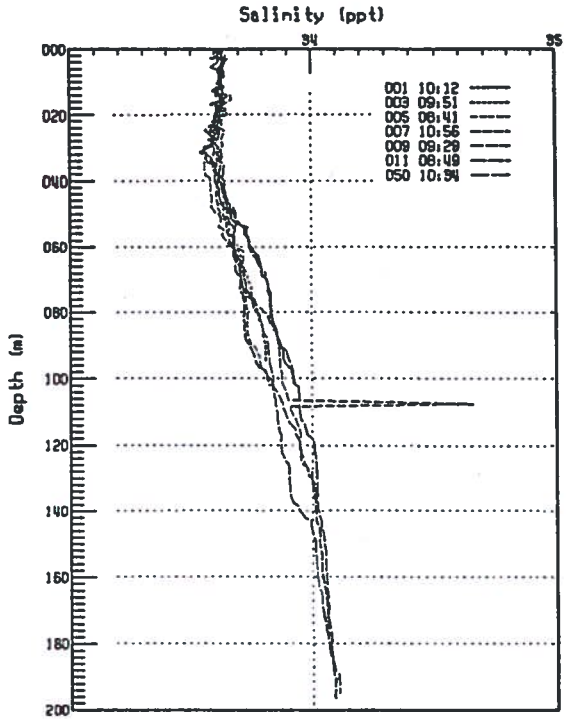

Hyperion Recovery - Cruise 8 (CD031,1989)

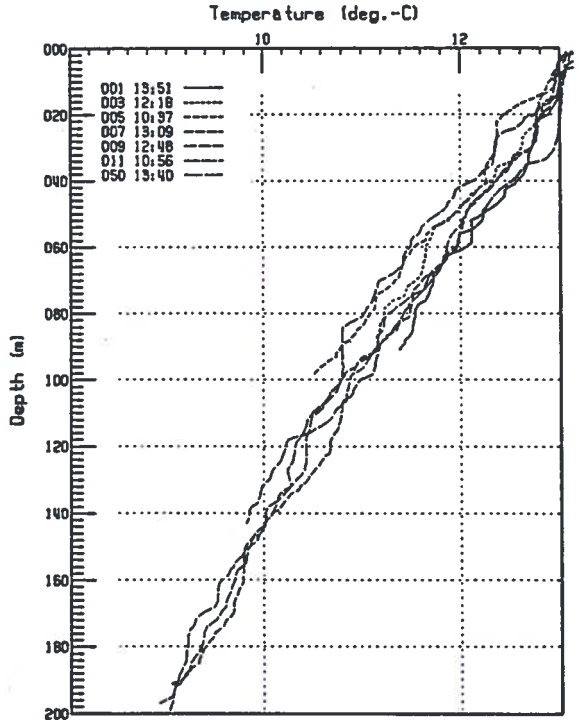

Hyperion Recovery - Cruise 9 (CD236,1989)

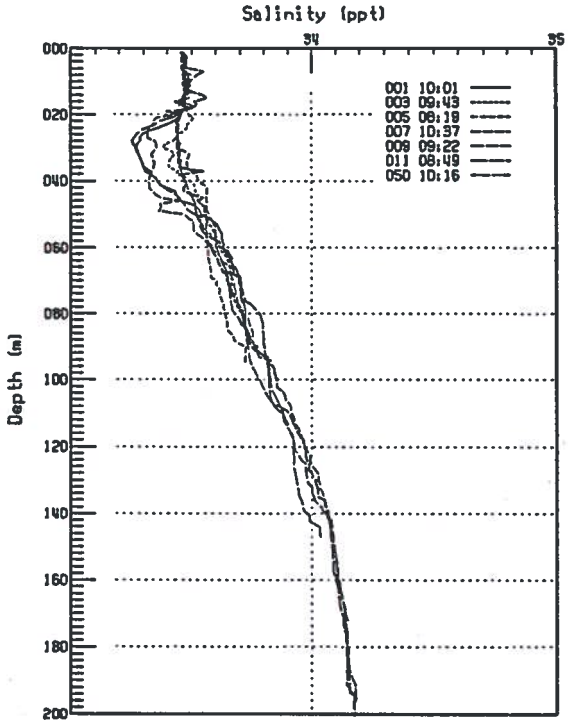

Hyperion Recovery - Cruise 10 (CD047, 1990)

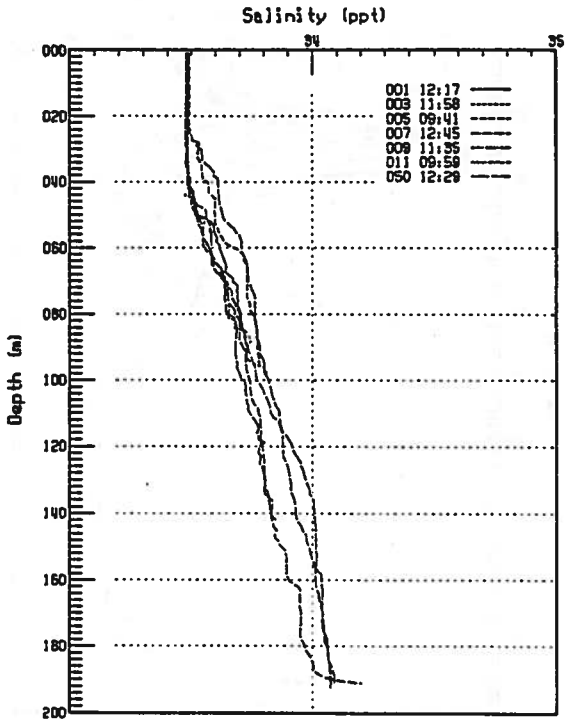

Hyperion Recovery - Cruise 11 (CD226, 1990)

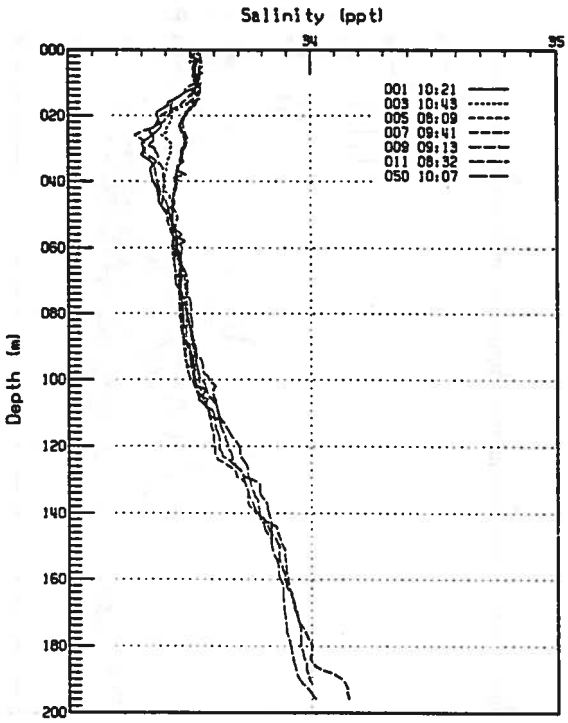

Hyperion Recovery - Cruise 4 (CD043, 1987)

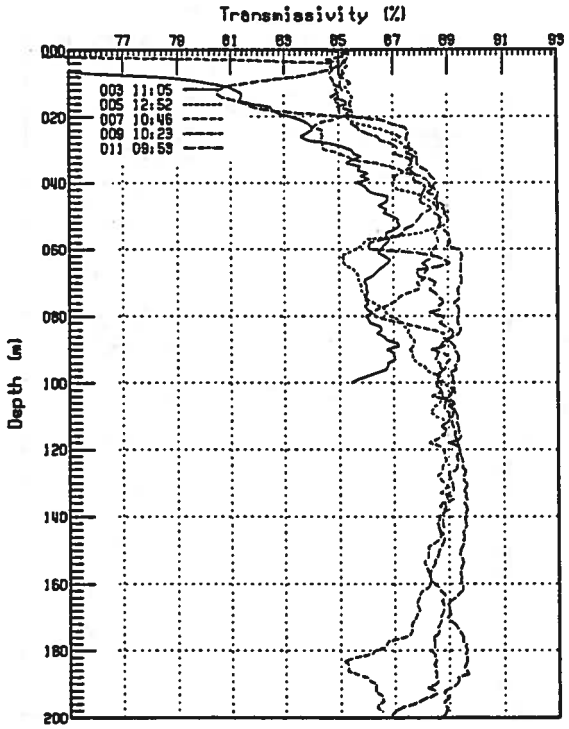

Hyperion Recovery - Cruise 6 (CD218, 1988)

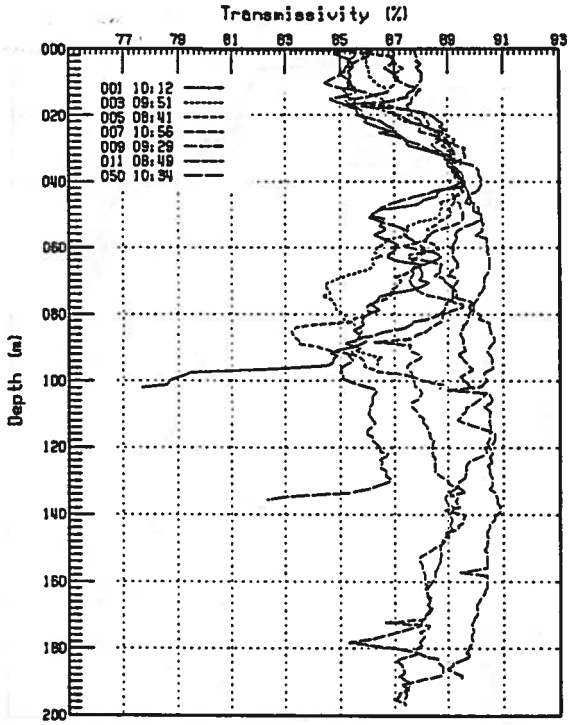

Hyperion Recovery - Cruise 8 (CD031, 1988)

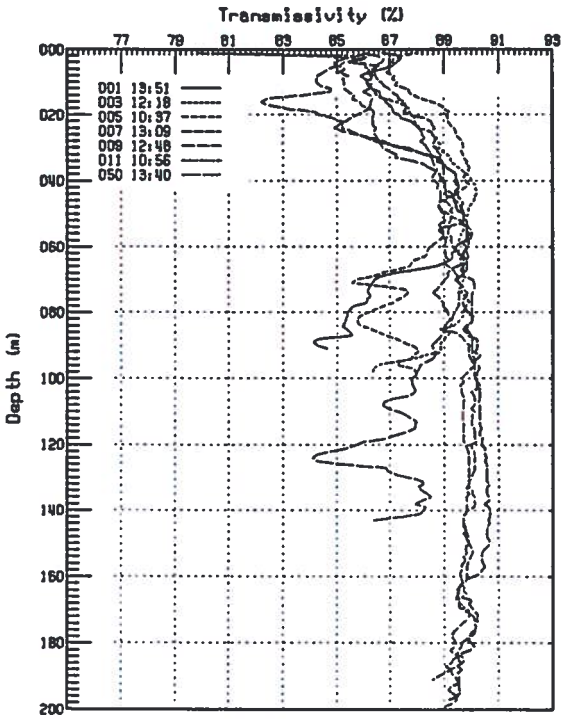

Hyperion Recovery - Cruise 9 (CD236,1989)

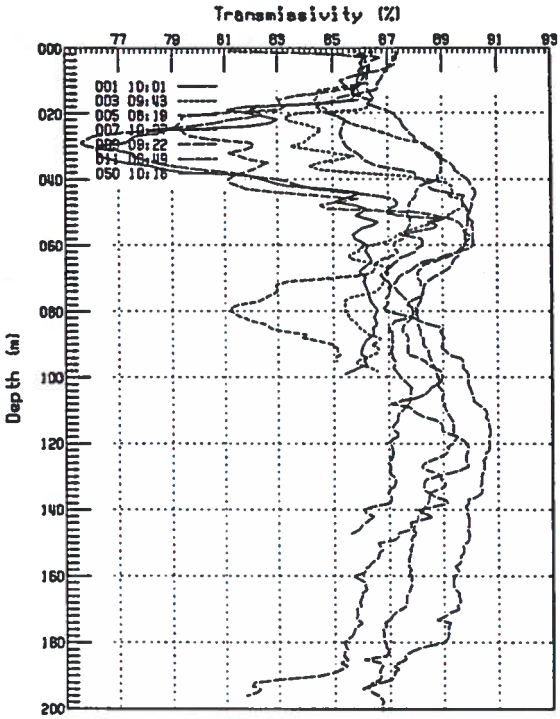

Hyperion Recovery - Cruise 10 (CD047, 1990)

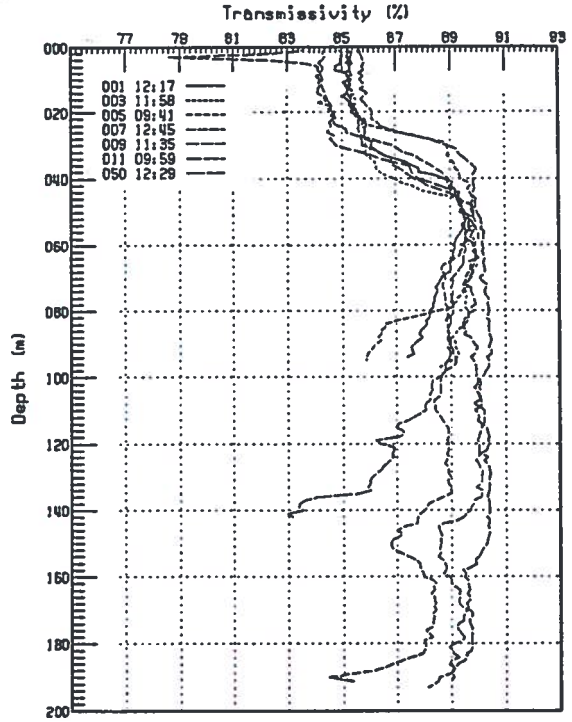

Hyperion Recovery - Cruise 11 (CD226, 1990)

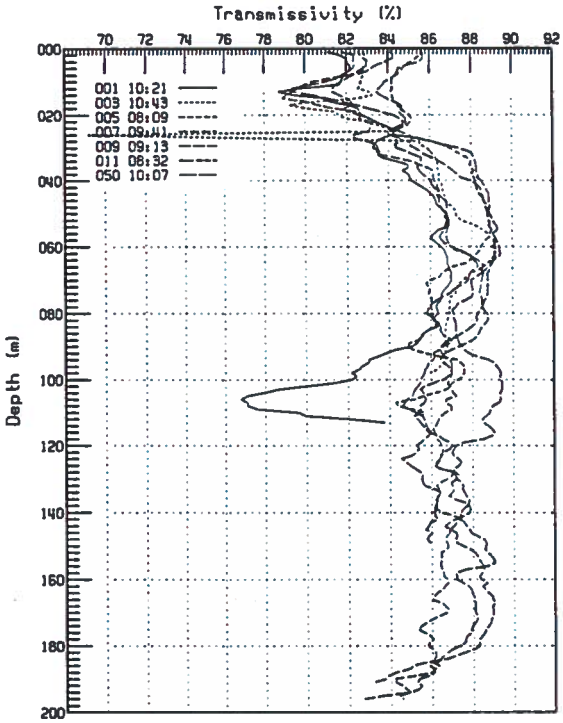

Hyperion Recovery - Cruise 2 (CD238-46,1986)

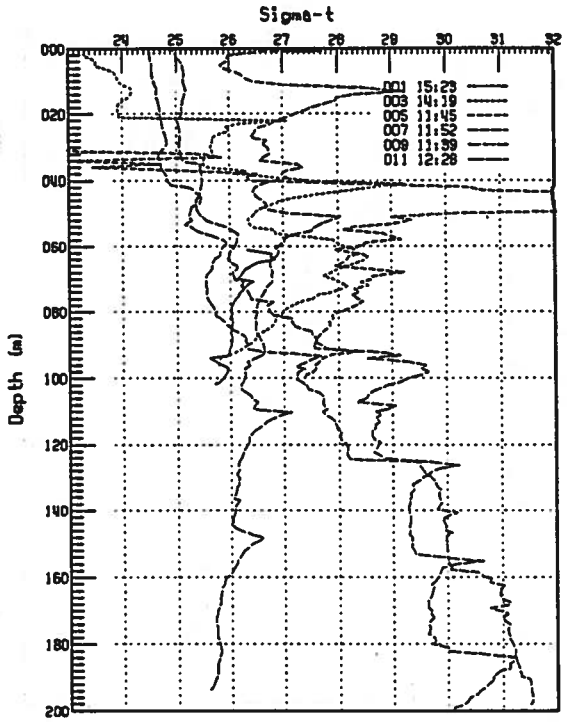

Hyperion Recovery - Cruise 4 (CD043, 1987)

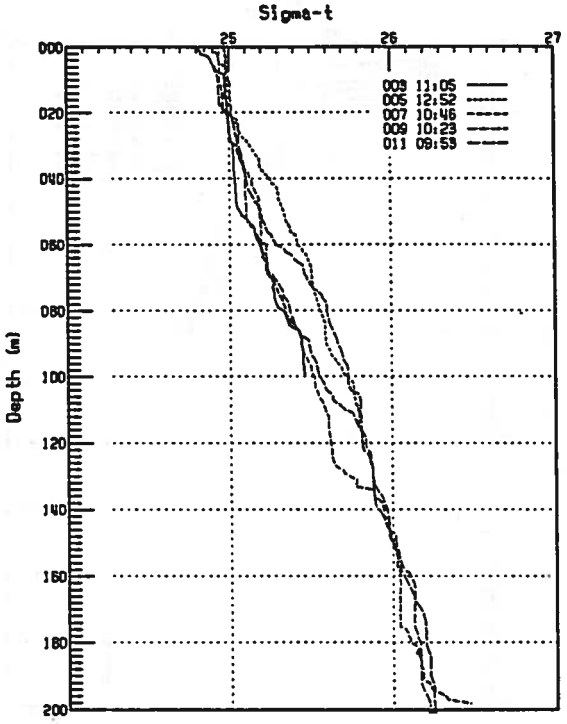

Hyperion Recovery - Cruise 6 (CD218, 1988)

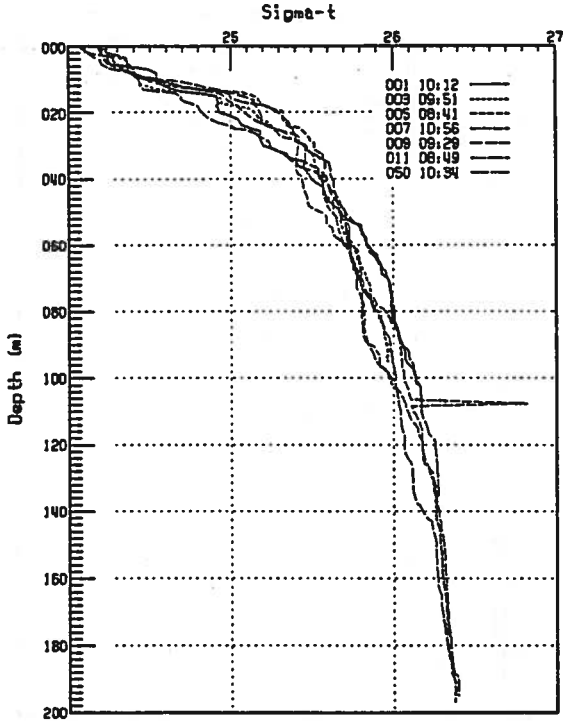

Hyperion Recovery - Cruise 8 (CD031, 1988)

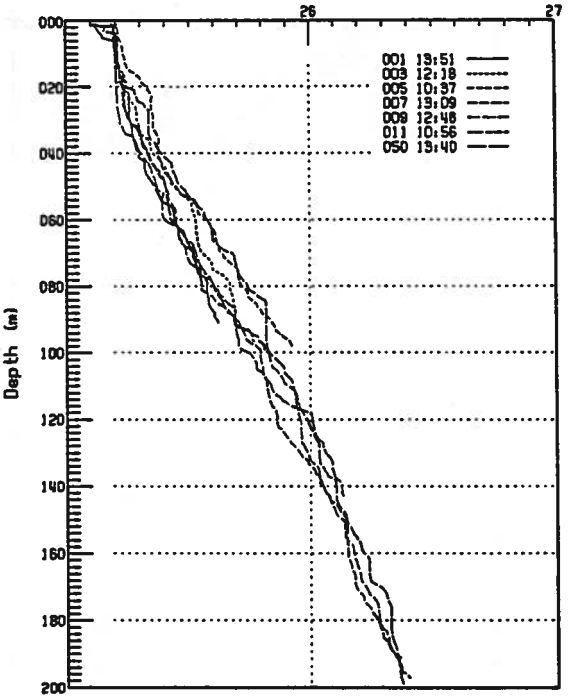

Hyperion Recovery - Cruise 9 (CD236,1989)

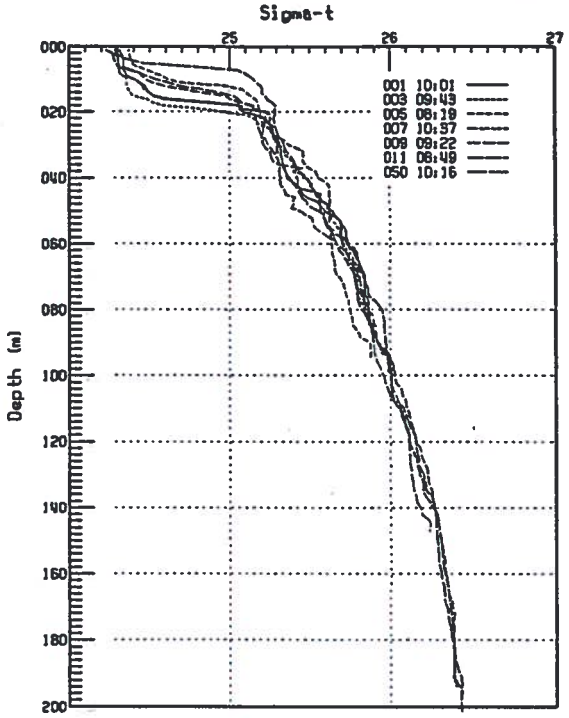

Hyperion Recovery - Cruise 10 (CD047, 1990)

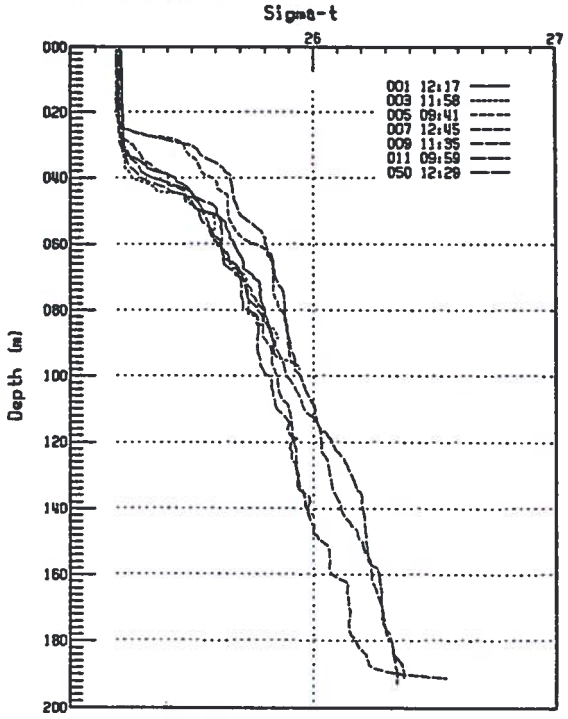

Hyperion Recovery - Cruise 11 (CD226, 1990)

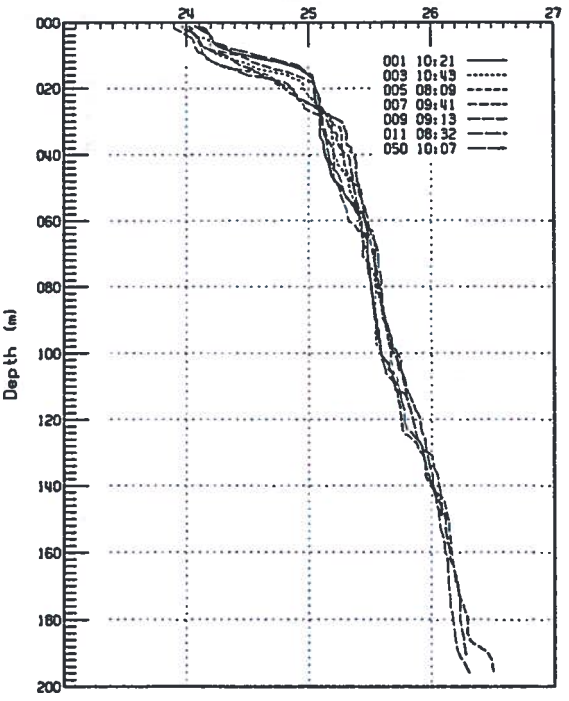

Hyperion Recovery - Cruise 4 (CD043, 1987)

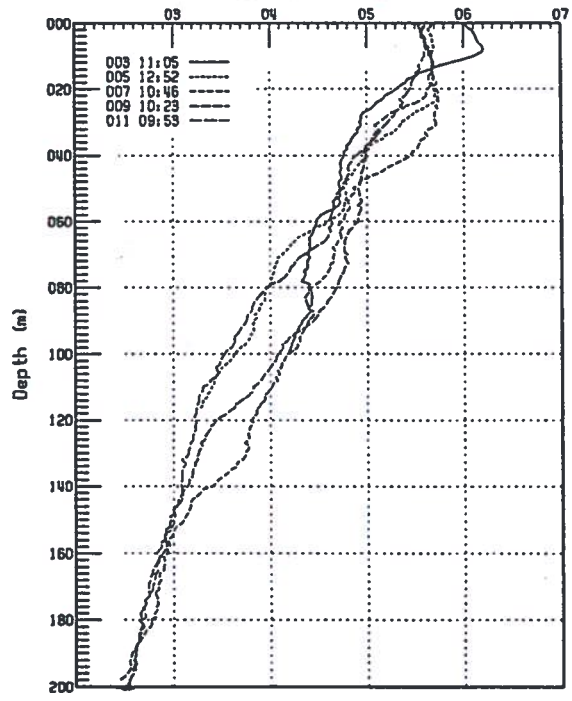

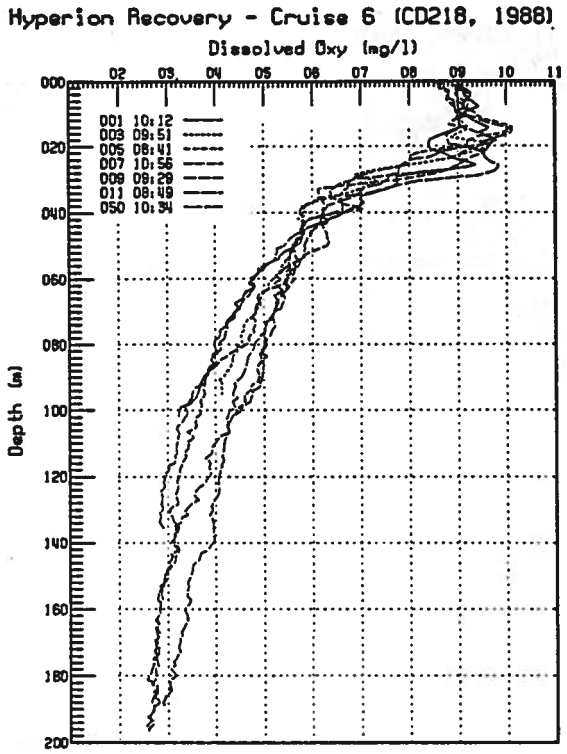
Hyperion Recovery - Cruise 6 (CD218, 1988)
Dissolved Oxy (mg/l)
Depth (m)
001 10:12
003 09:51
005 08:41
007 10:56
009 09:28
011 08:49
050 10:34

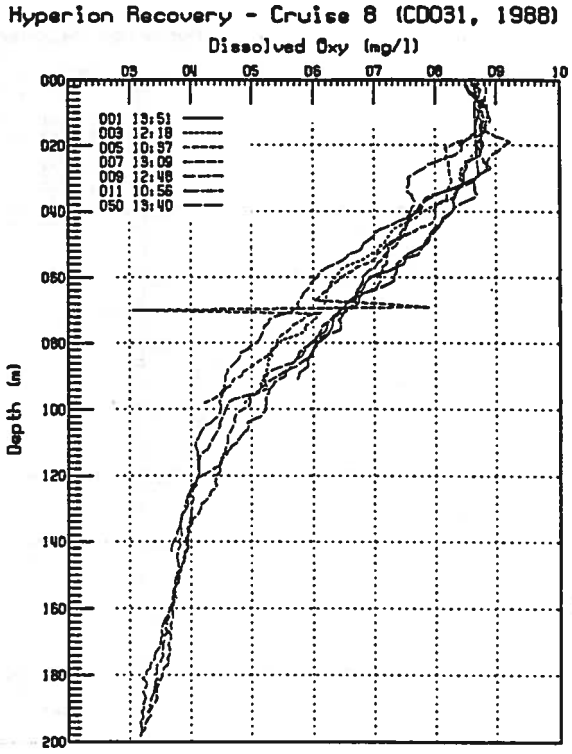
Hyperion Recovery - Cruise 8 (CD031, 1988)
Dissolved Oxy (mg/l)
Depth (m)
001 13:51
003 12:18
005 10:37
007 13:09
009 12:48
011 10:56
050 13:40

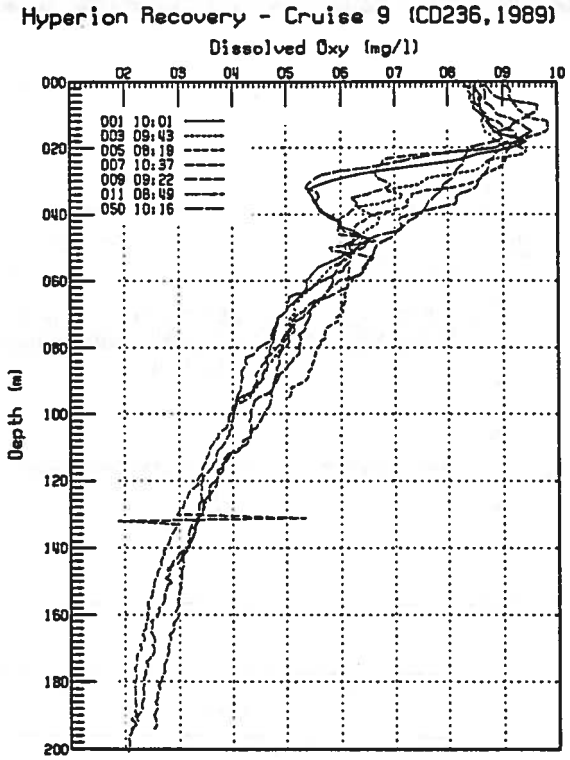
Hyperion Recovery - Cruise 9 (CD236,1989)
Dissolved Oxy (mg/l)
Depth (m)
001 10:01
003 09:43
005 08:19
007 10:37
009 09:22
011 08:49
050 10:16

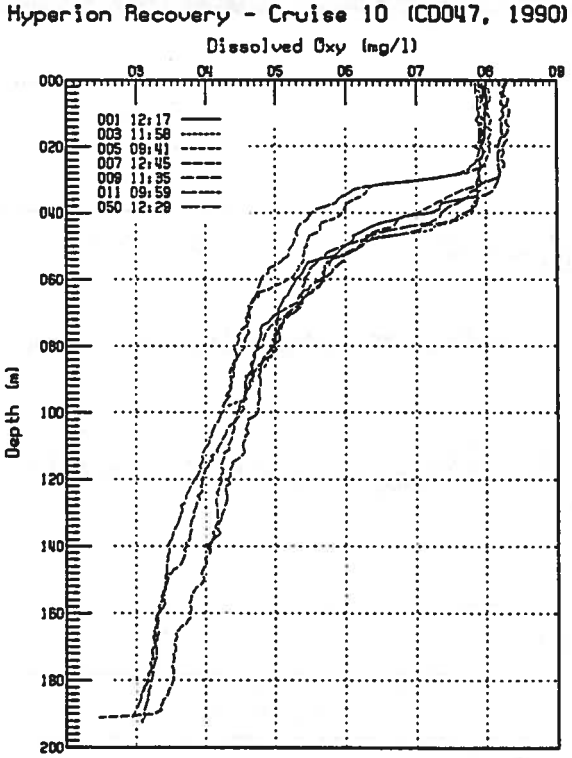
Hyperion Recovery - Cruise 10 (CD047, 1990)
Dissolved Oxy (mg/l)
Depth (m)
001 12:17
003 11:58
005 09:41
007 12:45
009 11:35
011 09:59
050 12:29

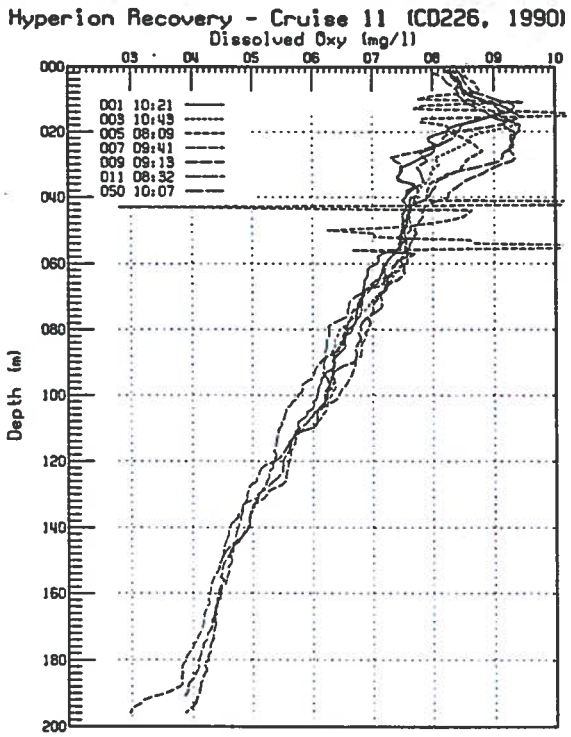

Appendix 6

Current meter velocity time series. Stations and dates are shown on each figure, see section for details (Pages 107 - 111).

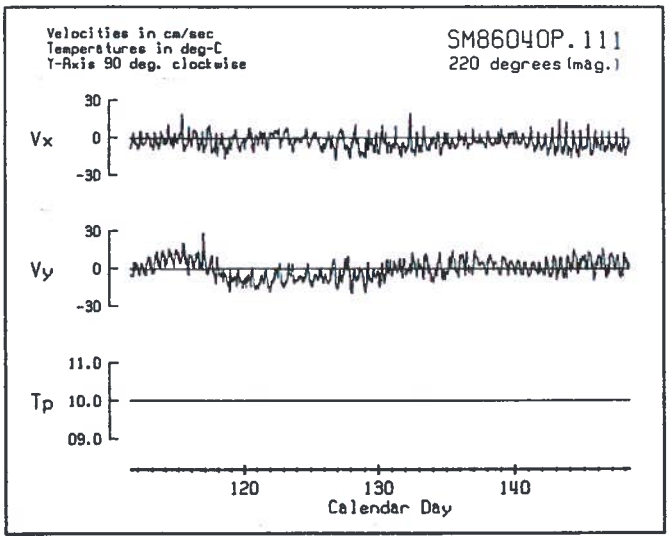

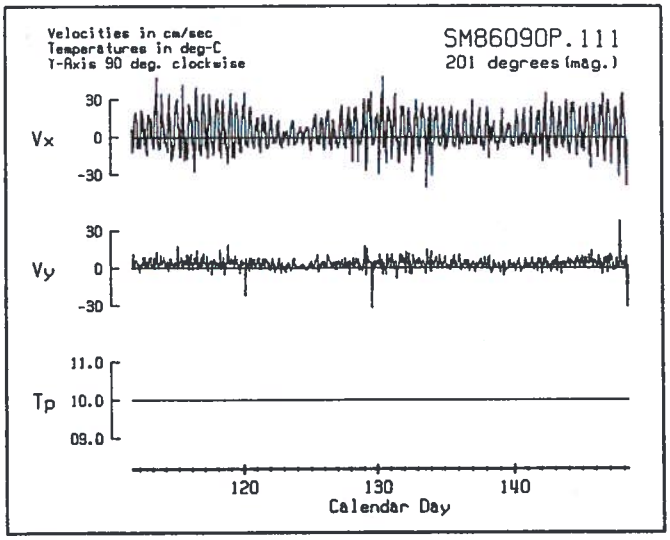

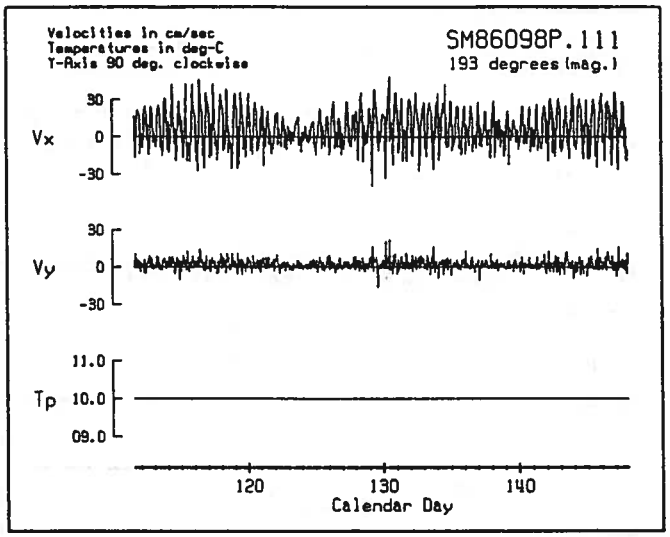
Velocities in cm/sec
Temperatures in deg-C
Y-Axis 90 deg. clockwise
SM86098P.111
193 degrees (mag.)
Vx
Vy
Tp
30
0
-30
11.0
10.0
09.0
120
130
140
Calendar Day

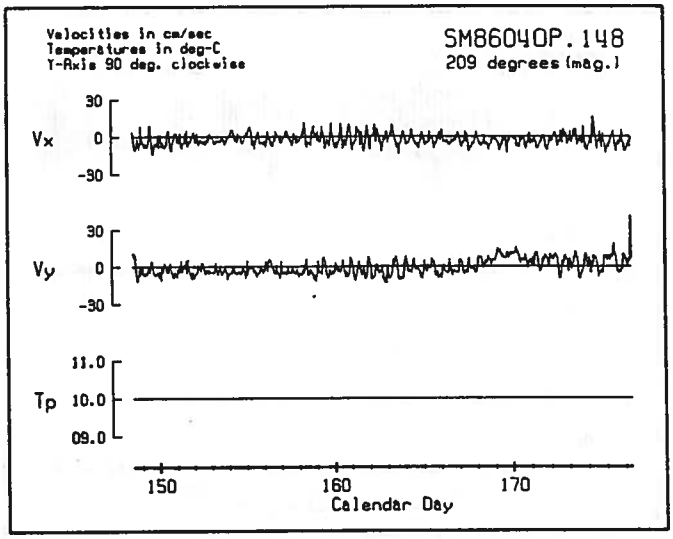
Velocities in cm/sec
Temperatures in deg-C
Y-Axis 90 deg. clockwise
SM86040P.148
209 degrees (mag.)
Vx
Vy
Tp
30
0
-30
11.0
10.0
09.0
150
160
170
Calendar Day

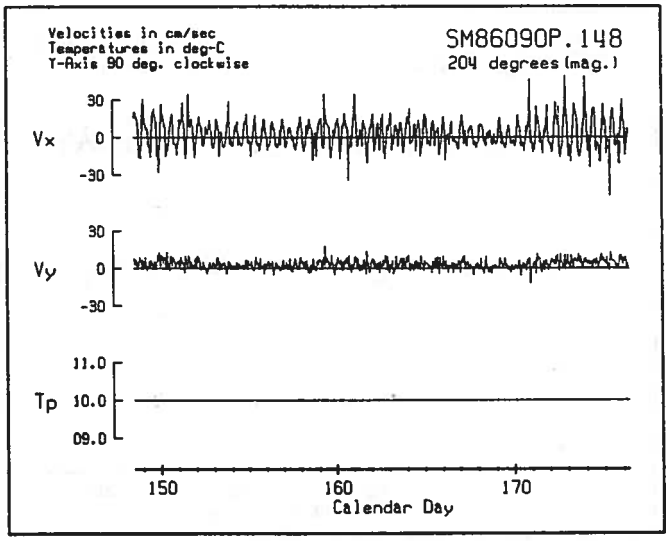
Velocities in cm/sec
Temperatures in deg-C
Y-Axis 90 deg. clockwise
SM86090P.148
204 degrees (mag.)
Vx
Vy
Tp
30
0
-30
11.0
10.0
09.0
150
160
170
Calendar Day

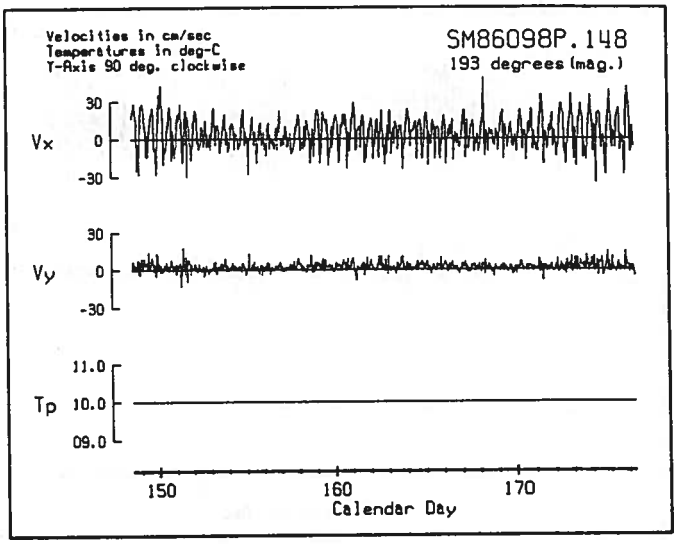
Velocities in cm/sec
Temperatures in deg-C
Y-Axis 90 deg. clockwise
SM86098P.148
193 degrees (mag.)
Vx
Vy
Tp
30
0
-30
11.0
10.0
09.0
150
160
170
Calendar Day

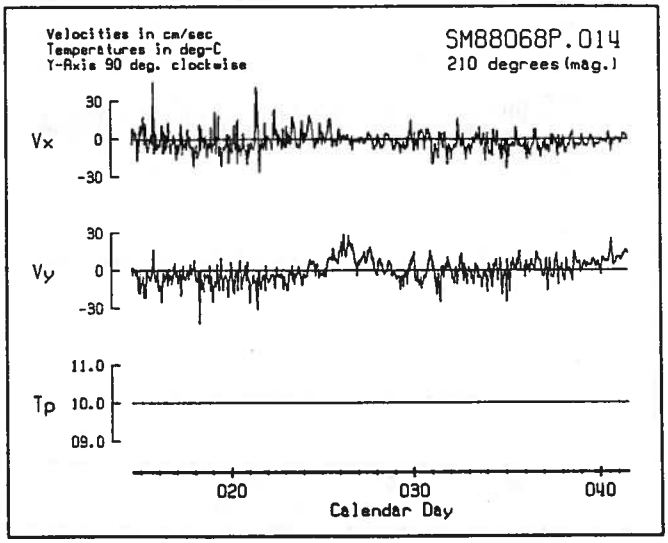
Velocities in cm/sec
Temperatures in deg-C
Y-Axis 90 deg. clockwise
SM88068P.014
210 degrees (mag.)
Vx
Vy
Tp
30
0
-30
11.0
10.0
09.0
020
030
040
Calendar Day

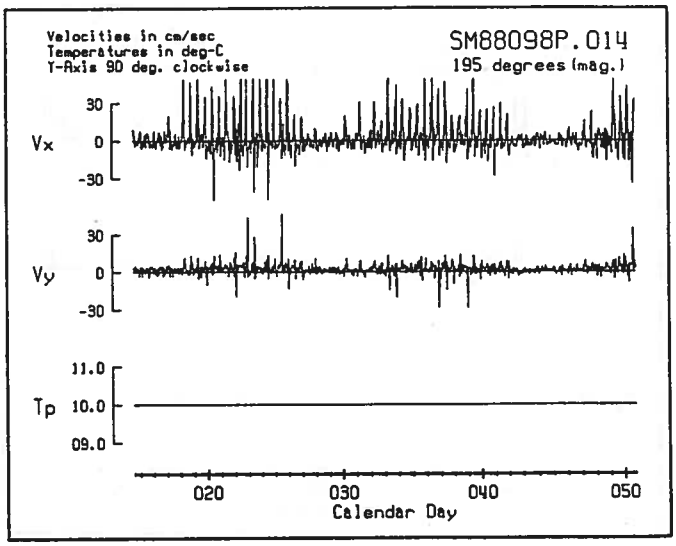
Velocities in cm/sec
Temperatures in deg-C
Y-Axis 90 deg. clockwise
SM88098P.014
195 degrees (mag.)
Vx
Vy
Tp
30
0
-30
11.0
10.0
09.0
020
030
040
050
Calendar Day

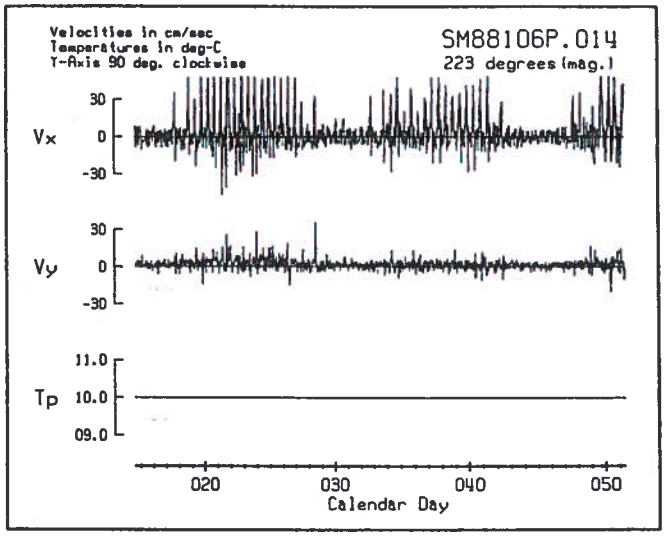
Velocities in cm/sec
Temperatures in deg-C
Y-Axis 90 deg. clockwise
SM88106P.014
223 degrees (mag.)
Vx
Vy
Tp
30
0
-30
11.0
10.0
09.0
020
030
040
050
Calendar Day

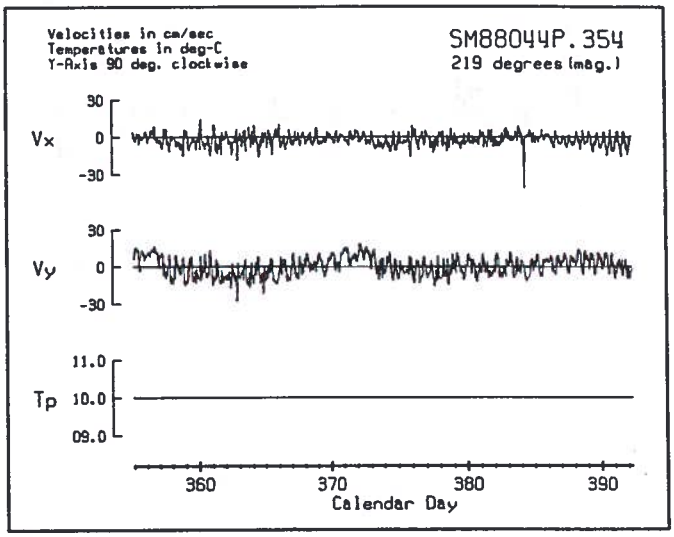
Velocities in cm/sec
Temperatures in deg-C
Y-Axis 90 deg. clockwise
SM88044P.354
219 degrees (mag.)
Vx
Vy
Tp
30
0
-30
11.0
10.0
09.0
360
370
380
390
Calendar Day

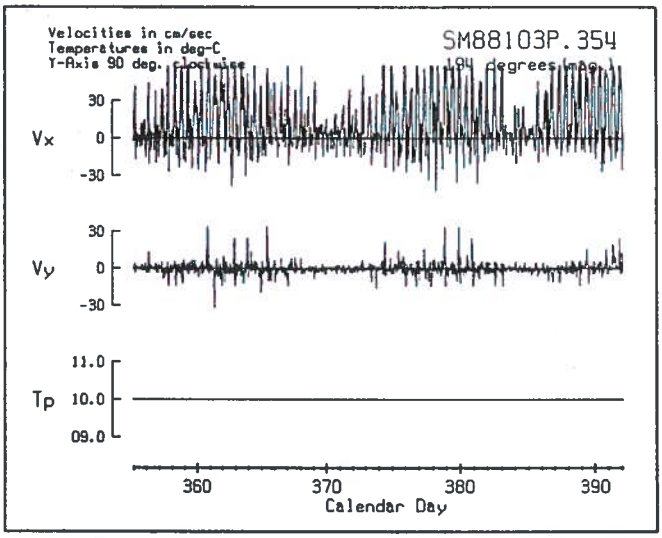
Velocities in cm/sec
Temperatures in deg-C
Y-Axis 90 deg. clockwise
SM88103P.354
184 degrees (mag.)
Vx
Vy
Tp
30
0
-30
11.0
10.0
09.0
360
370
380
390
Calendar Day

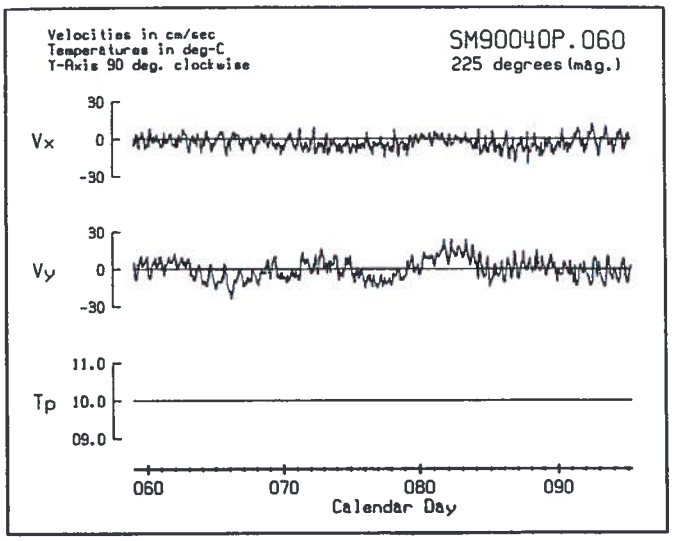
Velocities in cm/sec
Temperatures in deg-C
Y-Axis 90 deg. clockwise
SM90040P.060
225 degrees (mag.)
Vx
Vy
Tp
30
0
-30
11.0
10.0
09.0
060
070
080
090
Calendar Day

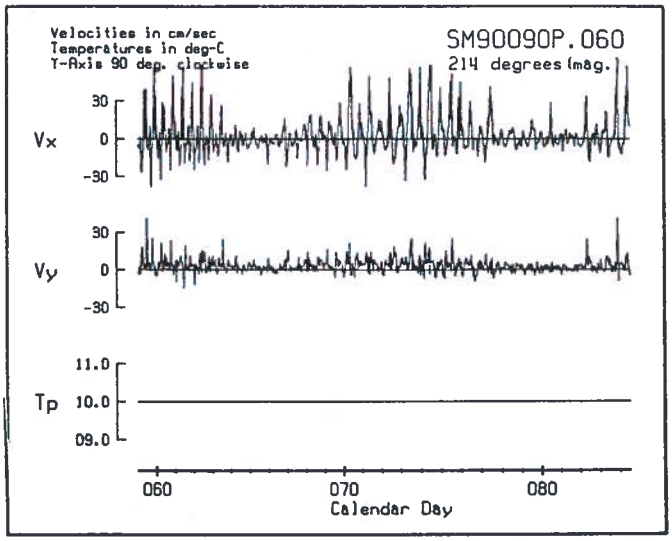
Velocities in cm/sec
Temperatures in deg-C
Y-Axis 90 deg. clockwise
SM90090P.060
214 degrees (mag.)
Vx
Vy
Tp
30
0
-30
11.0
10.0
09.0
060
070
080
Calendar Day

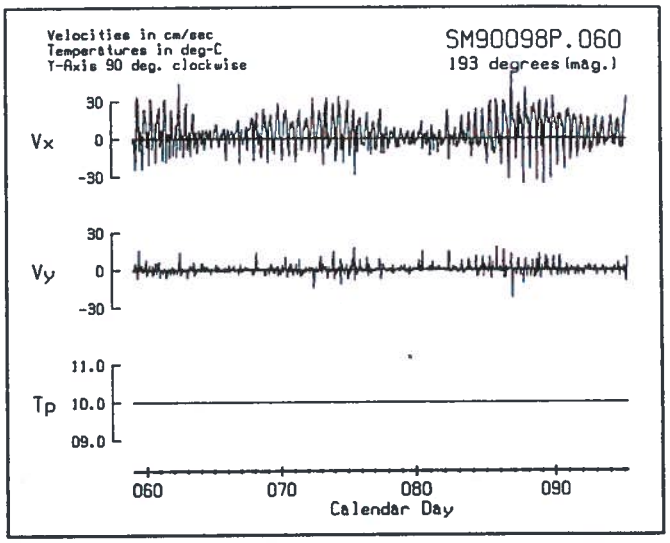
Velocities in cm/sec
Temperatures in deg-C
Y-Axis 90 deg. clockwise
SM90098P.060
193 degrees (mag.)
Vx
Vy
Tp
30
0
-30
11.0
10.0
09.0
060
070
080
090
Calendar Day

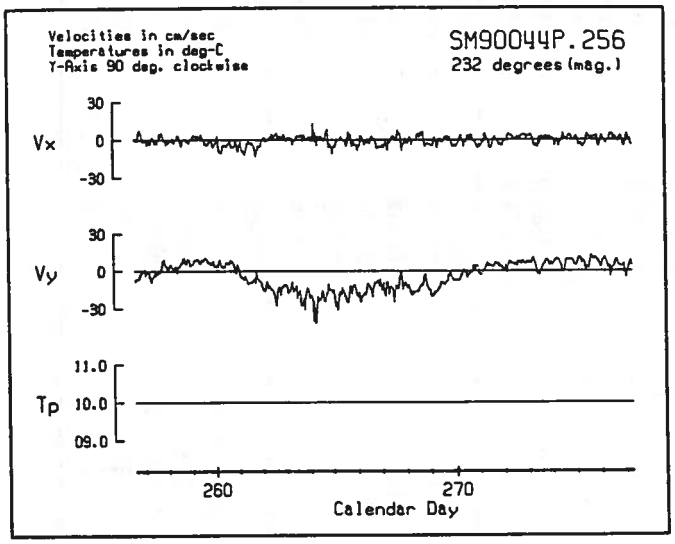
Velocities in cm/sec
Temperatures in deg-C
Y-Axis 90 deg. clockwise
SM90044P.256
232 degrees (mag.)
Vx
Vy
Tp
30
0
-30
11.0
10.0
09.0
260
270
Calendar Day

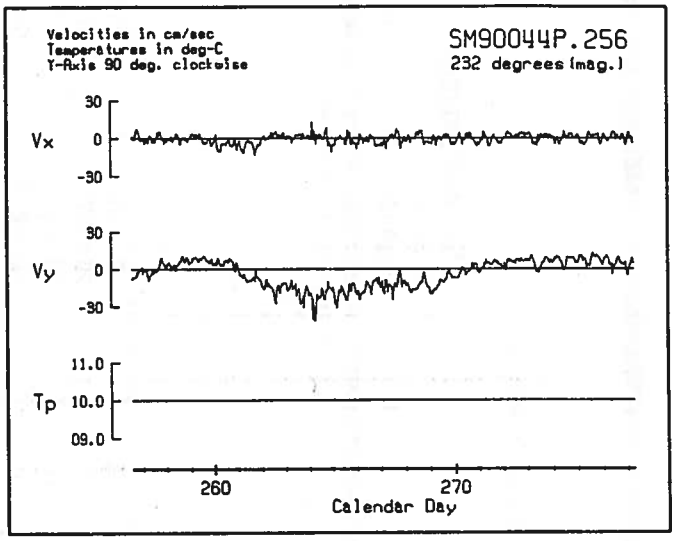
Velocities in cm/sec
Temperatures in deg-C
Y-Axis 90 deg. clockwise
SM90044P.256
232 degrees (mag.)
Vx
Vy
Tp
30
0
-30
11.0
10.0
09.0
260
270
Calendar Day

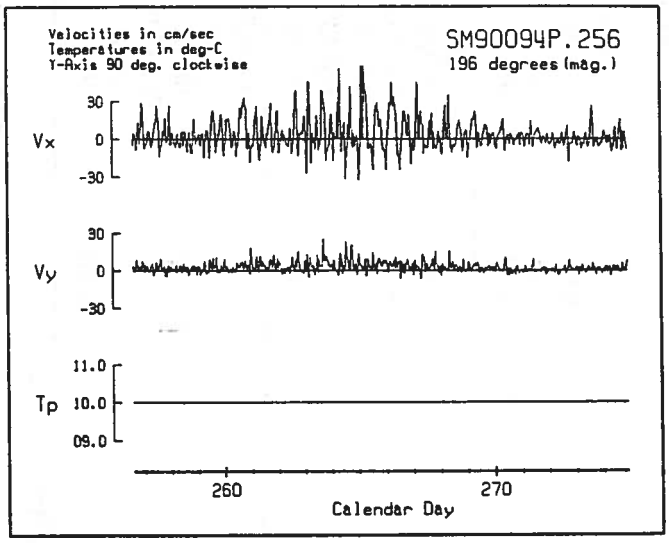
Velocities in cm/sec
Temperatures in deg-C
Y-Axis 90 deg. clockwise
SM90094P.256
196 degrees (mag.)
Vx
Vy
Tp
30
0
-30
11.0
10.0
09.0
260
270
Calendar Day

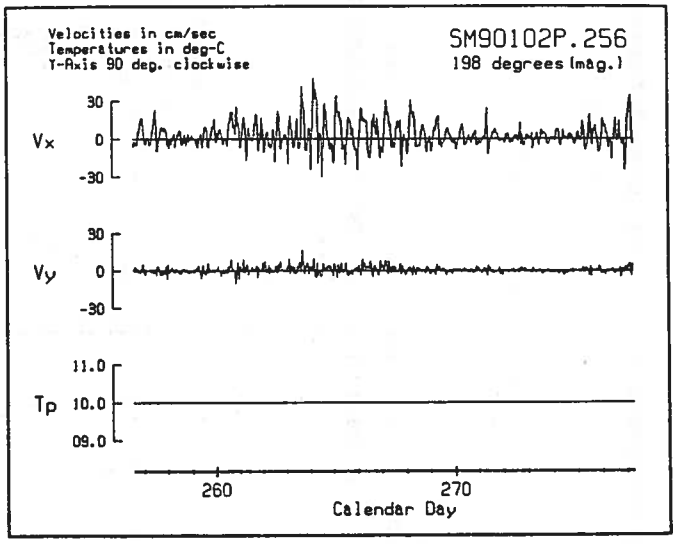
Velocities in cm/sec
Temperatures in deg-C
Y-Axis 90 deg. clockwise
SM90102P.256
198 degrees (mag.)
Vx
Vy
Tp
30
0
-30
11.0
10.0
09.0
260
270
Calendar Day

Appendix 7

Dissection Information for Dover sole & Sicyonia ingentis (Tissue Composite Info.)

Cruise	Station	Dover sole No. Composited	Dover sole Size range (cm)	Dover sole Sex	Sicyonia ingentis No. Composited	Sicyonia ingentis Size range (cm)	Sicyonia ingentis Sex
2	HR1	0	Dissection Logs Lost		None collected for tissues		
	2	0	" "		" "		
	3	0	" "		" "		
	4	0	" "		" "		
	5	0	" "	composited	" "		
	6	0	" "	composited	" "		
3	1	5	160-208	3F,2M	17	22.5-46.3	17F
	2	4	176-209	2 each	7	26.8-37.7	5F,2M
	3	6	174-245	2F,4M	6	24.5-37.3	5F,1M
	4	7	132-198	4F,3M	10	28.3-42.2	9F,1M
	5	3	63-132	1M,2I	12	19-39.9	8F,4M
	6	1	125	F	12	20.3-32.4	7F,5M
6	1	8	15.5-18.8	6F,2M	4	26.8-42.4	1F,3M
	2	8	9.4-23.7	4F,2M,2I	13	16.5-42.5	9F,4M
	3	13	7.1-19.3	6F,4M,3I	None	None	None
	4	7	17.8-23.3	6F,1M	8*/10*	26.3-43.0	*/*
	5	8	11.9-21.2	5F,3M	2	27.1-29.0	2M
	6	8	15.4-22.6	3F,5M	4	28.3-34.7	2F,2M
9	1	8	15-21	3F,5M	7	32-50	5F,2M
	2	7	14-21	2F,5M	6	33-42	5F,1M
	3	8	13-28	5F,2M,1I	None	None	None
	4	7	10-20	3F,4M	7	32-44	6F,1M
	5	6	11-19	2F,2M,2I	5	27-42	4F,1M
	6	5	13-24	2F,3M	7	24-49	5F,2M
11	1	7	16-19	1F,4M,2I	11	30-47	11F
	2	7	17-19	5F,2M	5 for muscle	33-45	4F,1M
	3	6	17-20	5F,1M	None	None	None
	4	6	11-19	4F,1M,1I	6 for muscle	28.4-47	6F
	5	3	7-18	2F,1I	15	24-32	8F,7M
	6	6	16-20	3F,3M	6	26-34	4F,2M

8* = for muscle 6F,2M & 10* = for hepato 7F,3M